



UNIVERSITY OF READING

Department of Meteorology

Downstream Transformation of African Easterly Waves:
Criteria for Development

Simon Rowell

A dissertation submitted in partial fulfilment of the requirements for
the degree of Master of Science in Applied Meteorology

August 16th 2010

Abstract

Each year North Atlantic hurricanes cause deaths and billions of dollars worth of damage to property and infrastructure. The majority of them originate from African Easterly Waves (AEWs) which propagate from the West African coast across the Atlantic. This investigation looks into the downstream transformation of AEWs into tropical hurricanes, and aims to identify specific differences between developing and non-developing AEWs to aid in the forecast and tracking of tropical hurricanes.

Methods of tracking and identifying AEWs are investigated and the automatic tracking of maxima of the vertical mean of relative vorticity between 850 and 600 hPa is chosen as the automatic tracking parameter to be used after AEWs have moved over the Atlantic. Direct observation and manual AEW identification using the 600 hPa relative vorticity field is the method chosen for identifying AEWs as they cross the West African coast. Case studies of developing and non-developing AEWs are presented and from these the hypotheses posed that cyclogenesis from an AEW depends on the downstream relationship with the African Easterly Jet (AEJ), the relative humidity distribution and the presence of deep convection.

These hypotheses are then investigated using a compositing technique for all the AEWs for the period June to September of 2005 to 2009 from the Interim ECMWF Re-Analysis data (ERA-I) in two regions – the West African coastal region and also a region referenced to the initial over-ocean automatic tracking point for each AEW.

Analysis of these composite data sets shows that developing AEWs are characterised by a stronger AEJ to the north of the 600 hPa relative vorticity maximum both at the coastal region and downstream, by more organised convection at both regions, and by a markedly different relative humidity distribution for the downstream composites.

Acknowledgements

I would like to thank my supervisors, Dr Rosalind Cornforth of the Department of Meteorology and Dr Kevin Hodges of the Environmental Systems Science Centre at the University of Reading. Their help and encouragement has been excellent, as has their gentle but necessary and always timely guidance. Most importantly I would like to thank my wife Gail, whose hard work, support and sacrifice have made this year possible.

Contents

1. Introduction	1
2. The Genesis and Development of AEWs	3
3. AEW Tracking	9
3.1. Automatic Tracking of Relative Vorticity Maxima	9
3.2. Automatic Tracking of Meridional Velocity Sign Reversal	9
3.3. Relative Merits of the Automatic Tracking Techniques.....	9
4. AEW Identification	12
4.1. AEW Identification During 2006.....	12
5. Case Studies	14
5.1. Hurricane Ernesto	14
5.2. Tropical Storm Chris	19
5.3. AEW 171	24
5.4. AEW 516.....	29
6. Manual Tracking and Identification of African Easterly Waves at the West African Coast	34
7. The Compositing of Coastal Region Data for Developing and Non-Developing AEWs	36
7.1. Zonal Wind	37
7.2. Meridional Wind	38
7.3 Vertical Wind.....	39
7.4 Relative Humidity	39
7.5. Equivalent Potential Temperature (θ_e)	43
7.6. Relative Vorticity	45
8. Downstream Tracking and Identification of African Easterly Waves	49
9. The Compositing of Downstream Data for Developing and Non-Developing AEWs	52
9.1 Wind Speed Composites.....	53
9.2 Relative Humidity Composites	56
9.3 Equivalent Potential Temperature Composites	58
9.4 Potential Vorticity on the 315 K Isentropic Surface Composites	60
10. Discussion, Conclusions and Further Questions	61
10.1. Tracking and Identifying AEWs	61
10.2. Case Studies of Developing and Non-Developing AEWs.....	61
10.3. Hypotheses for Experiments	62
10.4. AEW Development at the West African Coast.....	63
10.5. AEW Downstream Development	64
10.6. Overall Conclusions and Areas for Further Investigation	65
11. References	66

1. Introduction

During the northern hemisphere summer months African Easterly Waves (AEWs) propagate from east to west across the Atlantic approximately every 3 days at between 6 and 9 ms⁻¹ with a mean latitude of 11°N (Carlson, 1969). The surface effect of the passage of an AEW is not severe – the surface winds back and then veer and increased convection brings increased rainfall and the possibility of strong but short-lived squalls. Over land the increased convection associated with AEWs (Hopsch, et al., 2010) can lead to an increase in the number of meso-scale convective events (MSCs) which have a direct link to the rainfall in the West African and Sahel regions (Lebel, et al., 2009) and this can be extremely beneficial to the region's rainfall and therefore its ability to support its population. Once over the Atlantic they travel westwards towards the Caribbean and it is at this point that they change from being benign bringers of rainfall to the potential seeds of hurricanes. One of the criteria for cyclogenesis is that there should be an atmospheric disturbance as the trigger (Gray, 1978) and looking at 2005 as an example shows that of the 31 named storms, 25 could be directly linked to an AEW. In 2006, a much quieter year for cyclone activity, 7 out of 9 named storms resulted from an AEW (Tropical Prediction Center, 2010). In fact, analysis of the ERA-40 data set shows that over the period 1958 to 2002 approximately 40% of all AEWs in August and September become cyclones (Hopsch, et al., 2007).

The scientific interest in the evolution of AEWs into tropical storms is therefore clear – however, it is important to note the human, material and financial consequences of them. A hurricane in the middle of the North Atlantic, while a massive and meteorologically significant event, is of generally little consequence to society. Mariners have known for centuries the statistical forecasts of hurricanes and their paths (UK Hydrographic Office, 1987) and modern forecasting techniques and the technical advances in the promulgation of forecast information (UK Hydrographic Office, 2010) mean that it is a careless or very unlucky sailor who is caught unawares by one. For countries, cities and fixed installations in the path of a tropical cyclone the situation is very different. The best known north Atlantic example in recent years is Hurricane Katrina which devastated New Orleans in 2005, caused over 1800 confirmed fatalities (Knabb, et al., 2006) and cost, unadjusted for inflation since then, US\$81 billion (Blake, et al., 2007). Even relatively unknown hurricanes have significant effects – Hurricane Ernesto swept over Haiti and up the eastern seaboard of the United States in the last week of August 2006, directly causing 5 deaths in Haiti, widespread flood damage in Hispaniola and eastern North Carolina and estimated damage costs of up to US\$0.5 billion (Knabb, et al., 2006). Therefore a more comprehensive understanding of the evolution of AEWs into tropical cyclones would aid the downstream prediction and tracking of tropical cyclones, and possibly provide earlier and more accurate warnings of landfall.

The data used is taken from the ECMWF Interim Re-Analysis dataset (ERA-I) from 1989 to 2009. This uses improved data assimilation techniques and observation sets compared to the ERA-40 dataset, and has T255 horizontal resolution, which gives 0.7° resolution, using 16 pressure layers at 50 hPa intervals from 950 to 200 hPa. On occasion data has been taken from the publically available section on the ECMWF server at 1.5° resolution. This is referenced “ECMWF, 2010”.

The terms “hurricane” and “cyclone” are interchangeable and describe the same meteorological phenomenon. Traditionally they are described as hurricanes in the north Atlantic and east Pacific, cyclones in the south Pacific and Indian Oceans and typhoons in the west Pacific and over south-east Asia.

The aims for the work were to identify developing and non-developing AEWs over a selected time period, to generate composites and cross-sections using a technique previously only applied to extra-tropical storms and the ERA-I data set, to diagnose differences in composited AEW structure and to understand the role of dynamic processes in the development, or not, of AEWs.

The work is organised as follows. The genesis and development of AEWs are discussed, followed by the methods of tracking and identifying them. Case studies of developing and non-developing AEWs are presented, and from these hypotheses are drawn questioning the relationship both downstream and at then African coast between AEWs, the African Easterly Jet (AEJ), moisture content and convection. Using compositing techniques the AEWs from the period June to September (JJAS) 2005 to 2009 are analysed at the West African coast and downstream, and conclusions drawn from these analyses as to the differences between developing and non-developing AEWs.

2. The Genesis and Development of AEWs

AEWs are formed with components north and south of the African Easterly Jet (AEJ) (Carlson, 1969). The AEJ is a mid-tropospheric jet which is present all year round and becomes most defined with a core velocity of greater than 10 ms^{-1} during the boreal summer months in between April and November. The AEJ is primarily due to the reversal of the expected meridional surface temperature gradient caused by the intense heat of the Sahara (Hastenrath, 1991) illustrated by the mean monthly surface temperature for June to September (JJAS), 1989 to 2009 (Figure 2.1), using sea surface temperature and land 2m temperature.

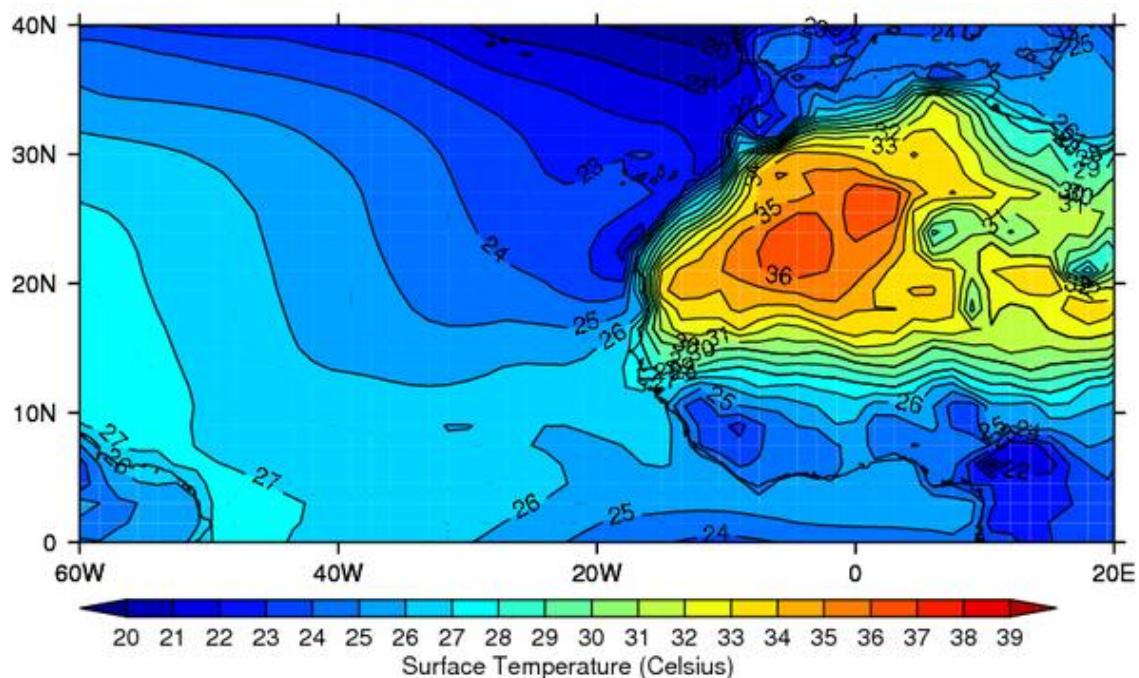


Fig 2.1: mean surface temperatures ($^{\circ}\text{C}$) for JJAS, 1989 to 2009 (ECMWF, 2010)

The AEJ generally sits at 600 hPa as above this level the temperature gradient reverses with the cooler temperatures on the poleward side (Burpee, 1972). AEWs are formed through a combination of barotropic and baroclinic energy conversions (Thorncroft, et al., 1994). The barotropic interaction occurs between the negative meridional potential vorticity gradient ($d\bar{q}/dy$) in the AEJ core and the positive $d\bar{q}/dy$ south of the AEJ, and the baroclinic interaction occurs between the negative $d\bar{q}/dy$ north of the AEJ and the positive surface temperature gradient (Pytharoulis, et al., 1999). This is illustrated by the JJAS mean of potential vorticity on the 315K potential temperature surface (PV315), which generally goes through the AEJ core, for 1989 to 2009 (Figure 2.2). Over land north of the AEJ there is usually a deep, well mixed boundary layer due to the high surface temperature and this, combined with the vertical flux of sensible heat allows efficient conversion of available eddy potential energy into eddy kinetic energy – this is the baroclinic instability forming the low level northern

vortex, while to the south of the AEJ meridional momentum flux occurs, which provides the barotropic instability for the southern vortex (Fink, et al., 2004).

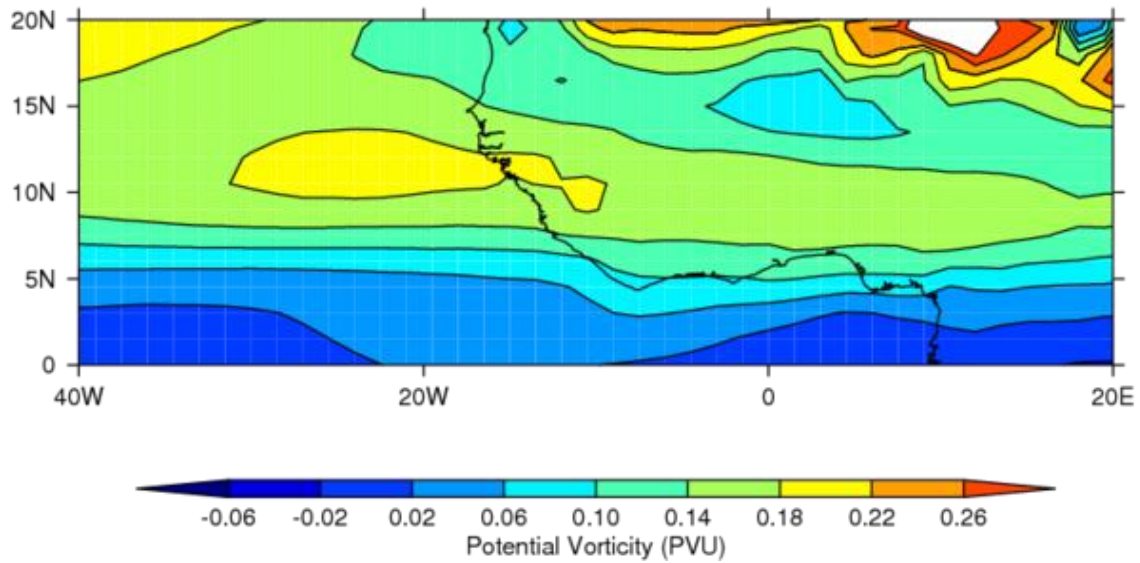


Fig 2.2: potential vorticity at 315 K potential temperature ($\text{PVU}=10^{-6}\text{m}^2\text{Ks}^{-1}\text{kg}^{-1}$) for JJAS 1989 to 2009 (ECMWF, 2010)

The University of Reading's Intermediate General Circulation Model, version 2 (IGCM2), has been used (Cornforth, et al., 2009) to investigate the effects of moisture and surface fluxes on the AEW/AEJ system. In a dry system, baroclinic energy conversion dominates barotropic, and the AEJ development depends more on heat flux than momentum flux. The introduction of moisture causes a faster AEJ growth but a slightly weaker maximum strength, and strongly modifies the structure, location and magnitude, particularly the diabatic heating associated with moist convection. The AEW eddy kinetic energy correlates with the daily average precipitation south of the AEJ, confirming the strong link between AEWs and West African rainfall. Deep moist convection in the AEW trough appears to strengthen the AEW.

The barotropic and baroclinic interactions form a vortex at each end of the AEW (Thorncroft, et al., 2001) – a low level one usually tracked by using relative vorticity maxima (Serra, et al., 2010) at 850 or 925 hPa poleward of 15°N, and a 600 hPa vortex which runs south of the AEJ usually between 5° and 10°N over the African continent, illustrated by the example of the 2006 relative vorticity maxima which passed between 10° and 20° W at those two levels for 2005 (*Figure 2.3*). The consensus of research has shown (e.g. Pytharoulis & Thorncroft, 1999; Fink, et al., 2004; Cornforth, et al., 2009) that the AEWs are usually composed of both northern and southern components with good correlation between the two but there is disagreement here with other work treating them as separate entities (Chen, 2006). This study, while not specifically investigating that, has found several examples where

the automatic relative vorticity maxima tracking routines have not picked up both the northern low level vortex and the southern mid-level vortex (seen by the visible difference in track numbers in the 2006 example). However, when manually observing the relative vorticity data for AEWs crossing the West African coast evidence of both was always present (see Case Studies, *section 5*).

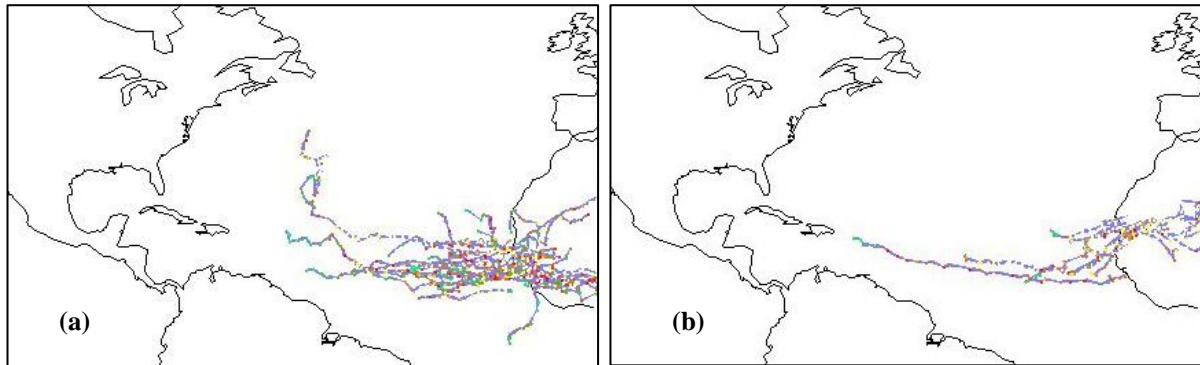


Fig 2.3: relative vorticity track for JJAS 2005 passing between 10^o and 20^oW and 5^o and 20^oN for (a) 600 hPa and (b) 925 hPa

The northern low level vortices are reinforced by the convergence of the north east Harmattan and the south west monsoon winds (Chen, 2006), and the presence of the dry Saharan Air Layer (SAL) prevents vortex stretching upwards, illustrated by the meridional vertical section at 19.5°N of vertical velocity overlaid on relative humidity for JJAS 1989 to 2009 (*Figure 2.4(a)*). Along the southern set of tracks (illustrated by a similar meridional section at 10.5°N, *Figure 2.4(b)*) there is no similar barrier to vertical propagation, and the 600 hPa vortex can gradually extend downwards.

The geographical location of the AEW genesis points depends on orography as well as tropospheric conditions. The southern barotropic vortices associated directly with the AEJ have their greatest genesis density at the West African coast at around 10° to 17°W, but there is a significant region on the lee side of the Ethiopian highlands west of around 10°N, 35°W (Thorncroft, et al., 2001). These two longitudinal regions can clearly be seen on the example of a longitude-time plot of the vertical mean relative vorticity from 850 to 600 hPa for JJAS 2005 (*Figure 2.5(a)*). Four main genesis regions for the low level northern vortices have been found (Chen, 2006) at the coast to 10°W, 10°W to 5°E, 10° to 20°E and 25° to 30°E. The second and most significant is just downstream of the Hoggar Mountains (the highest point of which is Mount Tahat with an elevation of 2918 m at 23°N, 5.5°W (Philip's, 2002)), and these regions can be seen in the example of the 925 hPa longitude-time plot for JJAS 2005 (*Figure 2.5(b)*). On the leeward side of these areas of high ground vertical vortex stretching takes place, aiding their genesis and growth.

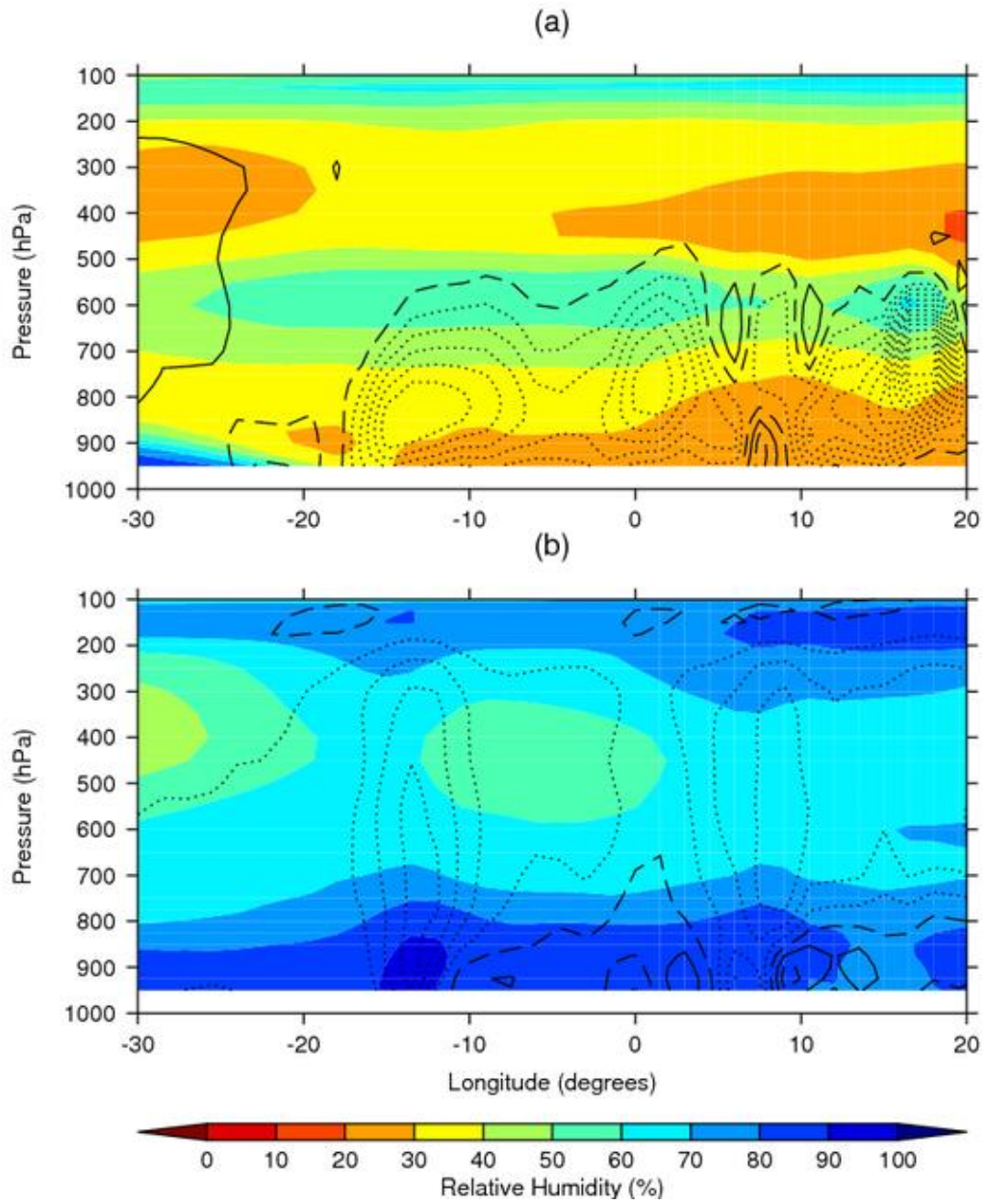


Fig 2.4: vertical velocity (contour spacing $2 \times 10^{-4} \text{hPa s}^{-1}$, zero line long dashed, negative, i.e. upwards, dotted) overlaid on meridional relative humidity (%) for JJAS 1989 to 2009 at (a) 19.5°N and (b) 10.5°N (ECMWF, 2010)

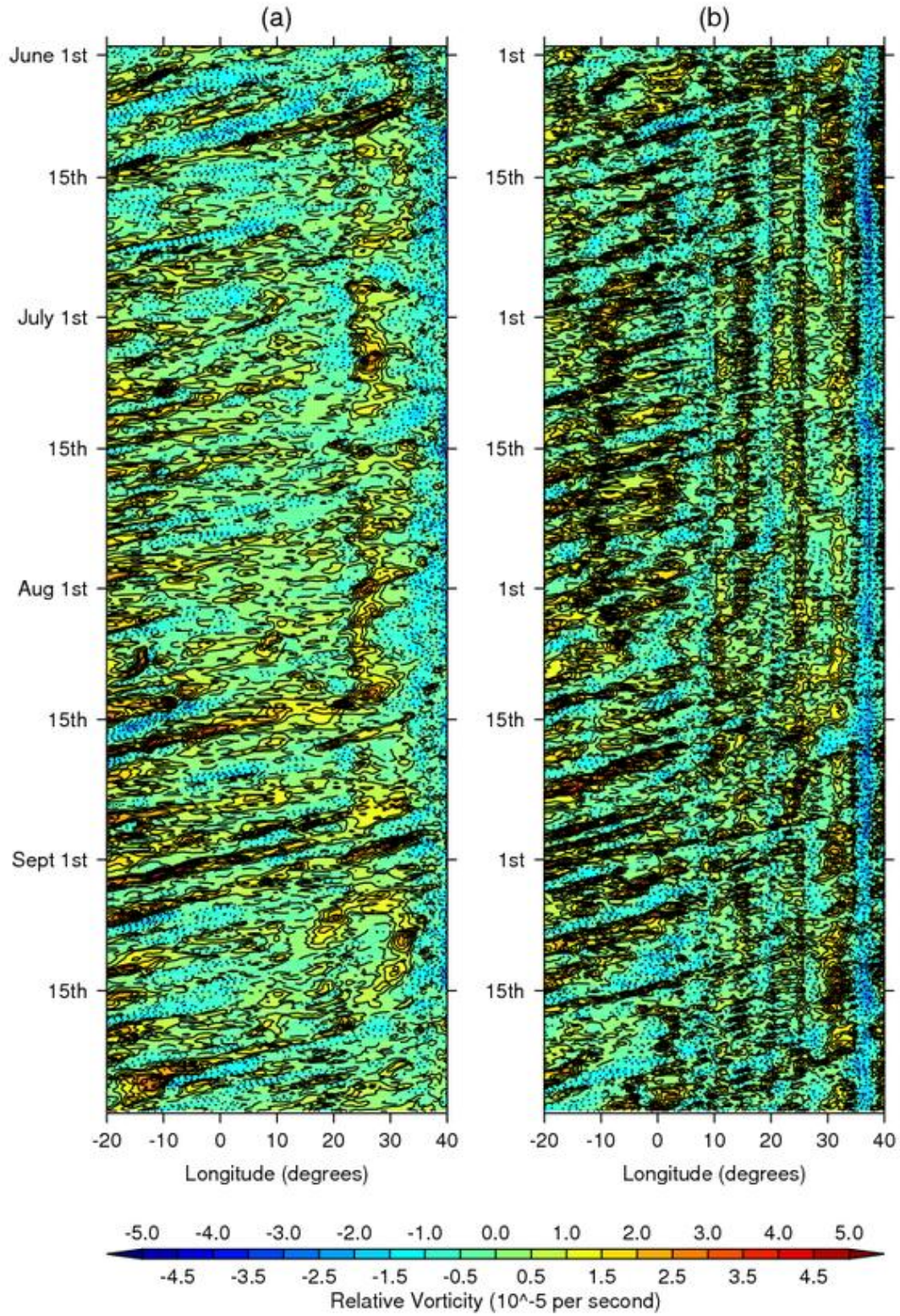


Fig 2.5: longitude-time plots for JJAS 2005 showing:
 (a) vertical mean relative vorticity ($\times 10^{-5} \text{ s}^{-1}$) from 850 to 600 hPa, averaged meridionally from 9° to 16°N
 (b) relative vorticity ($\times 10^{-5} \text{ s}^{-1}$) at 925 hPa, averaged meridionally from 12° to 24°N

The main development region (MDR) for hurricane development is defined as 10° - 20° N, 20° - 80° W. Hurricane development seems to be associated with moist convection over the Guinea Highlands, and the convergence of the northern low level vortices with the southern mid-level ones (Hopsch, et al., 2007). A second peak occurs at about 10° N, 38° W, possibly due to warming sea surface temperature underneath AEWs. The peak hurricane development months are July to September, and these coincide with peak AEW months, especially the peak hurricane development month of September and the peak northern 925 hPa vortex month of September (Hopsch, et al., 2007). There is more variability to the 850 hPa waves than the 600 hPa ones, and from 1985 to 1998 there is excellent correlation between this 600 hPa variability and hurricane development (Thorncroft, et al., 2001). This is contradicted somewhat by later work (Hopsch, et al., 2007) which shows that over the ERA-40 period as a whole (1958 to 2002) the 600 hPa tracks did not correlate significantly with TRS activity, but that there was correlation between 850 hPa meridional wind variance and MDR hurricane generation. Barotropic energy conversion at 700 hPa gave a robust indicator for the evolution of AEWs into hurricanes (Zipser et al, 2009). The same research indicated that developing AEWs were characterised by NE/SW wave axis tilt, a wind maximum ahead of the wave axis, and a strong, positive barotropic energy conversion. If the AEWs travel across the entire Atlantic they can reinvigorate over the Intra-Americas Sea (IAS) and Central America into the eastern Pacific (Thorncroft, et al., 2001).

3. AEW Tracking

Two types of AEW tracking methods are used, firstly the manual identification and following of relative vorticity maxima at 600 hPa and secondly the automatic detection of either relative vorticity maxima at various levels or the sign reversal in meridional wind at the AEW trough axis. Manual identification is used to identify the time that each individual AEW crosses the African coast at 17°W and is explained in detail in *section 6*. Automatic track identification is used to assemble the individual AEW data fields for the composite downstream analysis.

3.1. Automatic Tracking of Relative Vorticity Maxima

The automatic tracking technique used (Thorncroft, et al., 2001) was applied to relative vorticity data in various combinations of levels from 925 hPa to 600 hPa to capture both the barotropic vortices at 600 hPa south of the AEJ, and the low level baroclinic vortices north of it. It is important to remove very short lived and small scale vortices which would otherwise add spurious tracks to the analysis, and so T42 spectral resolution was used. A temporal filter was applied in that the tracks had to last for at least 48 hours, and spatially they had to travel at least 10° , which is at least 1000 km. Finally, only systems with closed vorticity contours of greater than $+0.5 \times 10^{-5} \text{ s}^{-1}$ were captured, which also helps to remove weaker relative vorticity centres which may come from other sources. This does, however, mean that a number of developing AEWs are lost from the tracking as they pass over the eastern Atlantic before becoming stronger as they spin up into tropical depressions.

3.2. Automatic Tracking of Meridional Velocity Sign Reversal

A tracking technique was applied to the sign reversal of meridional wind at the 925 and 700 hPa levels. These were tracked using a 2 to 6 day bandpass filter, then tracking the positive and negative anomalies.

3.3. Relative Merits of the Automatic Tracking Techniques

The combinations tested were relative vorticity tracking at 925, 850 and 600 hPa, and the vertical mean of relative vorticity between 850 and 600 hPa. It was found that using the vertical mean relative vorticity gave the most consistent results, agreeing with recent studies (Serra, et al., 2010). The meridional wind sign reversal was tracked at 925 and 700 hPa, and while it gave sporadic early detection of AEWs was not consistent for all of them. Taking the developing systems which were directly linked to AEWs in 2006, it can be seen that while relative vorticity tracking gives results at all levels, meridional wind sign change tracking does not (*table 3.3.1*).

2006 Systems	RV 925 hPa	RV 850 hPa	RV 600 hPa	RV vertical mean	Mer. Wind 925 hPa	Mer. Wind 700 hPa
Chris	Y	Y	Y	Y	N	N
Debby	Y	Y	Y	Y	N	N
Ernesto	Y	Y	Y	Y	Y	Y
Florence	Y	Y	Y	Y	Y	Y
Gordon	Y	Y	Y	Y	N	N
Helene	Y	Y	Y	Y	Y	Y
Isaac	Y	Y	Y	Y	N	N

Table 3.3.1: named systems which developed from AEWs for 2006, showing whether a particular automatic tracking method picked them up or not

There is some difference in the initial pick up points and the actual position of the system centre, which is illustrated by looking at the tracks for the development of Hurricanes Ernesto (*Figure 3.3.1(a)*) and Gordon (*Figure 3.3.(b)*). Hurricane Ernesto is an example of a system that is picked up earlier by meridional wind sign reversal tracking, but it can be seen that the tracked path of the developed storm as it travels up the eastern seaboard of North America is considerably to the east of the relative vorticity tracks, probably because the track is for the positive meridional wind anomaly which will be in a different location to the vorticity centre, especially in extra-tropical storms. This displacement of the track of the developed system was noticed with Hurricanes Florence and Helene too (not shown). Hurricane Gordon was not tracked by meridional wind sign reversal, and it can be seen that the vertical mean relative vorticity track is picked much earlier than the others.

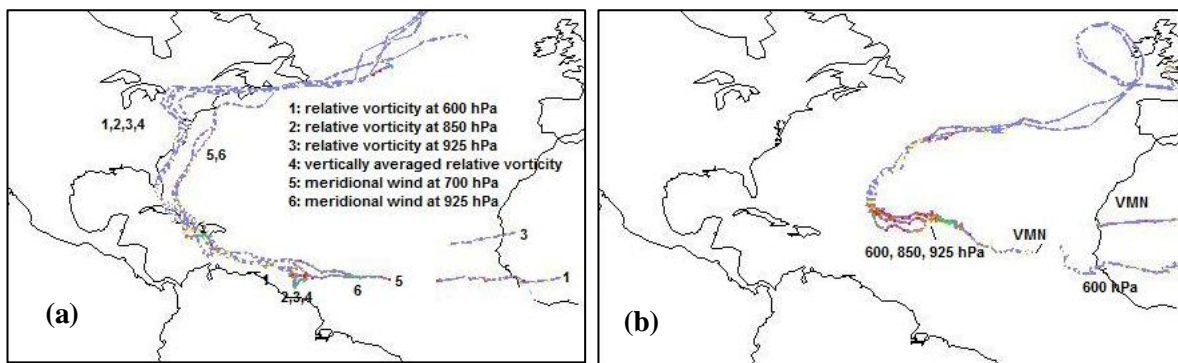


Fig 3.3.1: automatic tracking results for (a) Hurricane Ernesto and (b) Hurricane Gordon

It is also important to confirm whether a particular tracking method produces results that agree with the National Hurricane Center’s “best track” data (Tropical Prediction Center, 2010). Studies have shown (Thorncroft, et al., 2001) that relative vorticity maxima tracking closely follows best track data, and Hurricane Gordon is an example of this with the vertical mean relative vorticity track overlaying the best track data (*Figure 3.3.2*) until the system becomes an extra-tropical storm. The vertical mean relative vorticity track also picks up the developing system well before it is declared a tropical depression.

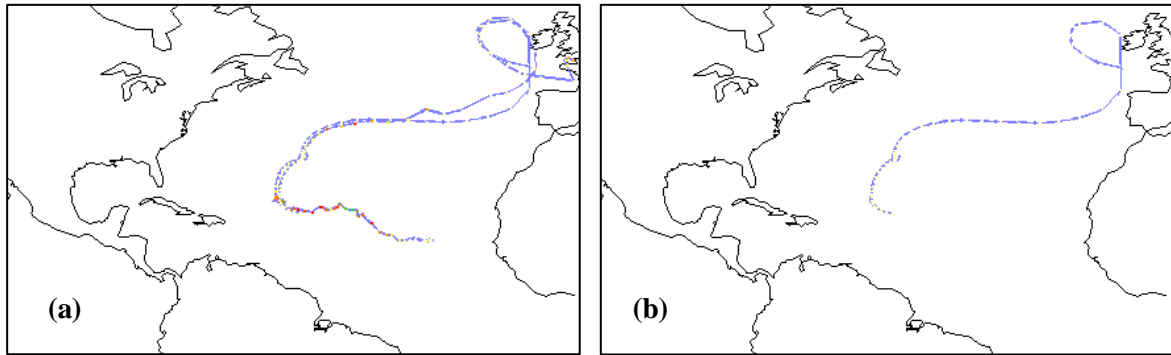


Fig 3.3.2: Hurricane Gordon showed with (a) vertical mean relative vorticity tracking overlaid on to best track data, and (b) best track data alone

From this it can be seen that the most consistent method of obtaining automatic AEW tracking is by using the relative vorticity maxima tracking system with vertical mean relative vorticity from 850 to 600 hPa. It is also important to note that there is a large gap for most AEWs where they fall below the detection threshold whilst moving across the Atlantic prior to being picked up again further west.

4. AEW Identification

For the chosen observation period of JJAS 2005 to 2009 each AEW needed to be identified as either a developing or a non-developing one, and each one also needed to be specified for two spatio-temporal reference points – the West African coastal crossing time, and the location and time that it was then detected again after passing into the Atlantic. For those AEWs that remain above the detection threshold for the entire Atlantic journey the second time will not be present. Interestingly, these are by no means all developing AEWs as will be seen. To illustrate the process it is best to use one year as an example.

4.1. AEW Identification During 2006

2006 was chosen as the first year to be processed, as it was a relatively quiet year for hurricane activity, with only 9 named systems of which 7 were the direct result of an AEW (*table 4.1.1*).

System	Origin
TS Alberto	Disturbed weather in C. America (Avila, et al., 2006)
TS Beryl	Started from a stalled frontal system (Pasch, 2006)
TS Chris	AEW that left the W African coast on 26 th July 2006 (Stewart, 2006)
TS Debby	AEW that left the W African coast on 20 th August 2006 (Franklin, 2006)
H Ernesto	AEW that left the W African coast on 18 th August 2006 (Knabb, et al., 2006)
H Florence	AEW that left the W African coast on 29 th August 2006; then joined by a faster AEW that left the W African coast on 31 st August 2006 (Beven, 2006)
H Gordon	AEW that left the W African coast on 1 st September 2006 (Blake, 2006)
H Helene	AEW that left the W African coast on 11 th September 2006 (Brown, 2006)
H Isaac	AEW that left the W African coast on 18 th September 2006 (Mainelli, 2006)

Table 4.1.1: 2006 named storms with their origins

The best track data for the 2006 storms are shown below (*Figure 2.1.1*). Two groups are clearly seen – those that develop in the east and recurve in the central or western Atlantic, and those that develop in the west and recurve over the Caribbean and along the eastern seaboard of North America.



Fig 2.1.1: Named Storm for the North Atlantic, 2006 (Tropical Prediction Center, 2010)

The automatic tracking routine was run separately for the vertical mean, 925 hPa, 850 hPa and 600 hPa relative vorticity with a regional filter set from 5° to 20°N and 90° to 10°W (Figure 4.1.2).



Fig 4.1.2: regional filter for automatic tracking method (UK Hydrographic Office, 1998)

Each run gave a track file containing the information for all AEWs, developing or not, which passed through the regional filter (table 4.1.2). Looking at the vertical mean tracks (Figure 4.1.3), the relative vorticity maxima tracks north and south of the AEJ can be clearly seen over the African continent, and the developing AEWs are seen as recurring tropical and then extra-tropical systems.

Level	Number of AEW Tracks
925 hPa	65
850 hPa	90
600 hPa	94
Vertical Mean	97

Table 4.1.2: tracks detected at each level with the regional filter

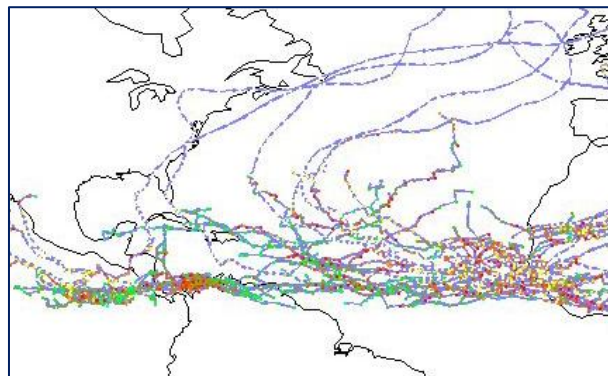


Fig 4.1.3: AEW tracks plotted for JJAS 2006 using vertical mean relative vorticity and a 5°-20°N, 90°-10°W regional filter

These tracks were then compared to the best track data to identify the developing AEWs, and then those that started over land (either West Africa or the northern part of South America) were removed to leave the non-developing AEWs which were first detected over the Atlantic. These are identified manually and studied in the coastal region analysis, but are left out of the automatically detected set as this set is used for downstream analysis, as will be explained in section 8. This whole process was then done for JJAS 2005 to 2009, with the only difference being that only the vertical mean relative vorticity was used.

5. Case Studies

AEWs over the African continent are characterised by low level baroclinic instability caused by surface heating, and mid-level barotropic instability developing from the AEJ. With this in mind, the progress of the AEW across the Atlantic are observed in three ways – the 925 hPa relative vorticity and sea surface temperature, the vertical mean relative vorticity and the 600 hPa geopotential height, and finally the 600 hPa relative vorticity and the 600 hPa wind speed. The thermal infrared (TIR) satellite image is also used to observe any organised convection. Two developing and two non-developing AEWs are used as case studies.

5.1. Hurricane Ernesto

For the developing AEWs, Hurricane Ernesto from the 2006 season was the first chosen as it displays the “typical” characteristics of a North Atlantic hurricane – it occurs in the second half of August, is formed by an AEW travelling virtually due west from the West African coast to the Caribbean, spins up over the Windward Islands and then recurves poleward across Cuba, Florida and the eastern seaboard of North America before becoming an extra-tropical depression moving north eastwards across the North Atlantic.

The AEW that developed into Hurricane Ernesto crossed the West African coast on 18th August 2006 (Knabb, et al., 2006) where it was detected by vorticity maximum tracking at 925 and 600 hPa (*Figure 5.1.1(a)*) before this went below the detection threshold just north of the Cape Verde islands. It was then picked up again approximately 8° to the east of the initial “best track” (*Figure 5.1.1(b)*) designation of being a tropical depression and from this point on it shows up well at the 925 hPa, 850 hPa and vertically averaged from 850 to 600 hPa levels. There is, however, a large and significant gap over the mid-Atlantic where the AEW is not tracked by any automatic method.

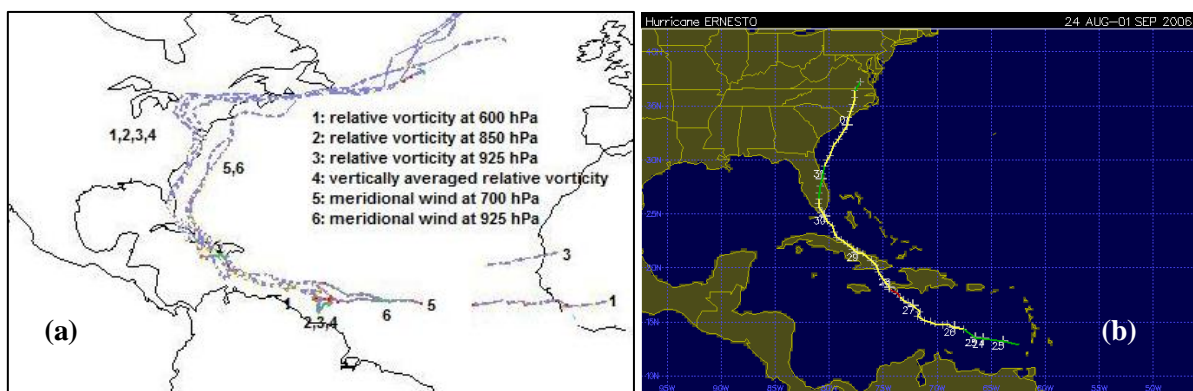


Fig 5.1.1: (a) automatic tracking results for Hurricane Ernesto compared to the (b) best track data (Tropical Prediction Center, 2010)

When the AEW is at the coast the northern 925 hPa vortex (*Figure 5.1.2 (a)*) is by far the strongest, the vertical mean relative vorticity maximum is positioned just downstream of the AEW trough axis (*Figure 5.1.2 (b)*) and the AEJ at the 600 hPa level has a maximum speed of 21 ms^{-1} and is adjacent to the north of the 600 hPa relative vorticity maximum (*Figure 5.1.2 (c)*).

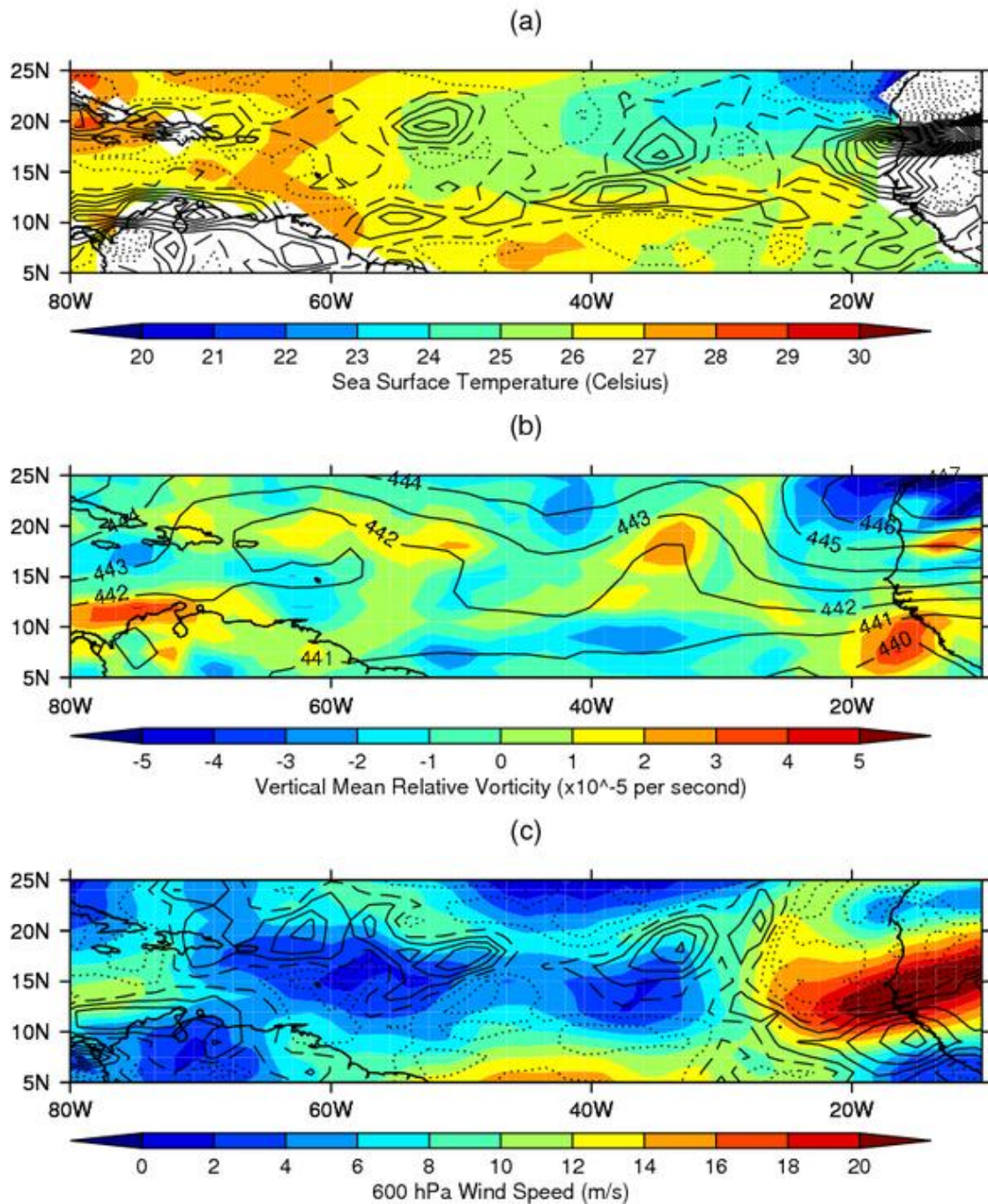


Fig 5.1.2: the precursor AEW for Hurricane Ernesto on 18th August 2006, 0600 UTC, showing
 (a) 925 hPa relative vorticity ($2 \times 10^{-5} \text{ s}^{-1}$ contour intervals) overlaid on to sea surface temperature ($^{\circ}\text{C}$)
 (b) 600 hPa geopotential height (dm) overlaid on to vertical mean relative vorticity ($\times 10^{-5} \text{ s}^{-1}$)
 (c) 600 hPa relative vorticity ($1 \times 10^{-5} \text{ s}^{-1}$ contour intervals) overlaid on to 600 hPa easterly wind speed (ms^{-1})

Three days later this AEW is in mid-Atlantic at 35°W, and the 925 hPa relative vorticity has decreased (*Figure 5.1.3(a)*), probably due to the drop in surface temperature to 25°C from the Sahara to the relatively cool waters of the eastern Atlantic. The vertical mean relative vorticity has increased, and the AEW trough, though weak, is still discernible in the 600 hPa geopotential height (*Figure 5.1.3(b)*), and the 600 hPa relative vorticity has increased, with the AEJ at 18 to 20 ms⁻¹ just to the north of it (*Figure 5.1.3(c)*).

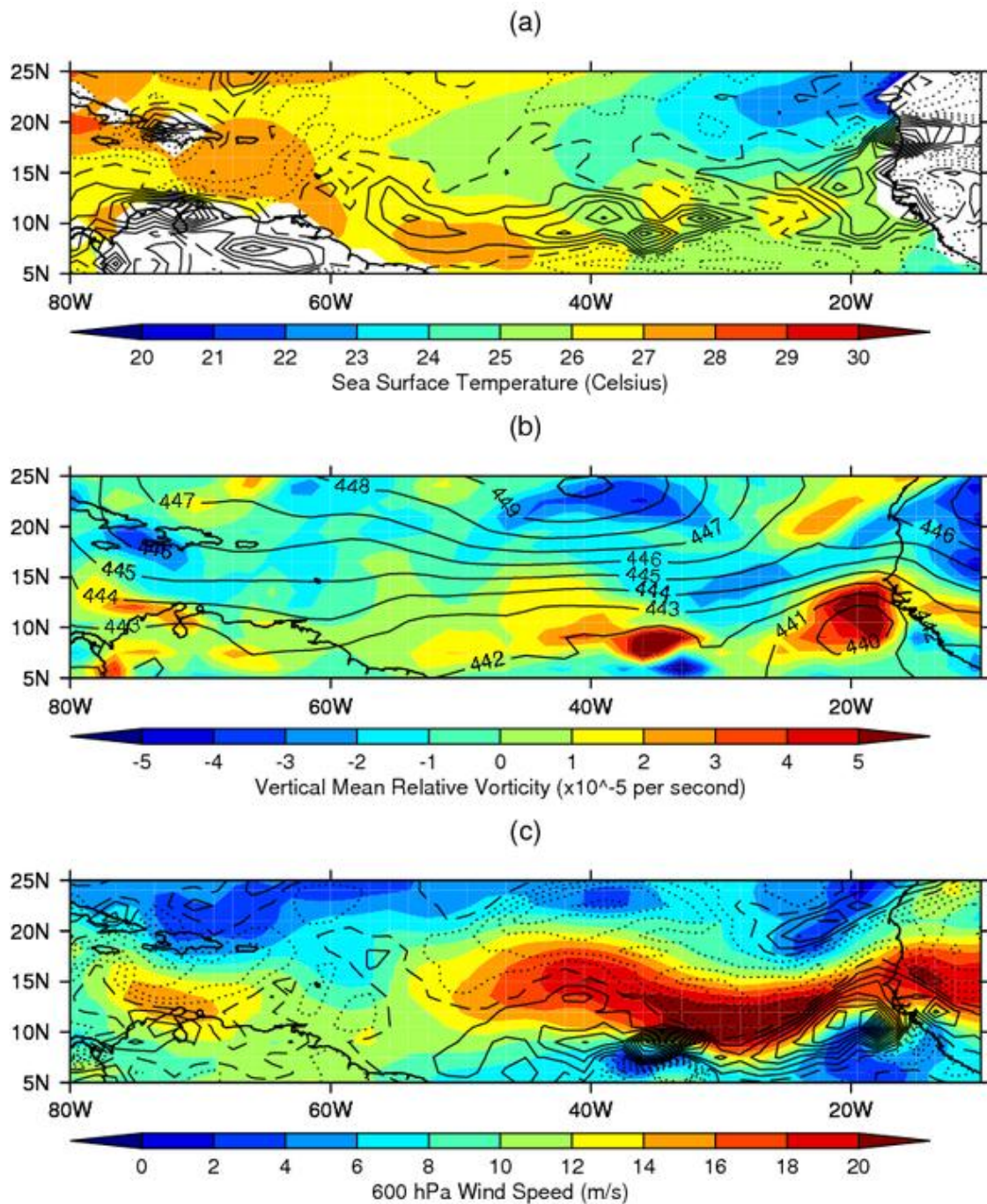


Fig 5.1.3: the precursor AEW for Hurricane Ernesto at 35°W on 21st August 2006, 0600 UTC, showing
 (a) 925 hPa relative vorticity ($2 \times 10^{-5} \text{ s}^{-1}$ contour intervals) overlaid on to sea surface temperature (°C)
 (b) 600 hPa geopotential height (dm) overlaid on to vertical mean relative vorticity ($\times 10^{-5} \text{ s}^{-1}$)
 (c) 600 hPa relative vorticity ($1 \times 10^{-5} \text{ s}^{-1}$ contour intervals) overlaid on to 600 hPa easterly wind speed (ms^{-1})

By the time the AEW reaches 55°W on 23rd August 2006 at 1800 UTC the 925 hPa relative vorticity is building up again (*Figure 5.1.4(a)*) which will be assisted by the system moving over warmer sea (the SST is now over 26°C, which is one of the criteria for tropical storm development (Gray, 1978)). The vertical mean relative vorticity is still in the AEW trough axis (*Figure 5.1.4(b)*) and the AEJ, though weaker, still has a maximum over 12ms⁻¹ just poleward of the 600 hPa relative vorticity maximum. This is 24 hours before it was declared a tropical depression (Knabb, et al., 2006).

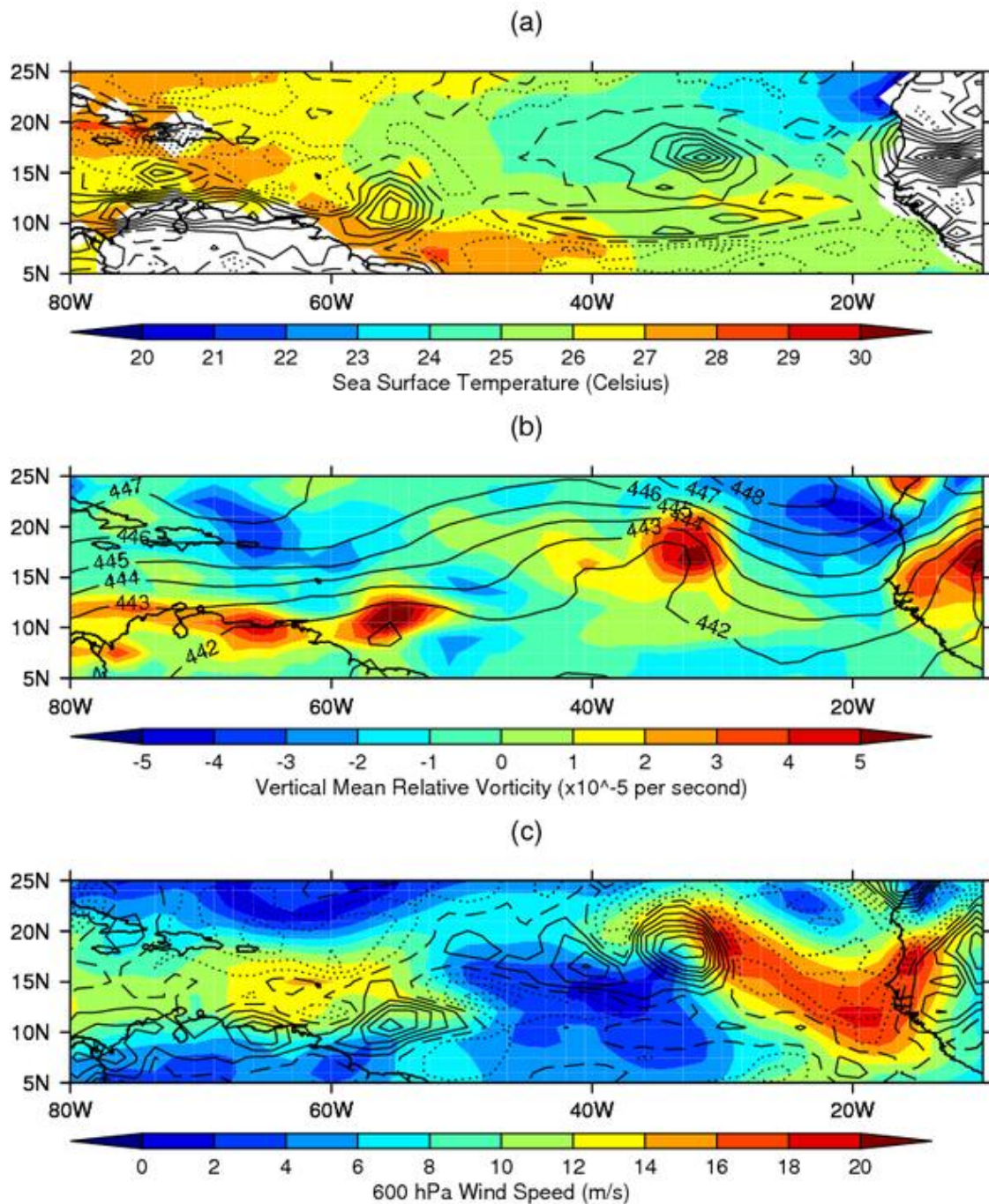


Fig 5.1.4: the precursor AEW for Hurricane Ernesto at 55°W on 23rd August 2006, 1800 UTC, showing
 (a) 925 hPa relative vorticity ($2 \times 10^{-5} \text{ s}^{-1}$ contour intervals) overlaid on to sea surface temperature ($^{\circ}\text{C}$)
 (b) 600 hPa geopotential height (dm) overlaid on to vertical mean relative vorticity ($\times 10^{-5} \text{ s}^{-1}$)
 (c) 600 hPa relative vorticity ($1 \times 10^{-5} \text{ s}^{-1}$ contour intervals) overlaid on to 600 hPa easterly wind speed (ms^{-1})

Convection is quite strong at the coast, with bright, cold cloud tops showing clearly at 9°N , 16°W on the TIR image (*Figure 5.1.5(a)*). This activity is still present in mid-Atlantic at 11°N , 35°W (*Figure 5.1.5(b)*) with a layer of lower cloud extending up to 500 km to the south and east from this, and by the time the system reaches the western Atlantic (*Figure 5.1.5(c)*) organised bands of high circulating cloud can be seen to the north and east of 11°N , 55°W . Broadly speaking, convection occurs throughout the passage of the AEW, becoming more organised as the system moves over the warmer waters to the west.

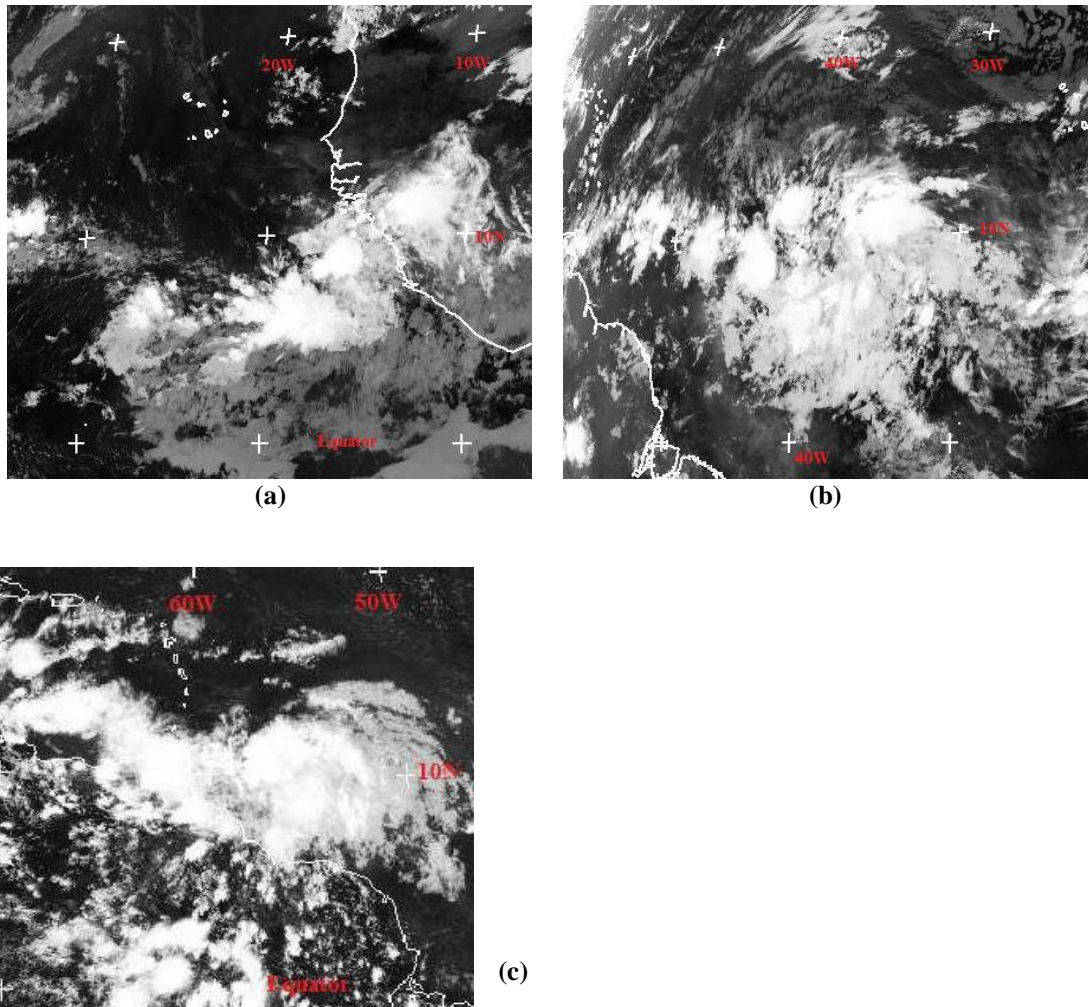


Fig 5.1.5: thermal infra-red images of the precursor AEW to Hurricane Ernesto at:

(a) 18th August 2006, 0600 UTC at 17°W

(b) 21st August 2006, 0600 UTC at 35°W

(c) 23rd August 2006, 1800 UTC at 55°W

(NERC Satellite Receiving Station, Dundee University, Scotland, 2010)

5.2. Tropical Storm Chris

Tropical Storm (TS) Chris was a relatively early season storm which, as with Hurricane Ernesto, was formed from an AEW that tracked across the Atlantic before becoming a depression approximately 370 km east of Antigua (Stewart, 2006). From this point it passed north of the Leeward Islands before dying out over Cuba.

The AEW that developed into TS Chris was detected over the West African coast by automatic tracking of the vertical mean relative vorticity on 26th July 2006, but over the next two days it weakened and was undetected over the central Atlantic until 43^oW where it was picked up on all the automatic relative vorticity tracking levels (*Figure 5.2.1(a)*). The system was declared a tropical depression (*Figure 5.2.1(b)*) at 60^oW on 1st August 2006, 0300 UTC (Stewart, 2006).

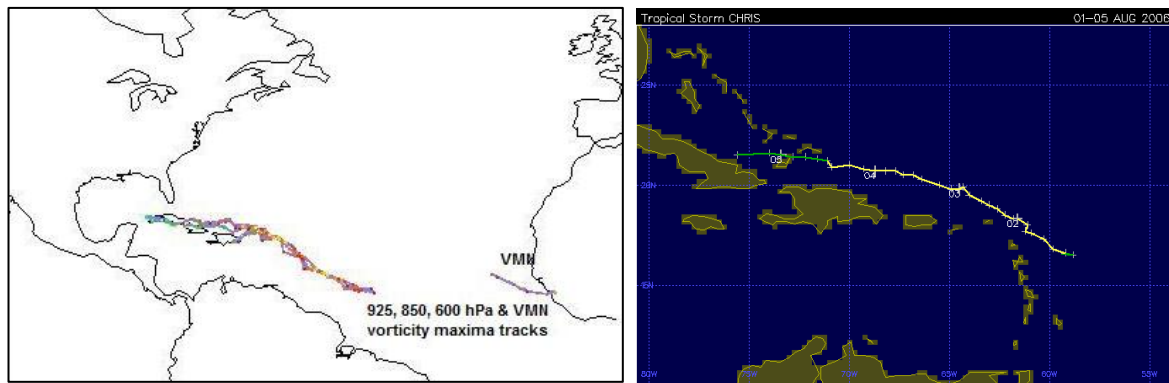


Fig 5.2.1: (a) automatic tracking results for TS Chris compared to the (b) best track data (Tropical Prediction Center, 2010)

When the AEW that develops into TS Chris crosses the West African coast the northern 925 hPa relative vorticity maximum is very well defined (*Figure 5.2.2 (a)*). There is a vertical mean relative vorticity maximum south of the AEJ (*Figure 5.2.2 (b)*) which sits in a not very well defined AEW trough axis. The 600 hPa relative vorticity maximum (*Figure 5.2.2 (c)*) is similarly not well defined, but is just to the south of an 18 ms⁻¹ section of the AEJ. Picking the coast crossing time for TS Chris was not as simple as for Hurricane Ernesto as the mid-troposphere relative vorticities were not well defined, and the chosen snapshot shows the 925 hPa maximum already over the Atlantic, with the southern 600 hPa maximum just crossing the coast.

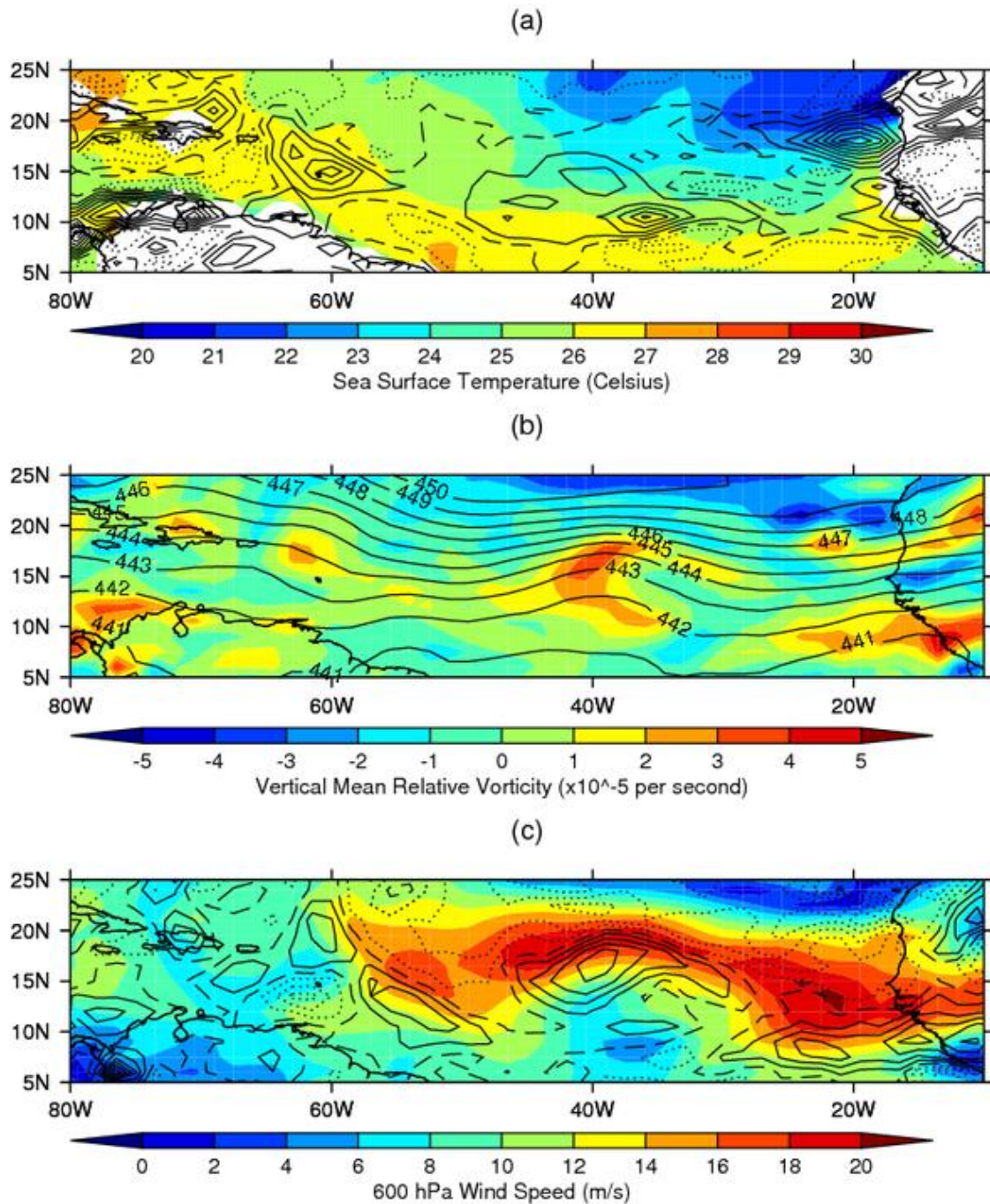


Fig 5.2.2: the precursor AEW for TS Chris on 26th July 2006, 1800 UTC, showing
 (a) 925 hPa relative vorticity ($2 \times 10^{-5} \text{s}^{-1}$ contour intervals) overlaid on to sea surface temperature ($^{\circ}\text{C}$)
 (b) 600 hPa geopotential height (dm) overlaid on to vertical mean relative vorticity ($\times 10^{-5} \text{s}^{-1}$)
 (c) 600 hPa relative vorticity ($1 \times 10^{-5} \text{s}^{-1}$ contour intervals) overlaid on to 600 hPa easterly wind speed (ms^{-1})

Over the Atlantic at 35°W the 925 hPa relative vorticity maximum has lost definition (*Figure 5.2.3(a)*) after having crossed over the tongue of cooler sea surface temperatures (21 to 25°C) in the Eastern Atlantic. The vertical mean relative vorticity maximum is also not well defined (*Figure 5.2.3(b)*), and the wave structure is spread zonally, looking at the geopotential heights. However, the meridional geopotential height gradient is greater at this longitude than east or west of it, and this

is reflected in the AEJ which still has a speed of over 18 ms⁻¹ at 600 hPa (*Figure 5.2.3(c)*). This drives the 600 hPa relative vorticity maximum, which has only decreased from $4 \times 10^{-5} \text{ s}^{-1}$ at the coast (*Figure 5.2.2(c)*) to $3 \times 10^{-5} \text{ s}^{-1}$.

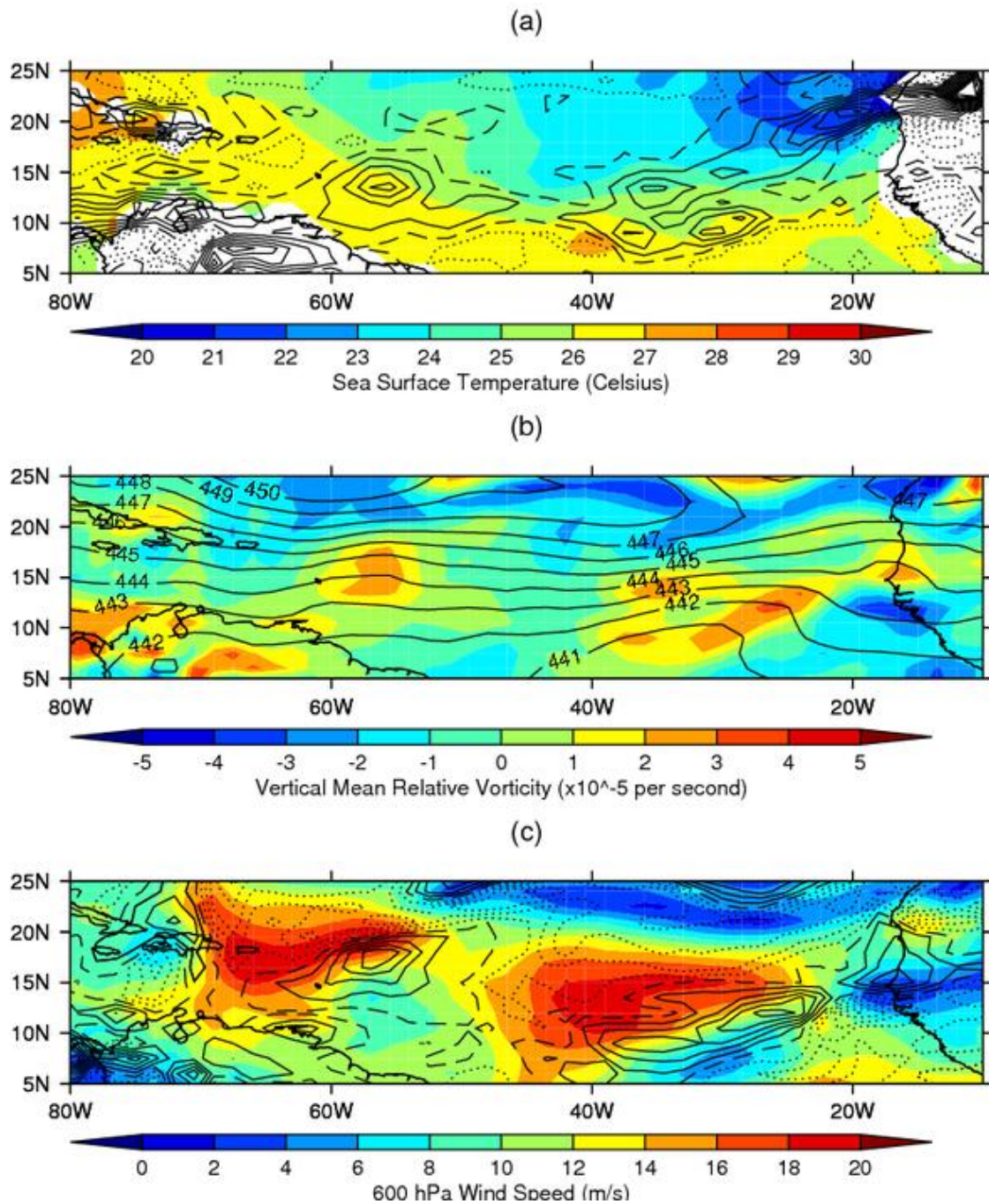


Fig 5.2.3: the precursor AEW for TS Chris at 35°W on 28th July 2006, 0600 UTC, showing:
 (a) 925 hPa relative vorticity ($2 \times 10^{-5} \text{ s}^{-1}$ contour intervals) overlaid on to sea surface temperature ($^{\circ}\text{C}$)
 (b) 600 hPa geopotential height (dm) overlaid on to vertical mean relative vorticity ($\times 10^{-5} \text{ s}^{-1}$)
 (c) 600 hPa relative vorticity ($1 \times 10^{-5} \text{ s}^{-1}$ contour intervals) overlaid on to 600 hPa easterly wind speed (ms^{-1})

At 52°W on 30th July 2006 over 24 hours before declaration as a depression (Stewart, 2006) the lower 925 hPa relative vorticity is well-defined (*Figure 5.2.4(a)*) and the system has moved into increasing sea surface temperatures (> 26°C). The AEW wave structure is also well-defined with the vertical mean relative vorticity maximum collocated with the wave trough (*Figure 5.2.4 (b)*). The AEJ has weakened to less than 12 ms⁻¹ (*Figure 5.2.4(c)*) but there is still a broadly east to west flowing band directly north of the 600 hPa relative vorticity maximum.

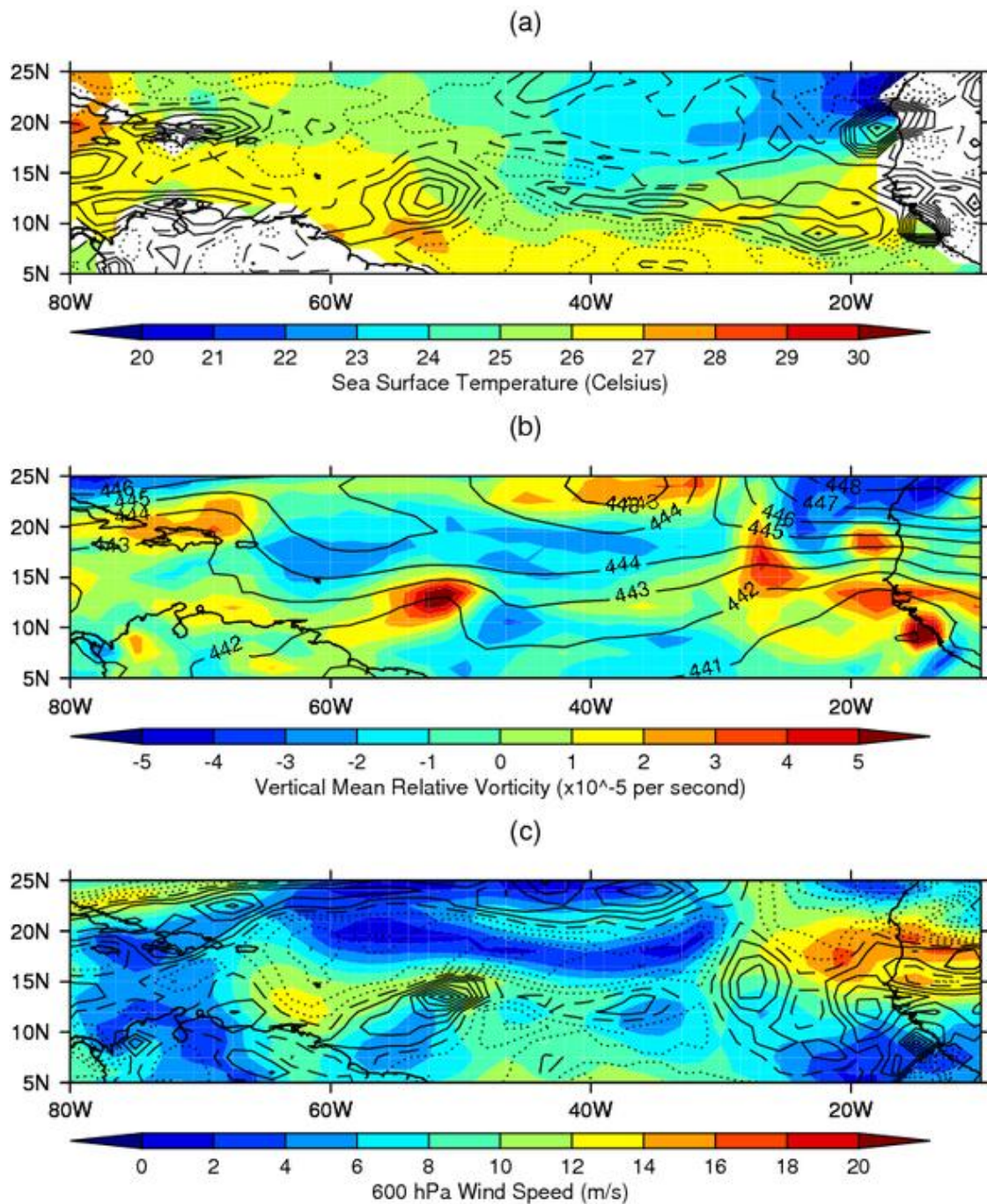
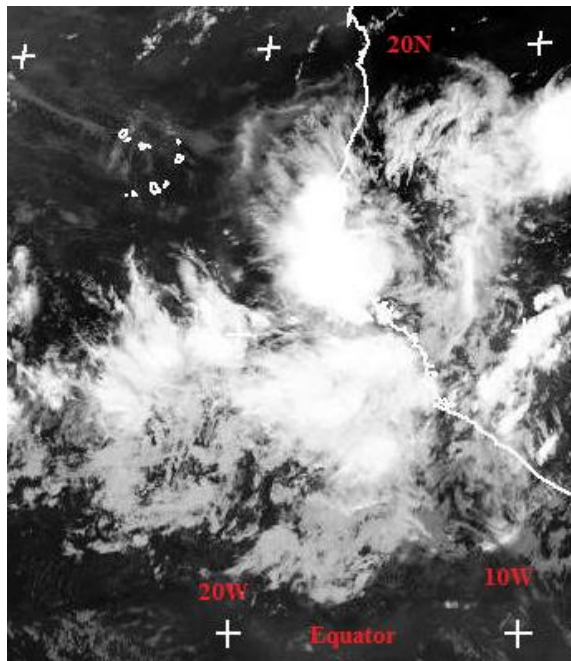
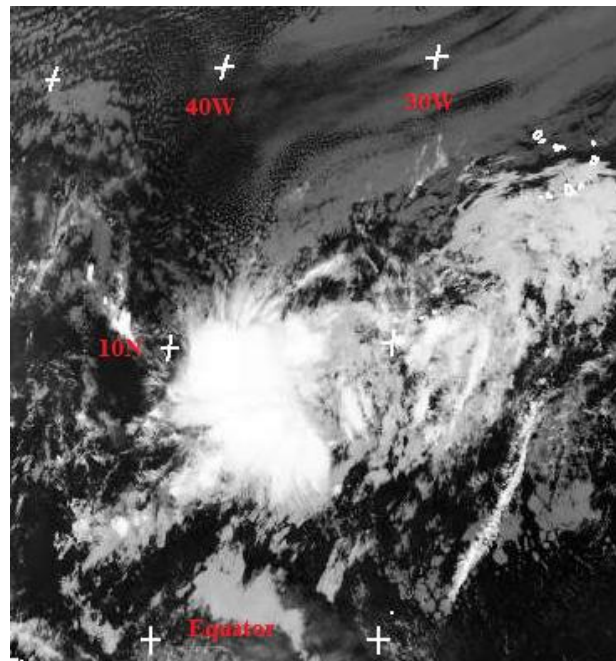


Fig 5.2.4: the precursor AEW for TS Chris at 52° W on 30th July 2006, 1800 UTC, showing
 (a) 925 hPa relative vorticity ($2 \times 10^{-5} \text{ s}^{-1}$ contour intervals) overlaid on to sea surface temperature ($^{\circ}\text{C}$)
 (b) 600 hPa geopotential height (dm) overlaid on to vertical mean relative vorticity ($\times 10^{-5} \text{ s}^{-1}$)
 (c) 600 hPa relative vorticity ($1 \times 10^{-5} \text{ s}^{-1}$ contour intervals) overlaid on to 600 hPa easterly wind speed (ms^{-1})

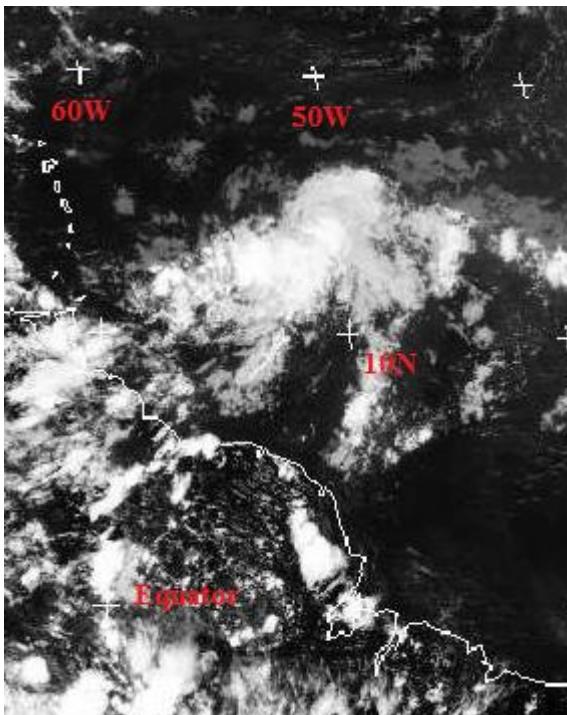
When the AEW is over the African coast (*Figure 5.2.5(a)*) deep convection is visible at 17°W by the cold cloud top temperatures visible in the TIR image. By 10°N, 37°W this has become more organised (*Figure 5.2.5(b)*), with a layer of lower cloud to the south and east of main convection. This lower layer is more visible at 13°N, 52°W but the area of convective cloud is less here (*Figure 5.2.5(c)*), just before the AEW evolves into a depression.



(a)



(b)



(c)

Fig 5.2.5: thermal infra-red images of the precursor

AEW to TS Chris at:

(a) 26th July 2006, 1800 UTC at 16°W

(b) 28th July 2006, 0600 UTC at 37°W

(c) 30th July 2006, 1800 UTC at 52°W

(NERC Satellite Receiving Station, Dundee University, Scotland, 2010)

5.3. AEW 171

AEW 171 (the label given it by the automatic tracking routine) is tracked using vertical mean relative vorticity tracking, and is first picked up just off the West African coast, finally being lost at 48°W (*Figure 5.3.1*). This is a very similar path to that taken by the AEWs that became Hurricane Ernesto and Tropical Storm Chris, and is an early season AEW, being tracked from the 21st to the 27th of June 2006.

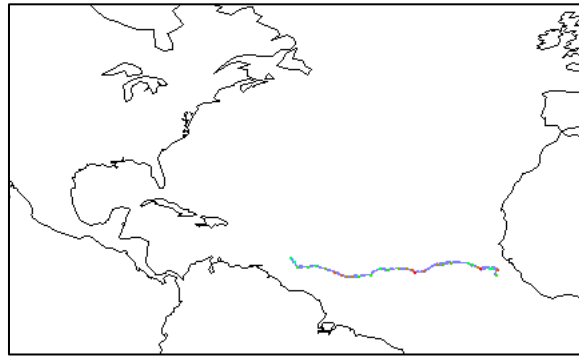


Fig 5.3.1: the vertical mean relative vorticity maximum track for AEW 171 (21st to 27th June 2006)

As AEW 171 leaves the coast, there is a 925 hPa relative vorticity maximum at 20°N (*Figure 5.3.2(a)*) which is starting to travel over a relatively cold sea surface (20°C). The shape of the AEW trough as given by the geopotential height contours (*Figure 5.3.2(b)*) is not well-defined and the vertically averaged relative vorticity maximum is co-located with it. At the 600 hPa level the AEJ is not strong (10 to 12 ms^{-1}) and is just to the north of the 600 hPa relative vorticity maximum (*Figure 5.3.2(c)*).

After 48 hours AEW 171 has moved to 31°W , and the lower 925 hPa relative vorticity maximum has increased with the increase in sea surface temperature to 25°C (*Figure 5.3.3(a)*). The synoptic shape of the AEW is visible in the 600 hPa geopotential height contours, and the vertical mean relative vorticity maximum is co-located with this trough (*Figure 5.3.3(b)*). The 600 hPa relative vorticity maximum is still present, but has become disconnected from the main stream of the AEJ (*Figure 5.3.3(c)*).

Another 72 hours downstream sees AEW 171 virtually dissipated at 48°W , with the 925 hPa relative vorticity maximum still quite pronounced (*Figure 5.3.4(a)*), and the vertical mean relative vorticity no longer co-located with the wave trough (*Figure 5.3.4(b)*). The 600 hPa relative vorticity maximum barely exists at $1 \times 10^{-5}\text{ s}^{-1}$ (*Figure 5.3.4(a)*) and has no west-going 600 hPa AEJ to its north.

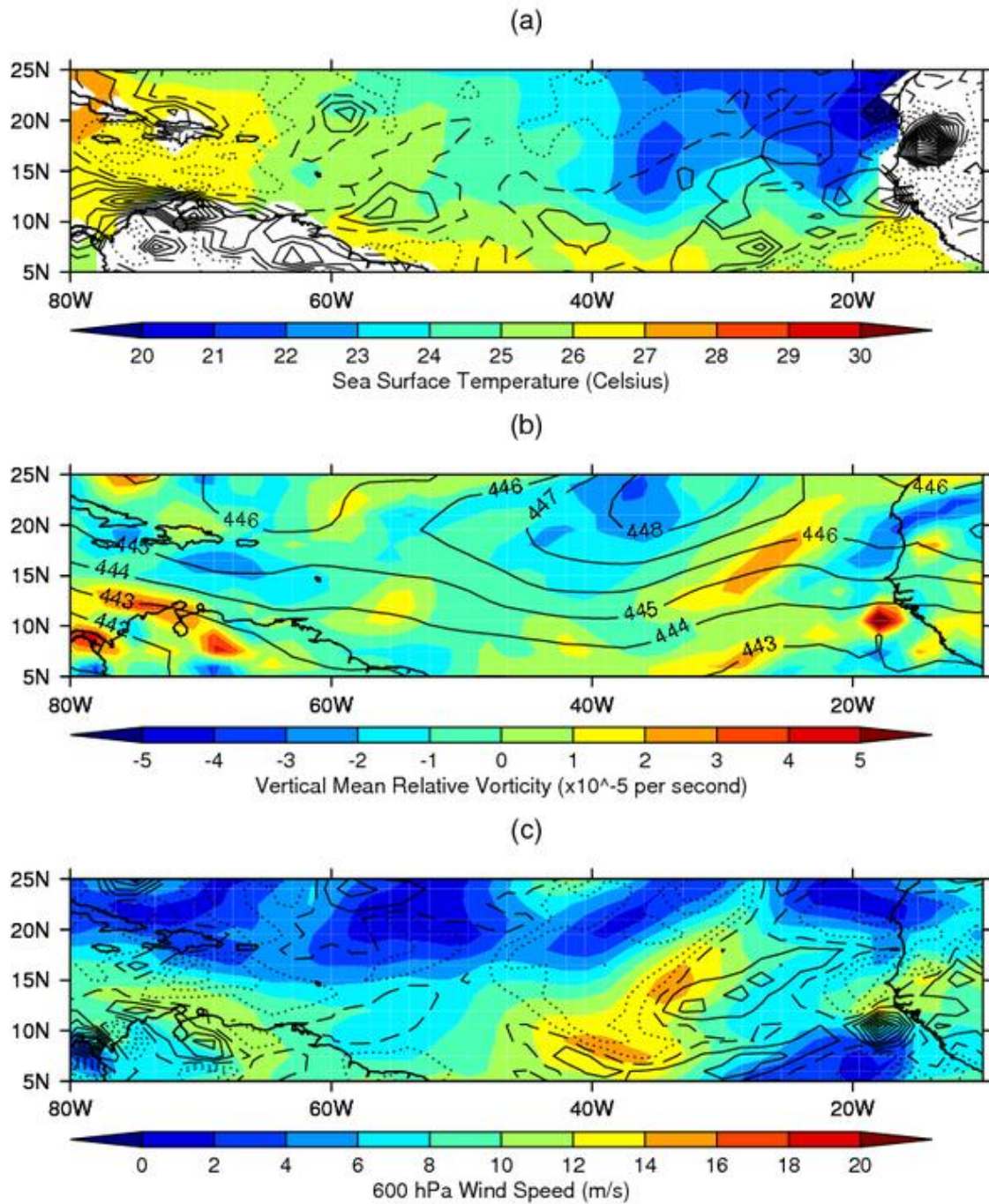
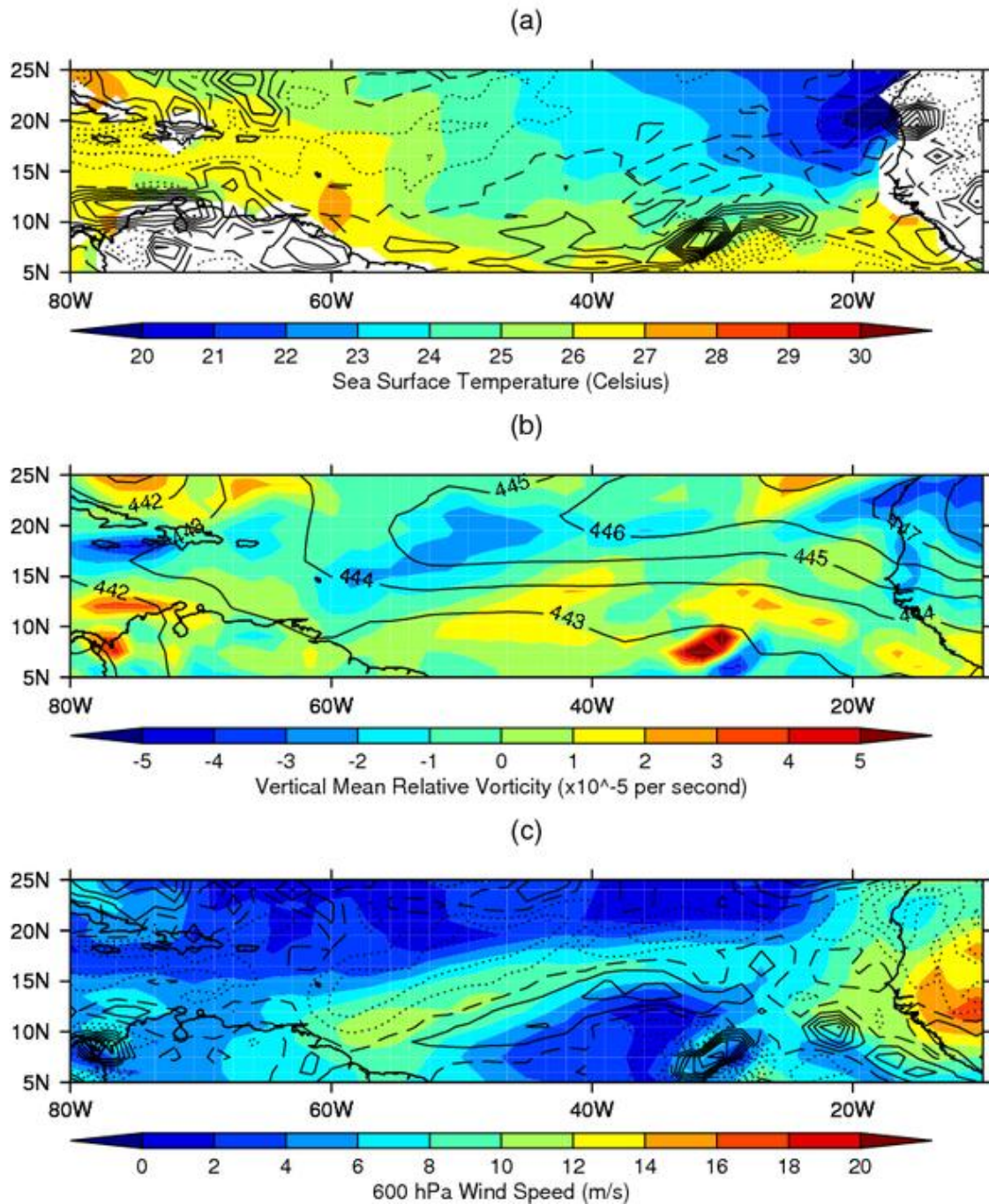


Fig 5.3.2: AEW 171 at 17°W on 22nd June 2006, 0000 UTC, showing
 (a) 925 hPa relative vorticity ($2 \times 10^{-5} \text{ s}^{-1}$ contour intervals) overlaid on to sea surface temperature ($^{\circ}\text{C}$)
 (b) 600 hPa geopotential height (dm) overlaid on to vertical mean relative vorticity ($\times 10^{-5} \text{ s}^{-1}$)
 (c) 600 hPa relative vorticity ($1 \times 10^{-5} \text{ s}^{-1}$ contour intervals) overlaid on to 600 hPa easterly wind speed (ms^{-1})



5.3.3: AEW 171 at 31°W on 24th June 2006, 0000 UTC, showing
 (a) 925 hPa relative vorticity ($2 \times 10^{-5} \text{s}^{-1}$ contour intervals) overlaid on to sea surface temperature ($^{\circ}\text{C}$)
 (b) 600 hPa geopotential height (dm) overlaid on to vertical mean relative vorticity ($\times 10^{-5} \text{s}^{-1}$)
 (c) 600 hPa relative vorticity ($1 \times 10^{-5} \text{s}^{-1}$ contour intervals) overlaid on to 600 hPa easterly wind speed (ms^{-1})

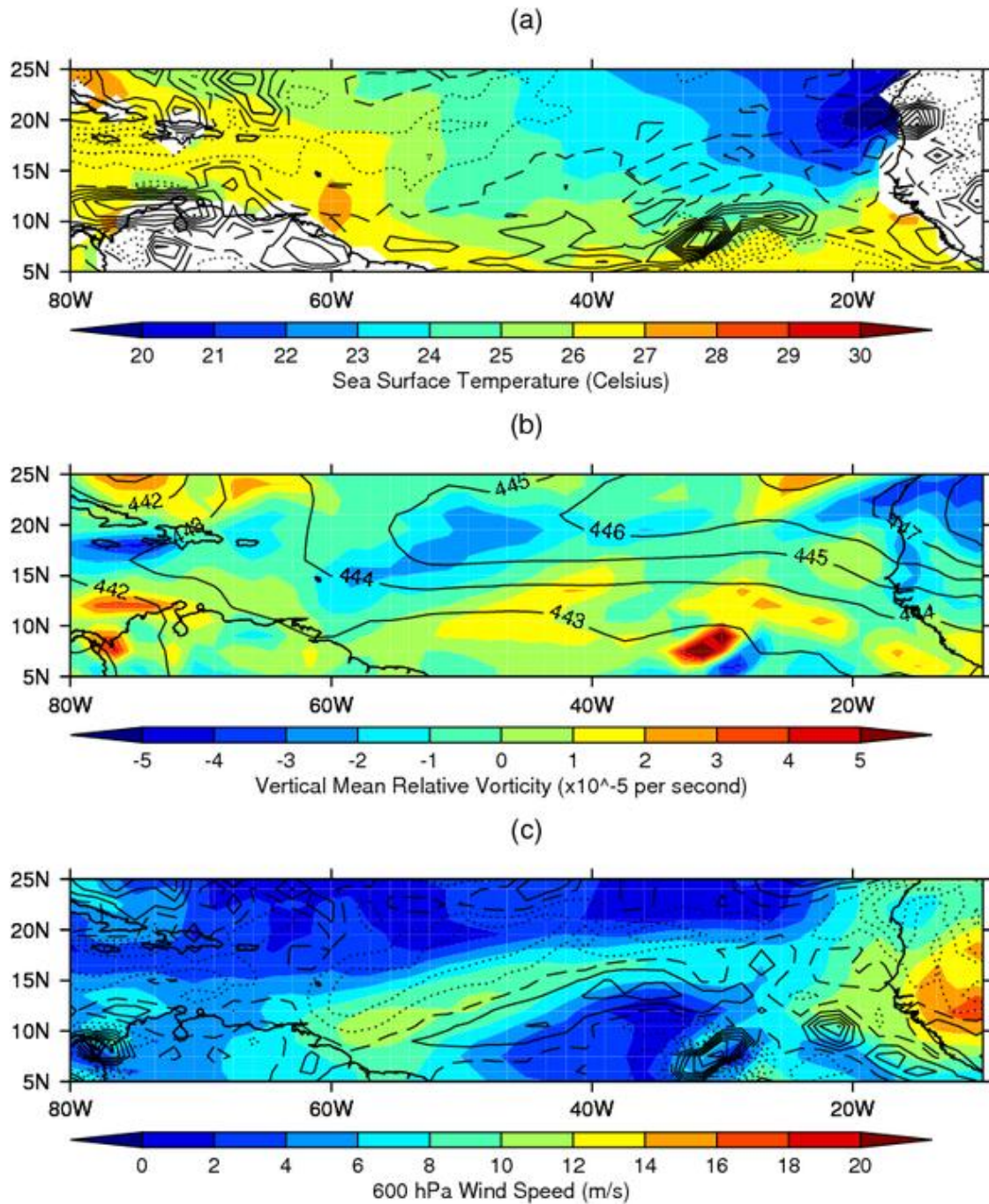


Fig 5.3.4: AEW 171 at 48°W on 27th June 2006, 0000 UTC, showing
 (a) 925 hPa relative vorticity ($2 \times 10^{-5} \text{s}^{-1}$ contour intervals) overlaid on to sea surface temperature ($^{\circ}\text{C}$)
 (b) 600 hPa geopotential height (dm) overlaid on to vertical mean relative vorticity ($\times 10^{-5} \text{s}^{-1}$)
 (c) 600 hPa relative vorticity ($1 \times 10^{-5} \text{s}^{-1}$ contour intervals) overlaid on to 600 hPa easterly wind speed (ms^{-1})

There is convection when AEW 171 leaves the West African coast (*Figure 5.3.5 (a)*), however this does not appear to be as deep as for the AEWs that evolved into Hurricane Ernesto and TS Chris (*Figures 5.1.5(a) and 5.2.5(a)*). 48 hours later at 31°W on 24th June 2006, 0000 UTC (*Figure 5.3.5 (b)*) the convection is disorganised, with individual sub-mesoscale features visible as high, cold cloud tops but no large convective feature present. This is seen again at 48°W (*Figure 5.3.5(c)*) where there is one large convective system about 1 degree across at 11°N 47°W , but no coincident bands of lower clouds becoming organised around it.

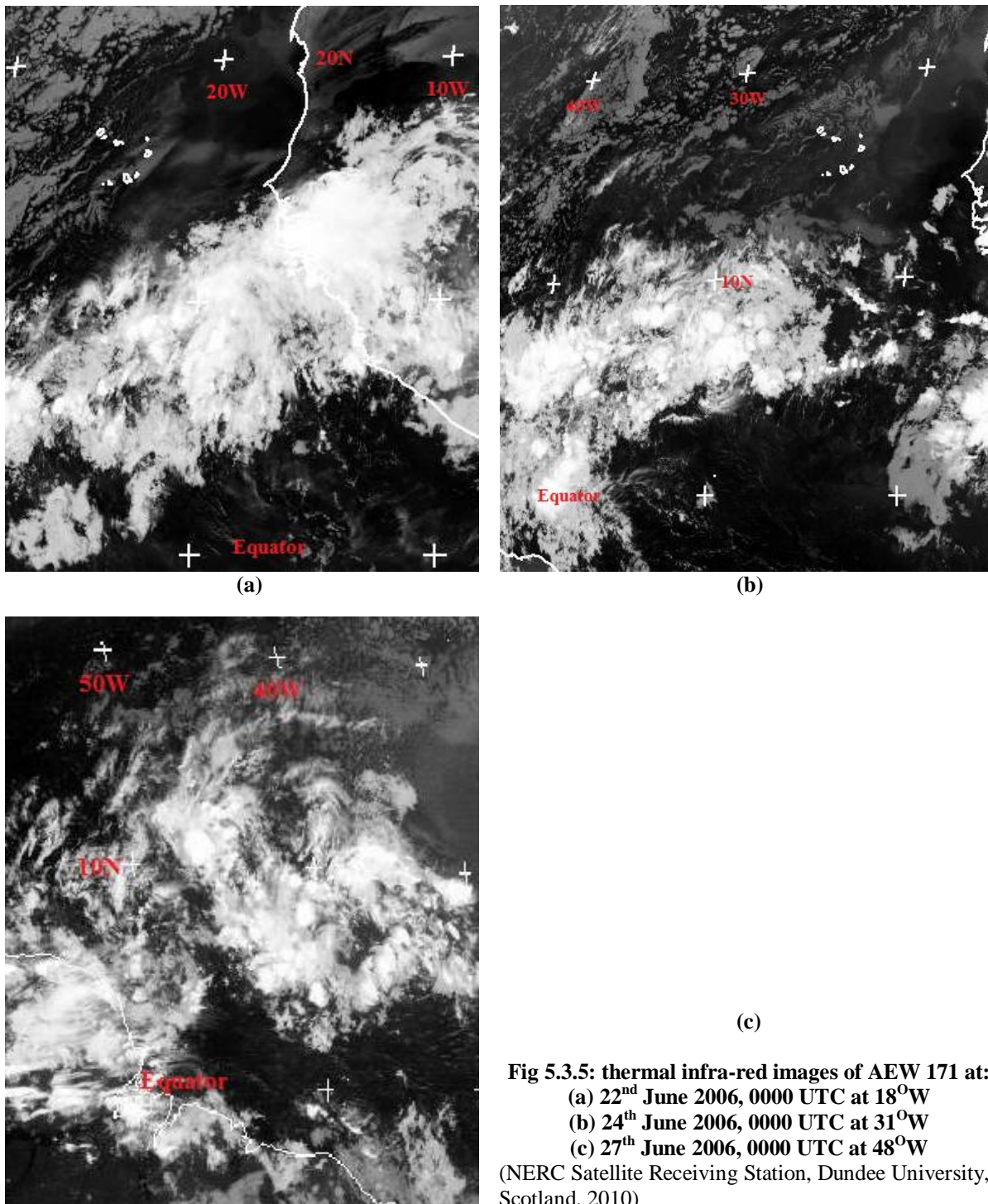


Fig 5.3.5: thermal infra-red images of AEW 171 at:
(a) 22nd June 2006, 0000 UTC at 18°W
(b) 24th June 2006, 0000 UTC at 31°W
(c) 27th June 2006, 0000 UTC at 48°W
 (NERC Satellite Receiving Station, Dundee University, Scotland, 2010)

5.4. AEW 516

AEW 516 was detected just off the West African by the vertical mean relative vorticity maxima automatic tracking (*Figure 5.4.1*) and was tracked until 57°W. As with AEW 171, this is a very similar path to the developing AEWs studied, with the difference being that it is later in the season.

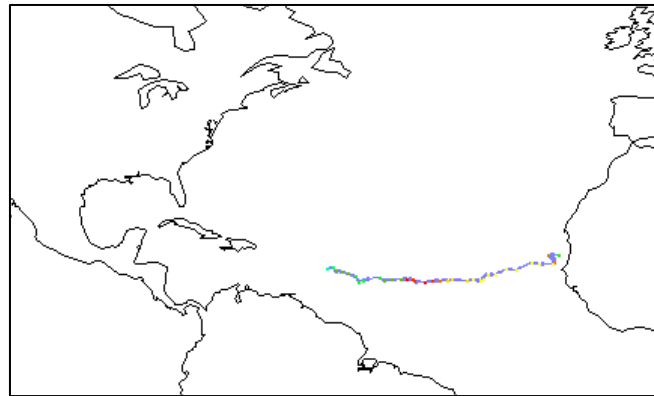


Fig 5.4.1: the vertical mean relative vorticity maximum track for AEW 516 (5th to 11th August 2006)

On 6th August 2006 at 1800 UTC, just after AEW 516 has crossed the West African coast the wave structure is visible at 19° to 20°W. The 925 hPa relative vorticity maximum is (*Figure 5.4.2(a)*) is present at 20°N, with another at 12°N, and the vertical mean relative vorticity maximum is co-located with the wave trough at 12°N. The AEJ is strong with a maximum of 20 ms⁻¹, and the 600 hPa relative vorticity vortex is not very well defined to the south of that.

48 hours down track on 8th August 2006 at 1800 UTC AEW 516's structure is still present at 31°W, with the 925 hPa relative vorticity maximum not as strong after passing over the relatively cool sea surface of the eastern Atlantic (*Figure 5.4.3(a)*). The vertical mean relative vorticity maximum is well defined with a peak of $4 \times 10^{-5} \text{ s}^{-1}$, and this peak is almost co-located with the trough of the AEW as shown by the 600 hPa geopotential height contours (*Figure 5.4.3(b)*). The 600 hPa relative vorticity maximum is well-defined at $5 \times 10^{-5} \text{ s}^{-1}$, but the AEJ, while still adjacent to this maximum, is beginning to weaken, down to less than 12 ms⁻¹ at 31°W.

A further 48 hours later, on 10th August 2006 at 1800 UTC at 42°W, AEW 516 starts to lose definition. The 925 hPa relative vorticity maximum spreads zonally (*Figure 5.4.3(a)*), and the vertical mean relative vorticity maximum, while still co-located with the AEW trough, has also spread zonally (*Figure 5.4.3(b)*). The AEJ has become much weaker, with speed less than 8 ms⁻¹ north of the weaker 600 hPa relative vorticity maximum (*Figure 5.4.3(c)*), and has also become less directionally stable, with weak meanders developing in the east to west flow. After this point AEW 516 steadily dissipates, losing all vertical structure.

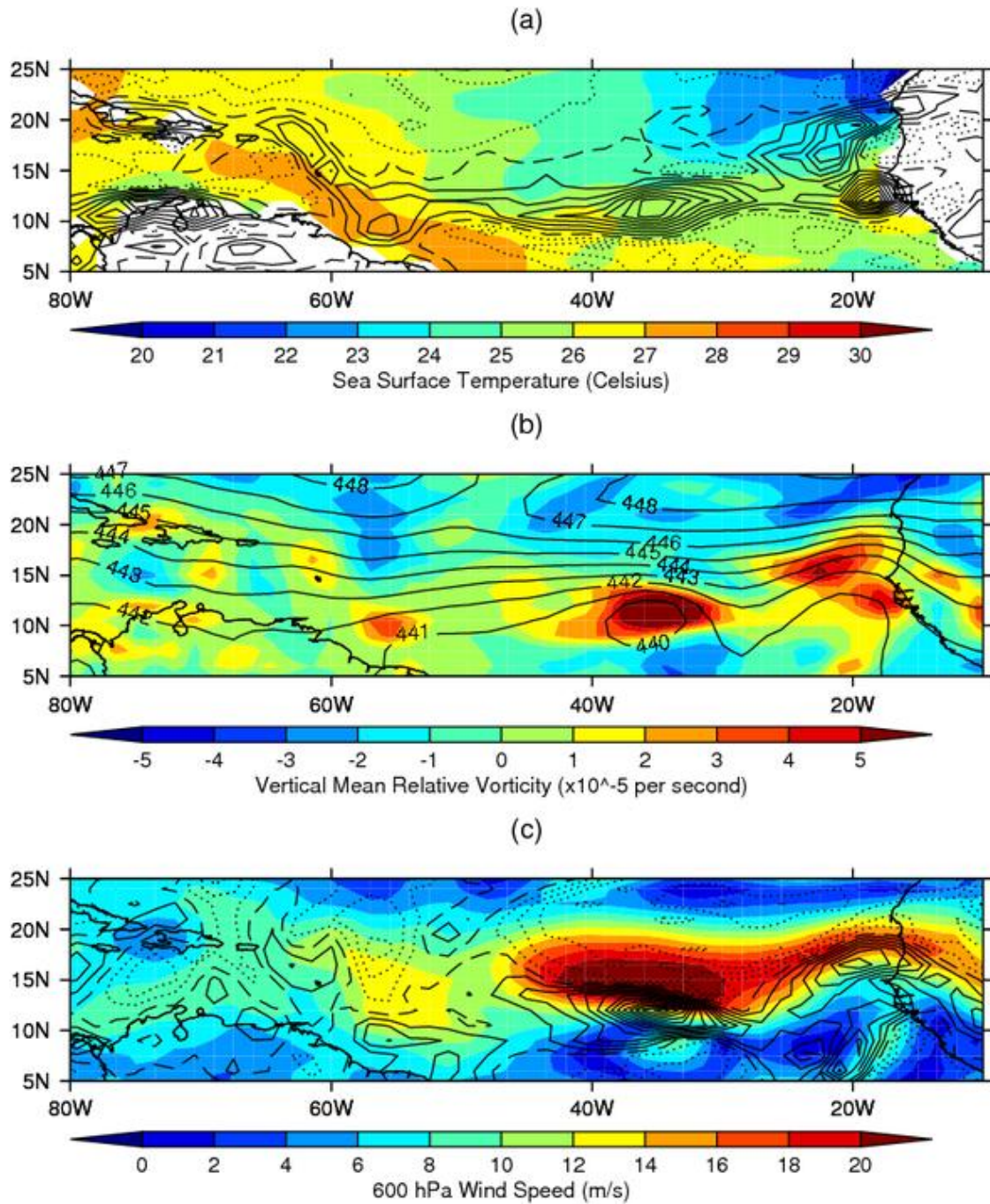


Fig 5.4.2: AEW 516 at 19°W on 6th August 2006, 1800 UTC, showing
 (a) 925 hPa relative vorticity ($2 \times 10^{-5} \text{ s}^{-1}$ contour intervals) overlaid on to sea surface temperature ($^{\circ}\text{C}$)
 (b) 600 hPa geopotential height (dm) overlaid on to vertical mean relative vorticity ($\times 10^{-5} \text{ s}^{-1}$)
 (c) 600 hPa relative vorticity ($1 \times 10^{-5} \text{ s}^{-1}$ contour intervals) overlaid on to 600 hPa easterly wind speed (ms^{-1})

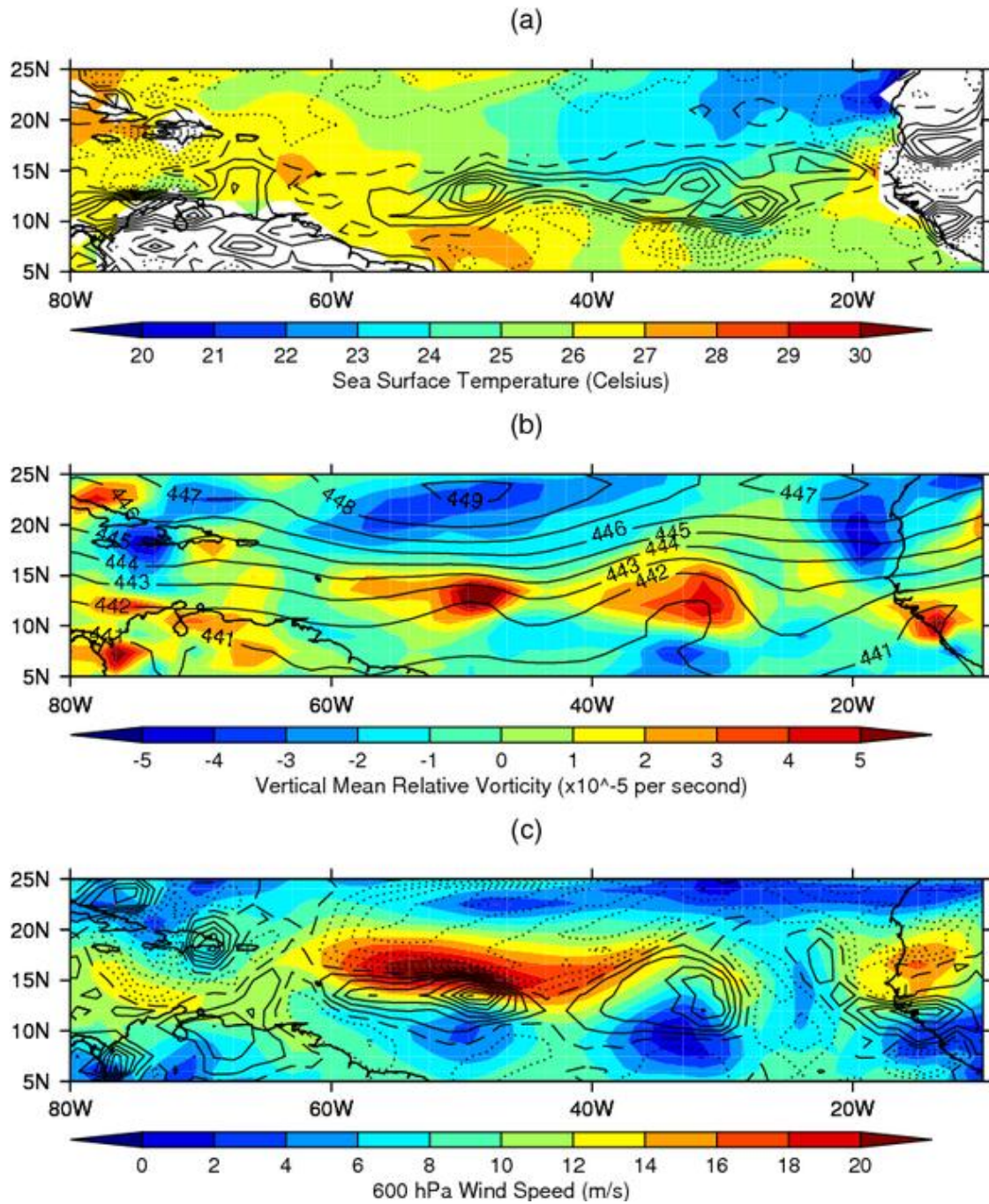


Fig 5.4.3: AEW 516 at 31°W on 8th August 2006, 1800 UTC, showing:
 (a) 925 hPa relative vorticity ($2 \times 10^{-5} \text{ s}^{-1}$ contour intervals) overlaid on to sea surface temperature ($^{\circ}\text{C}$)
 (b) 600 hPa geopotential height (dm) overlaid on to vertical mean relative vorticity ($\times 10^{-5} \text{ s}^{-1}$)
 (c) 600 hPa relative vorticity ($1 \times 10^{-5} \text{ s}^{-1}$ contour intervals) overlaid on to 600 hPa easterly wind speed (ms^{-1})

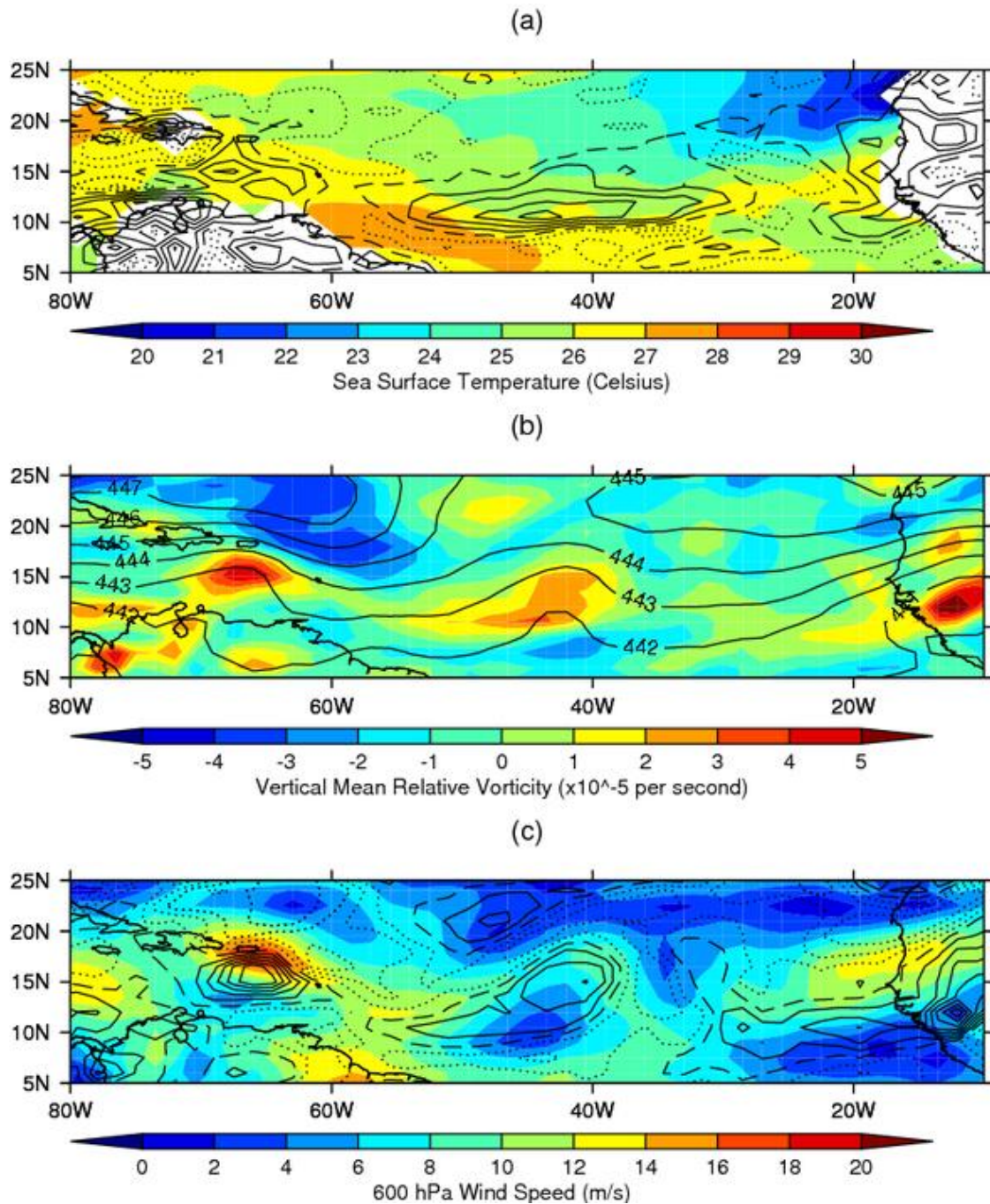
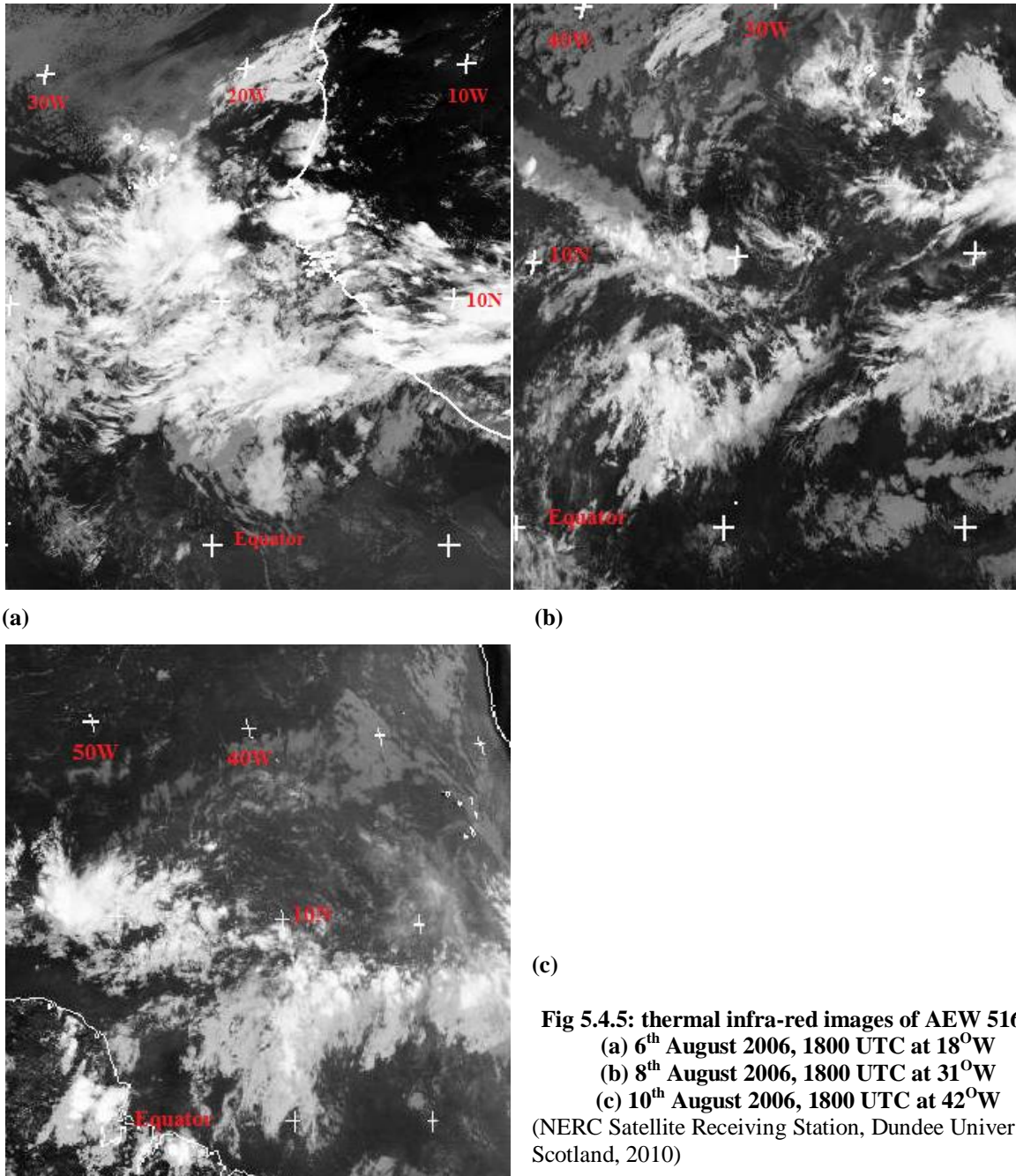


Fig 5.4.4: AEW 516 at 42°W on 10th August 2006, 1800 UTC, showing:
 (a) 925 hPa relative vorticity ($2 \times 10^{-5} \text{ s}^{-1}$ contour intervals) overlaid on to sea surface temperature ($^{\circ}\text{C}$)
 (b) 600 hPa geopotential height (dm) overlaid on to vertical mean relative vorticity ($\times 10^{-5} \text{ s}^{-1}$)
 (c) 600 hPa relative vorticity ($1 \times 10^{-5} \text{ s}^{-1}$ contour intervals) overlaid on to 600 hPa easterly wind speed (ms^{-1})

As AEW 516 leaves the West African coast (*Figure 5.4.5(a)*) there is much convection present, some of it deep looking at the cloud top colour. However, 48 hours later at 13°N, 31°W there is no organised convection with only scattered small pockets of deep convection (*Figure 5.4.5(b)*), and the same is true 48 hours after that at 13°N, 42°W (*Figure 5.4.5(c)*), with no organised convection showing.



6. Manual Tracking and Identification of African Easterly Waves at the West African Coast

The West African coast provides a consistent geographical marker for the development of AEWs as they pass from the African continent to the Atlantic. The meridional spread of the AEW tracks is small enough such that composites of the individual AEW data fields do not show significant blurring or smoothing of the data, and can be used for analysis (Hopsch, et al., 2010). The period for analysis was JJAS for 2005 to 2009.

The AEWs were identified manually using the ERA-Interim 1.5^o resolution data set (ECMWF, 2010) downloaded in GRIB format and viewed using Panoply software (version 2.9.4). The relative vorticity at 600 hPa was observed, and each AEW was identified as it crossed the West African coast at 17^oW (*Figure 6.1*). The AEW was then tracked with time across the Atlantic, and the developing ones were backtracked from the known tropical storms back to the coast to check. For some AEWs the 925 hPa relative vorticity maxima were also used to aid identification.

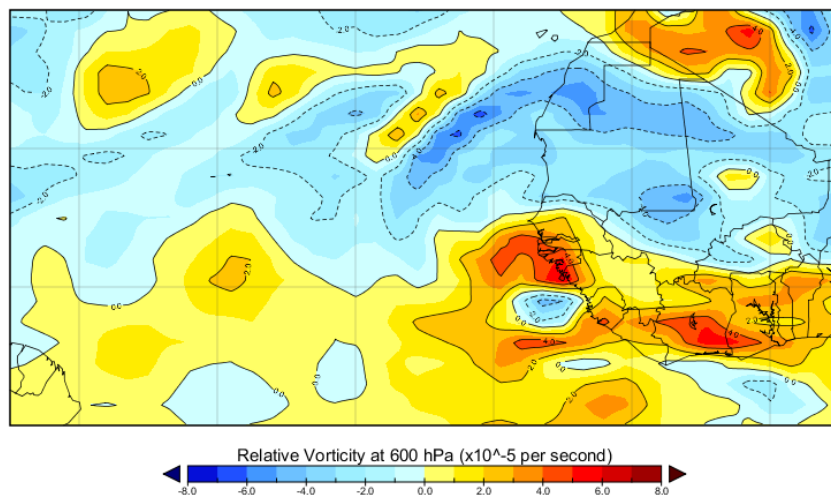


Fig 6.1: strong AEW shown crossing the West African coast at 17^oW at 0600 UTC, 1st July 2009. The RV maximum is clearly shown at 12^o N on the coast

This manual AEW identification process gave 42 developing and 170 non-developing AEWs (*table 6.1*), and this set was used for AEW analysis in the coastal region.

	Developing AEWs	Non-Developing AEWs
2005	12	28
2006	8	28
2007	7	38
2008	8	37
2009	7	39

Table 6.1: developing and non-developing AEWs identified manually from JJAS 2005 to 2009

There are approximately four times as many non-developing as there are developing AEWs, which raises concerns that the compositing process may smooth the non-developing AEW fields more than the developing ones, and so skew the data. To investigate this the non-developing AEWs were split into 4 pseudorandom groups, in the sense that each group had a similar number of AEWs from each month so as to ensure a good spread of the climatological conditions. A vertical section of the zonally averaged u-component of the wind for the coastal region was plotted for each of these groups and the overall non-developing AEW composite (*Figure 6.2*). The bars shown are the root mean square difference between the overall composite and each pseudorandom group, and it can be seen that the individual groups closely follow the overall mean, indicating that this approach does not skew the data in favour of developing AEWs due to the differential in group size between the developing and non-developing AEWs.

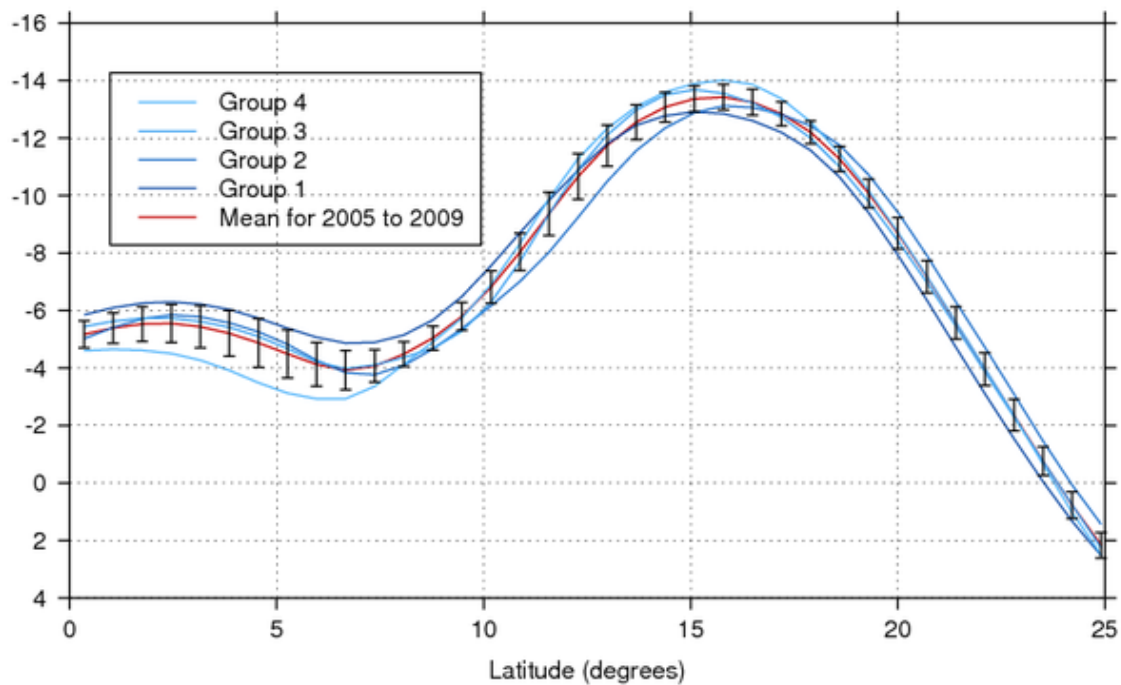


Fig 6.2: zonal wind at 600 hPa (ms^{-1}) plotted for the overall non-developing AEW composite (red) and the four pseudorandom individual groups. The bars are the root mean square difference between the overall composite and the individual groups.

7. The Compositing of Coastal Region Data for Developing and Non-Developing AEWs

The coastal region from the Equator to 25°N and from 20° to 14°W (*Figure 7.1*) was used as a geographical filter, with each AEW's characteristics taken in a three dimensional snapshot from 950 to 200 hPa at the coast crossing time. This crossing time is at 6 hour resolution, i.e. at 00, 06, 12 or 18 UTC on a particular day, and this is why the 6° longitudinal width of the geographic area was chosen as a particular AEW is unlikely to be at exactly 17°W at one of those 4 times. Unless stated otherwise, all the vertical sections for this region are zonally averaged from 20° to 14°W. These individual AEW representations were then made into two overall composites, one for developing and one for non-developing AEWs. These composites were then analysed for zonal, meridional and vertical wind, relative humidity and equivalent potential temperature. To observe the overall synoptic and regional conditions an area (not shown) bounded by the Equator and 40°N and 60°W to 20°E was used.

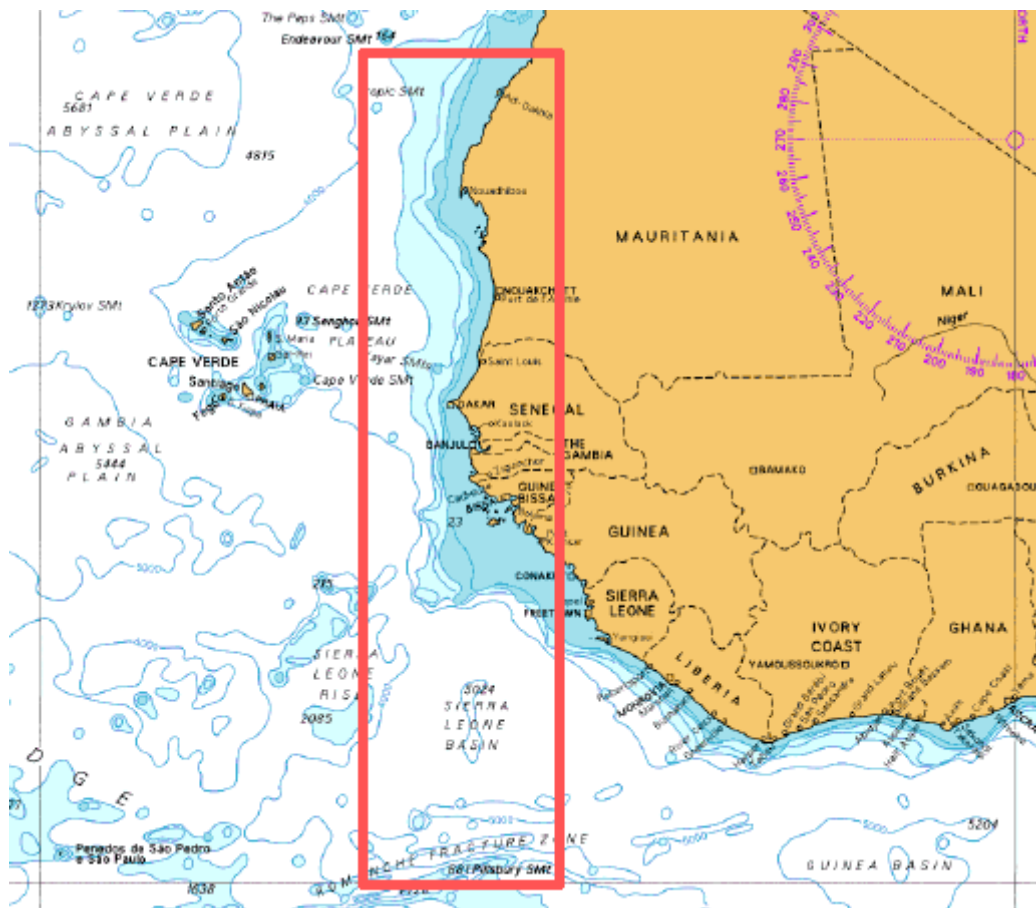


Fig 7.1: coastal region used for AEW analysis (UK Hydrographic Office, 1998)

7.1. Zonal Wind

The AEJ is the single most obvious feature of zonal wind in this region, and this is clearly shown in both the developing AEW composite (*Figure 7.1.1 (a)*) and the non-developing one (*Figure 7.1.1(b)*). The overall structure is very similar for both composites, and at first glance it seems the strength of the AEJ is not that different, with the developing composite having a maximum of 15 ms^{-1} compared to the non-developing case of just over 13 ms^{-1} . The more significant difference is not immediately obvious however, and is the rate of change of zonal wind speed to the south of the AEJ, in other words over the region where the 600 hPa vortices develop. This rate of change is noticeably larger for the developing case (*Figure 7.1.2*). It is this meridional rate of change of zonal velocity that contributes to the development of relative vorticity maxima at the 600 hPa level via barotropic instability.

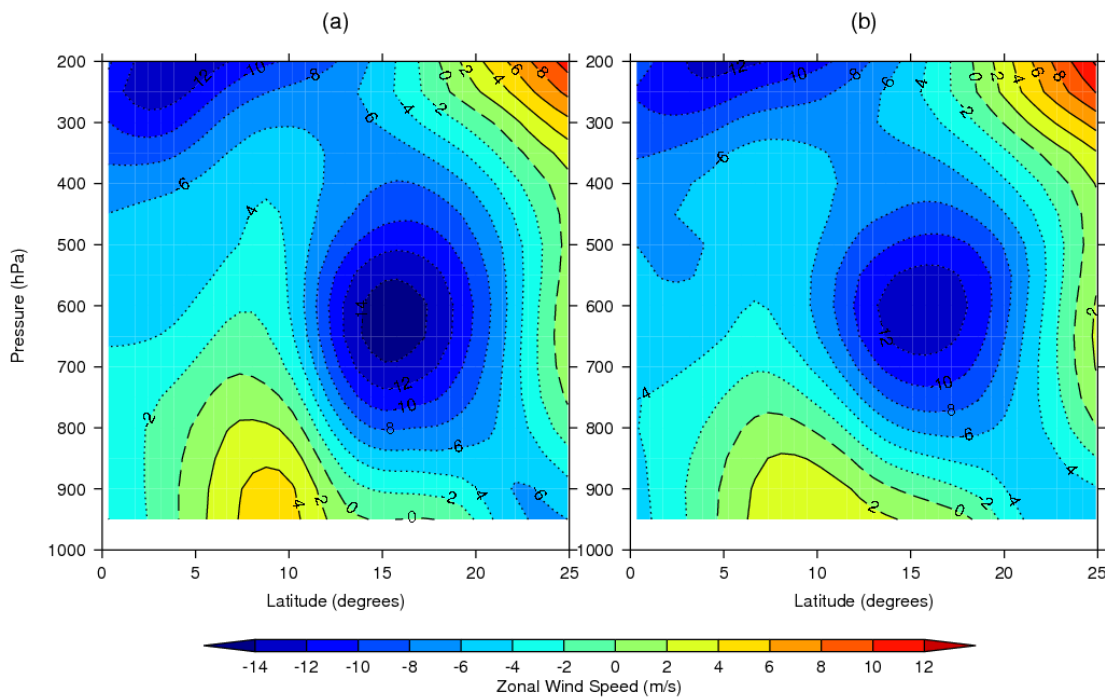


Fig 7.1.1: zonal wind velocity (ms^{-1}) from 20° to 14°W for the (a) developing and (b) non-developing AEW composites

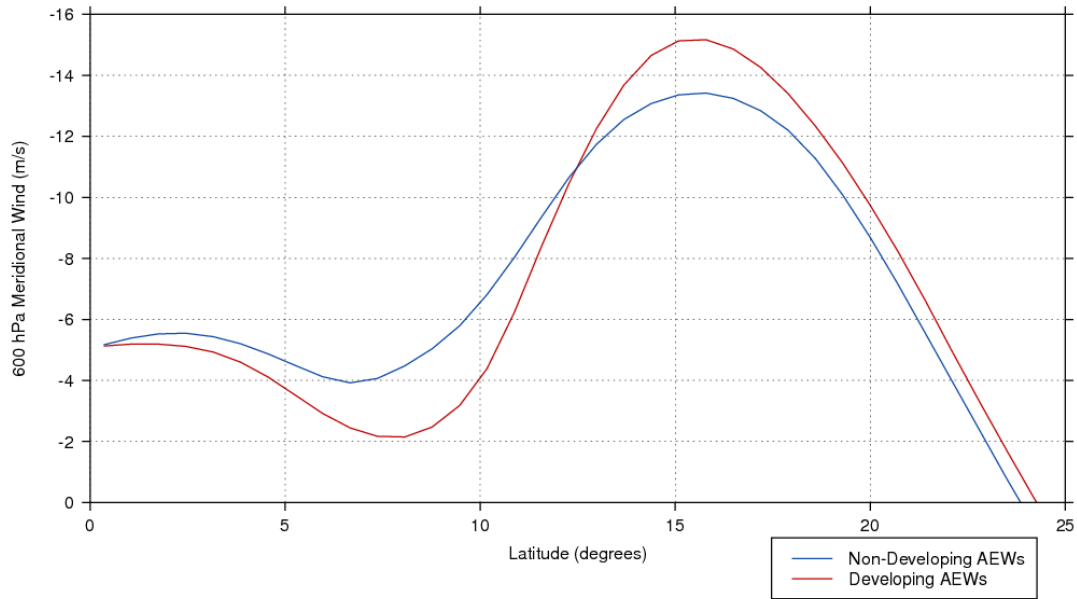


Fig 7.1.2: zonal wind velocity (ms^{-1}) at 600 hPa from 20° to 14°W for the developing and non-developing AEW composites

7.2. Meridional Wind

The AEJ is a zonal feature, so the expectation is that meridional composites will not show much variation between developing and non-developing AEWs. This is the case, and the only appreciable difference that can be seen between the developing (*Figure 7.2.1 (a)*) and non-developing (*Figure 7.2.1 (b)*) AEW composites is that the developing one has more equatorward meridional wind at 200 to 300 hPa, which is possibly indicative of more convection occurring in the developing AEWs.

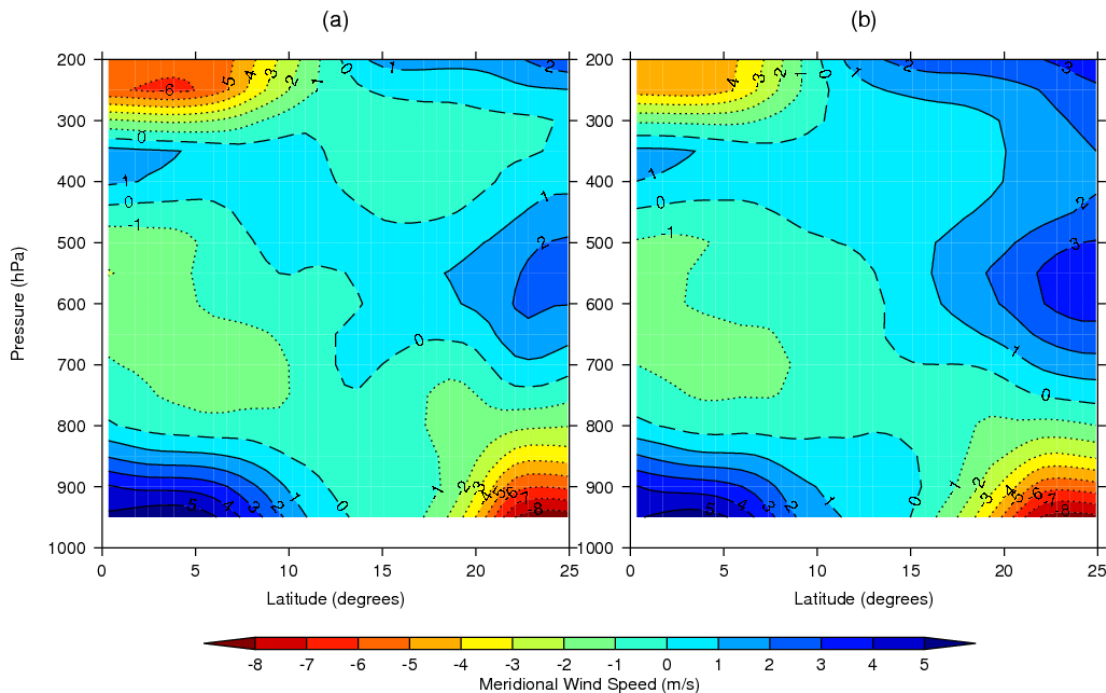


Fig 7.2.1: meridional wind velocity (ms^{-1}) from 20° to 14°W for the (a) developing and (b) non-developing AEW composites

7.3 Vertical Wind

The vertical wind component is expected to be higher if there is more convection present. It has been surmised that convection in the coastal region is important in the downstream development of AEWs into tropical cyclones (Hopsch, Thorncroft & Tyle, 2010; Cornforth, Hoskins & Thorncroft, 2009; Fink, Reiner & Speth, 2004), and therefore the developing AEW composite is expected to show more vertical wind than the non-developing one. This is the case, as is shown by the zonal mean of vertical velocity from 20° to 14°W for the developing composite (*Figure 7.3.1 (a)*) compared to the non-developing one (*Figure 7.3.1 (b)*). The maximum vertical velocity is seen at 17°W (*Figure 7.3.1 (c)* for the developing composite, *(d)* for the non-developing one).

7.4 Relative Humidity

Relative humidity (RH) is closely linked with vertical wind for the development of convection (Hopsch, et al., 2010). Initially the relative humidity was looked at in zonal vertical section, which shows that there is a distinct moist column centred on 10°N . The developing AEW composite (*Figure 7.4.1(a)*) has approximately 5% more RH at any given point in this column than the non-developing composite (*Figure 7.4.1(b)*), but the overall structure is the same for both cases. It is only when looking in meridional vertical section that a significant difference is seen. The meridional section is taken at 10°N , along the centre of the column of maximum RH seen in zonal vertical section, and the developing composite (*Figure 7.4.2(a)*) shows a zone of 70% or more RH for a spread of 8° around the coast (17°W), as compared to less than 3° for the non-developing composite (*Figure 7.4.1(b)*). Further downstream, particularly between 28°W and 40°W , the developing composite has up to 14% greater RH throughout the troposphere than the non-developing composite.

The great majority of AEWs have a 925 hPa north and a 600 hPa south track and the low level baroclinically unstable relative vorticity maxima are advected from the Sahara over the Atlantic. This would imply the advection of the relatively dry Saharan Air Layer (SAL) and this would have an effect on the availability of moisture to allow the continuation and growth of convection (Zipser et al, 2009). The meridional section along 9.5°N (*Figure 7.4.2*) suggests that this would be most visible at 400 hPa, and in the coastal region this is indeed the case (*Figure 7.4.3*). However, looking at the region as a whole and taking the difference between the relative humidity of the developing and the non-developing composites it can be seen that the largest difference is further downstream in the lower troposphere, with a tongue of over 10% more relatively humid air extending at the 850 hPa level co-located with and north of the AEJ out to 38°W (*Figure 7.4.3(c)*).

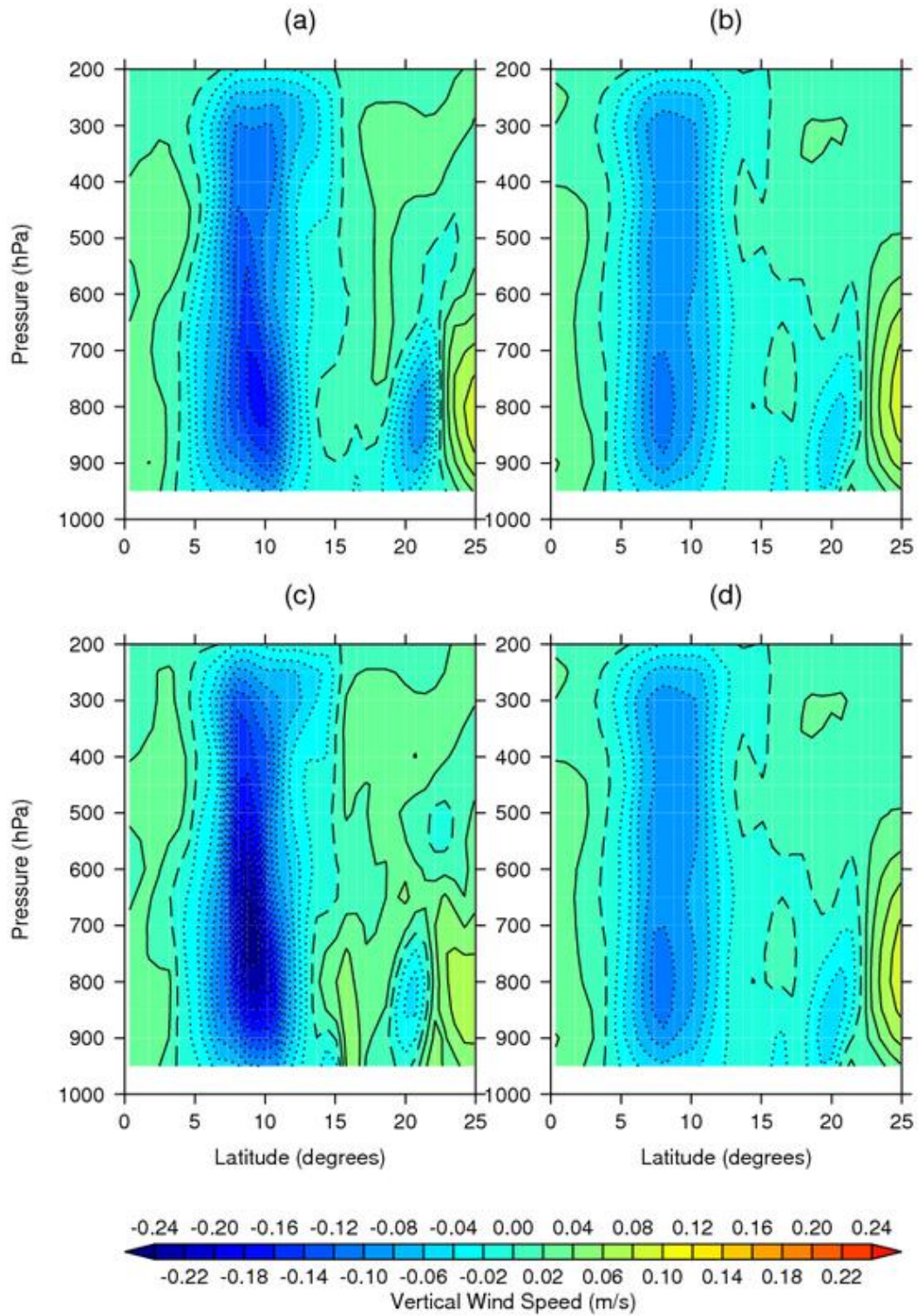


Fig 7.3.1: vertical velocity (ms^{-1}) for the zonal average from 20° to 14°W for the developing (a) and non-developing (b) AEW composite, and at 17°W for the developing (c) and non-developing (d) composites

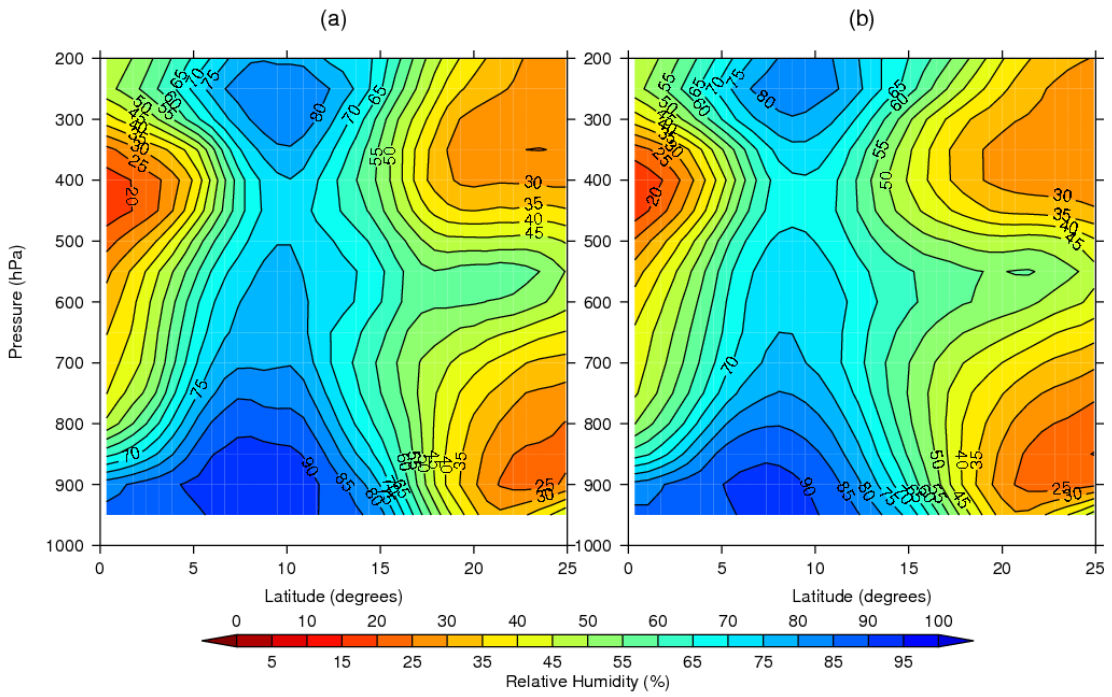


Fig 7.4.1: zonal section of RH (%) for (a) developing AEWs and (b) non-developing AEWs

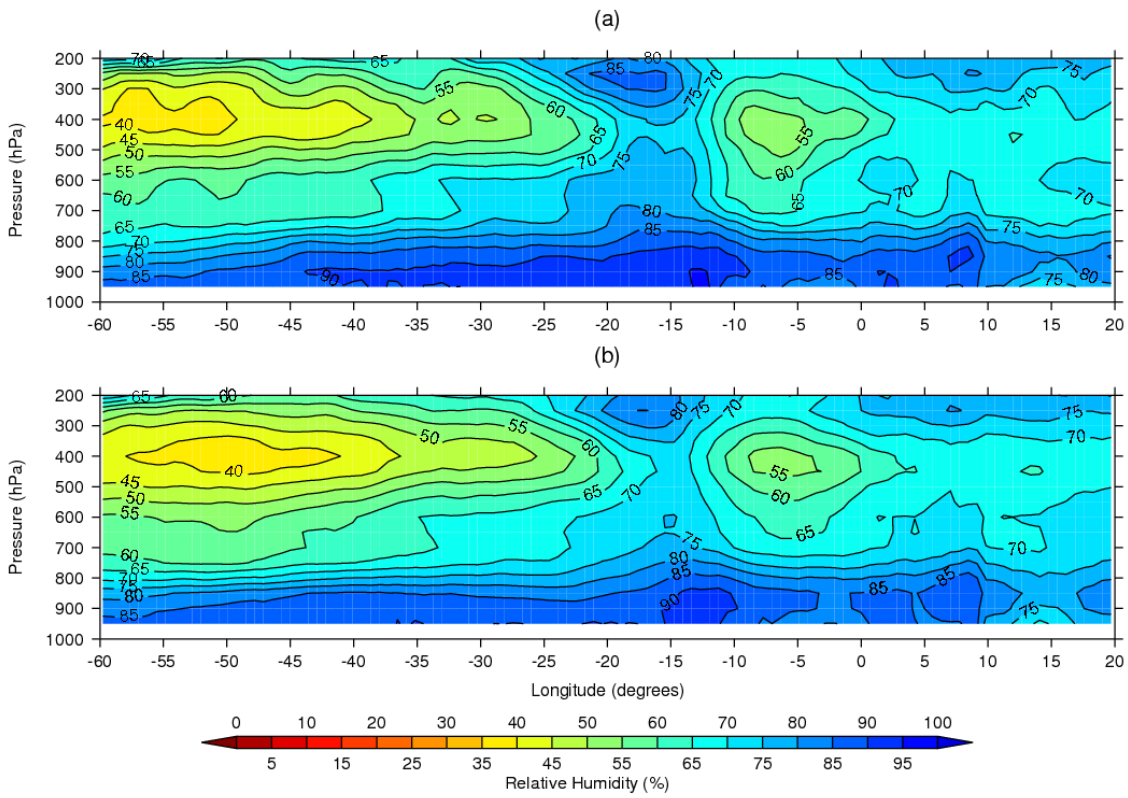


Fig 7.4.2: meridional section along 9.5°N of RH (%) for (a) developing AEWs and (b) non-developing AEWs

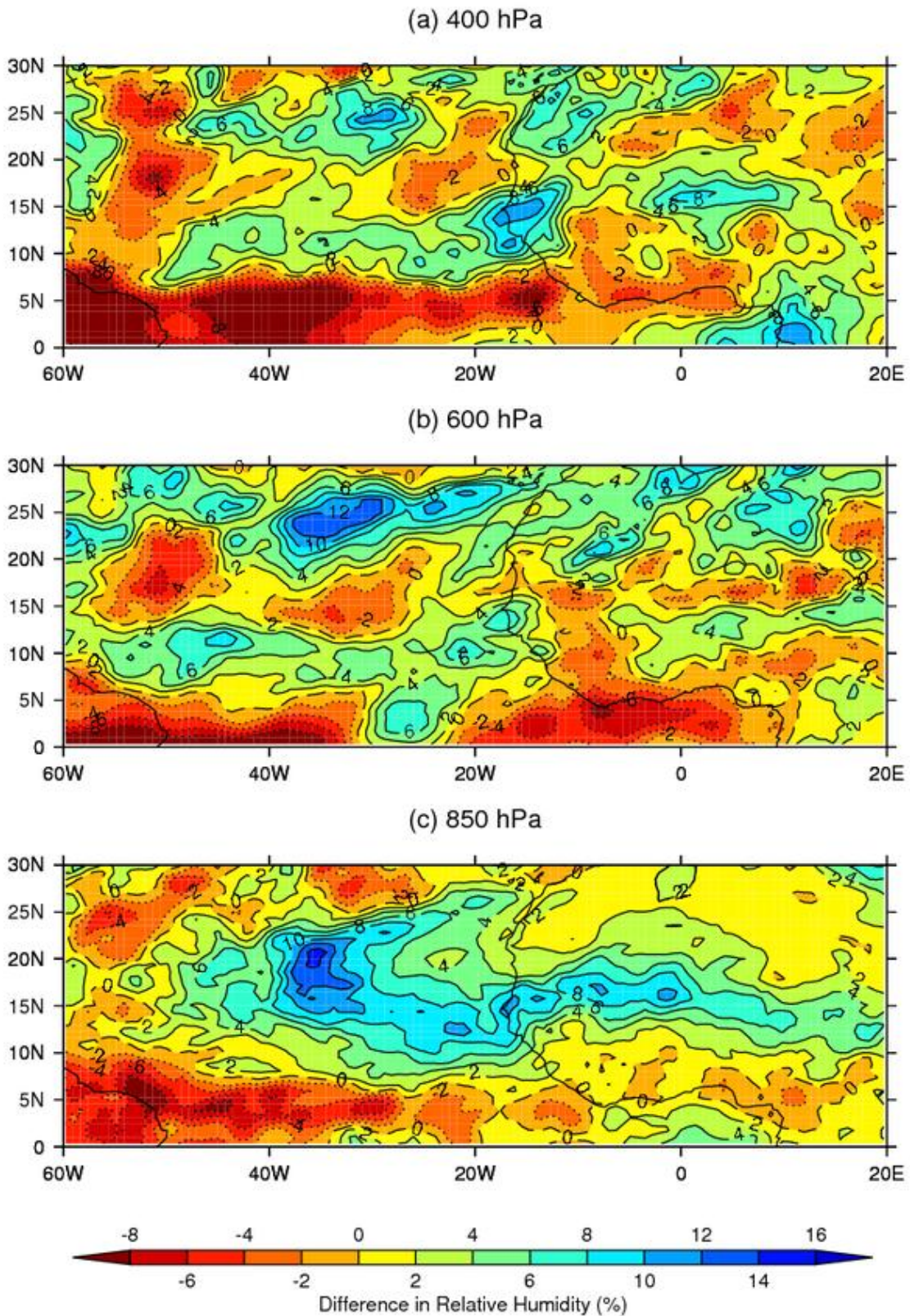


Fig 7.4.3: the difference in relative humidity (%) between developing and non-developing AEW composites at (a) 400 hPa, (b) 600 hPa and (c) 850 hPa

7.5. Equivalent Potential Temperature (θ_e)

As the AEWs pass over the West African coast it has been shown that they have more vertical wind velocity and more relative humidity, probably due to more convection being present (Hopsch, Thorncroft & Tyle, 2010; Cornforth, Hoskins & Thorncroft, 2009; Fink, Reiner & Speth, 2004). The θ_e data was analysed in the coastal region, and the zonal vertical section shows a slight increase in the developing AEW composite (Figure 7.5.1(a)) compared to the non-developing one (Figure 7.5.1(b)). This is more easily quantified by looking at the differences over the region through the troposphere (Figure 7.5.2), which shows that as with relative humidity there is a large region of air at low levels with a higher θ_e (up to 6K higher) in the area co-located and to the north of the AEJ out to 35°W (Figure 7.5.2(c)). At the coast itself it can be seen that from the surface up to 400 hPa there is a column of air which has consistently higher θ_e (4K at 850 hPa down to 1.5K at 400 hPa), which, when taken in conjunction with the vertical wind velocity and the relative humidity analyses, confirms that developing AEWs are warm-core structures as they cross the coast (Hopsch, et al., 2010).

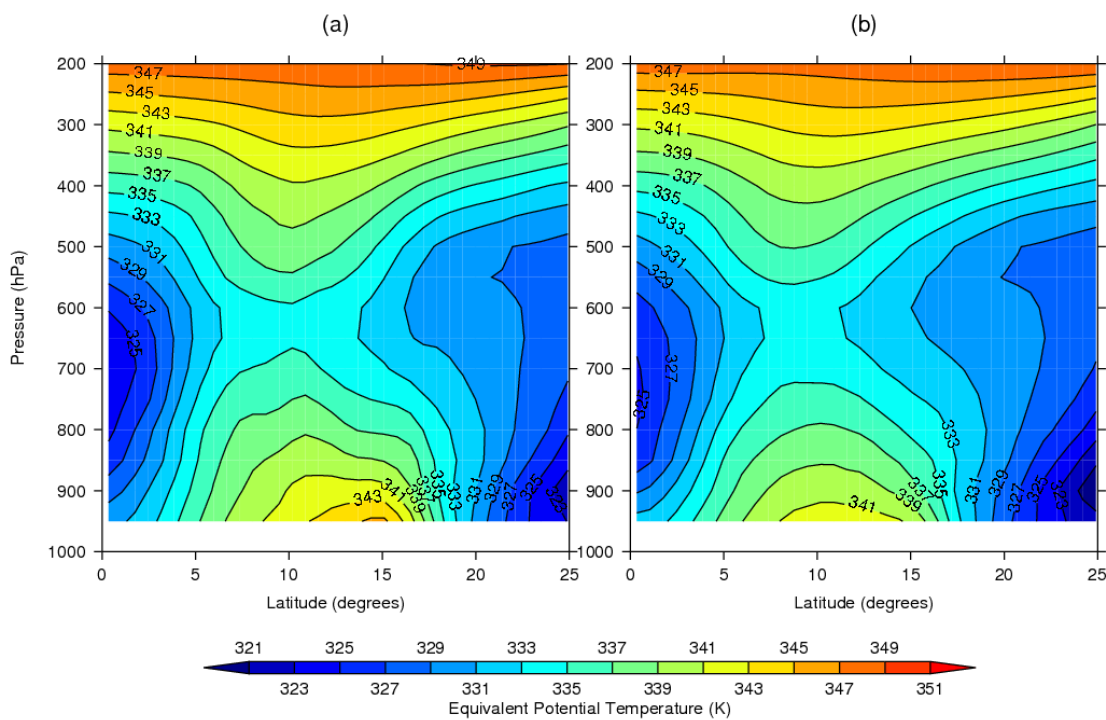


Fig 7.5.1: zonal vertical sections from 20° to 14°W showing θ_e (K) for (a) developing AEWs and (b) non-developing AEWs

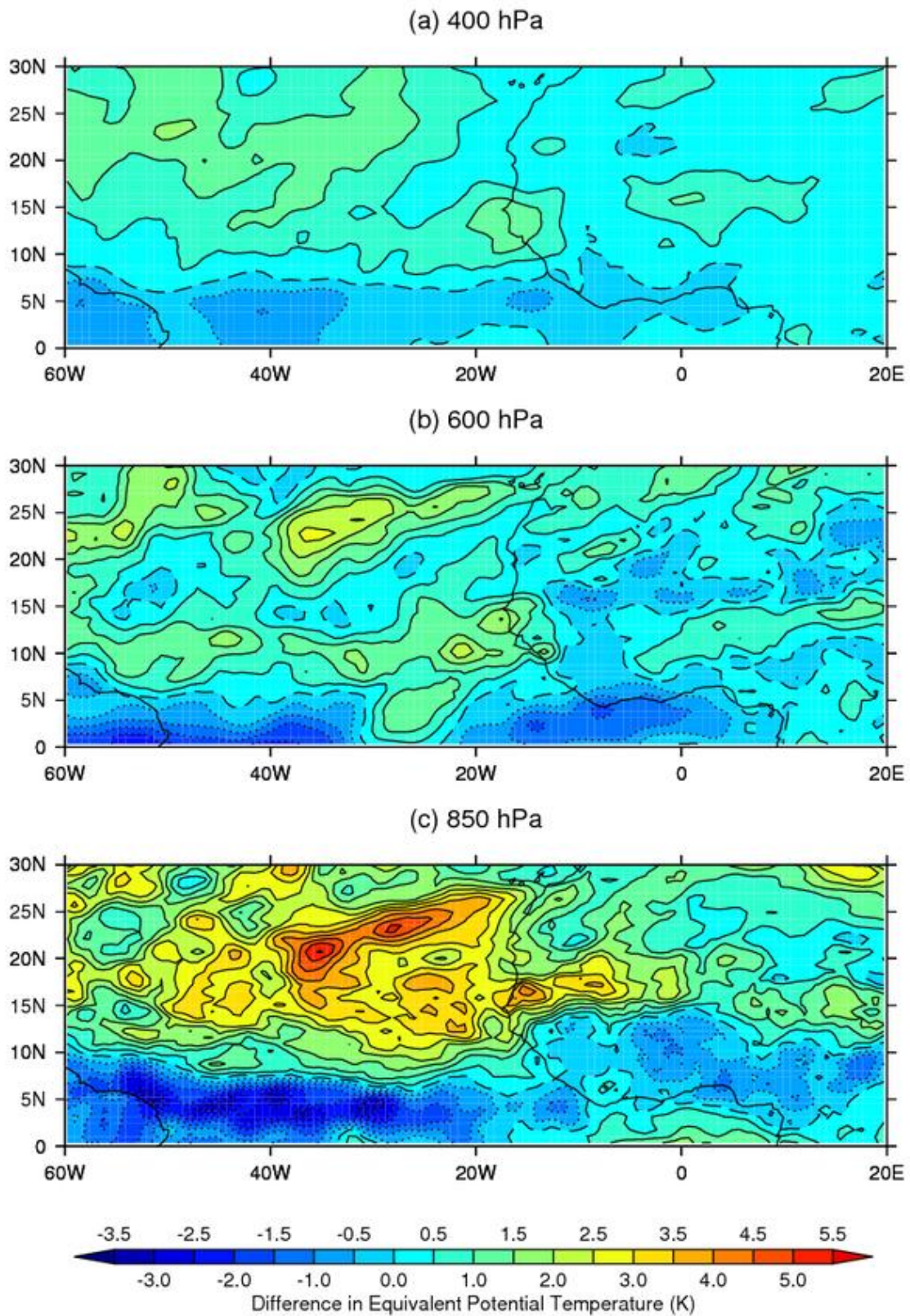


Fig 7.5.2: the difference in θ_e (K) between developing and non-developing AEW composites at (a) 400 hPa, (b) 600 hPa and (c) 850 hPa

7.6. Relative Vorticity

The vertical mean relative vorticity from 850 hPa to 600 hPa has been shown to be an effective AEW tracking field (Thorncroft & Hodges, 2001; Serra, Kiladis, & Hodges, 2010) but should be compared to the relative vorticity at the level of the AEJ to ensure that it can be used as an analysis field as well. The comparison of using the vertical mean relative vorticity against the 600 hPa relative vorticity shows no difference in maxima positioning at the West African coast (*Figure 7.6.1*).

AEWs have a wave structure, with a trough forming along a generally meridional axis (Carlson, 1969; Burpee, 1972) and this is shown for both the developing (*Figure 7.6.1 (a) and (b)*) and non-developing (*Figure 7.6.1 (c) and (d)*) AEW composites. What can be seen however is that the developing composite trough is more marked than the non-developing one, and that the position of the relative vorticity maxima for the developing case is on the trough axis, whereas for the non-developing case it is slightly upstream (to the east) of it. This means that the developing composite will have neither positive nor negative vorticity advection, whereas the non-developing one will have some negative vorticity advection, which will slightly inhibit convection, as seen by the vertical wind velocity analysis (*section 7.3*). This is also shown by the 600 hPa vector wind which shows the relative positioning of the vertical mean relative vorticity maximum for the developing (*Figure 7.6.2(a)*) and non-developing (*Figure 7.6.2(b)*) composites, as well as showing that there is no significant regional synoptic difference between the two cases.

The relationship between lower troposphere temperature and the position of the relative vorticity maximum is also interesting – in the developing composite (*Figure 7.6.3(a)*) there is a distinct zone ahead of the trough axis which is 2K higher in θ_e than for the equivalent zone in the non-developing case (*Figure 7.6.3(b)*). Looking at the difference between developing and non-developing composites (*Figure 7.6.4*) there is a relatively small zone where θ_e is up to 6K higher for the developing AEWs ahead of the AEW trough axis.

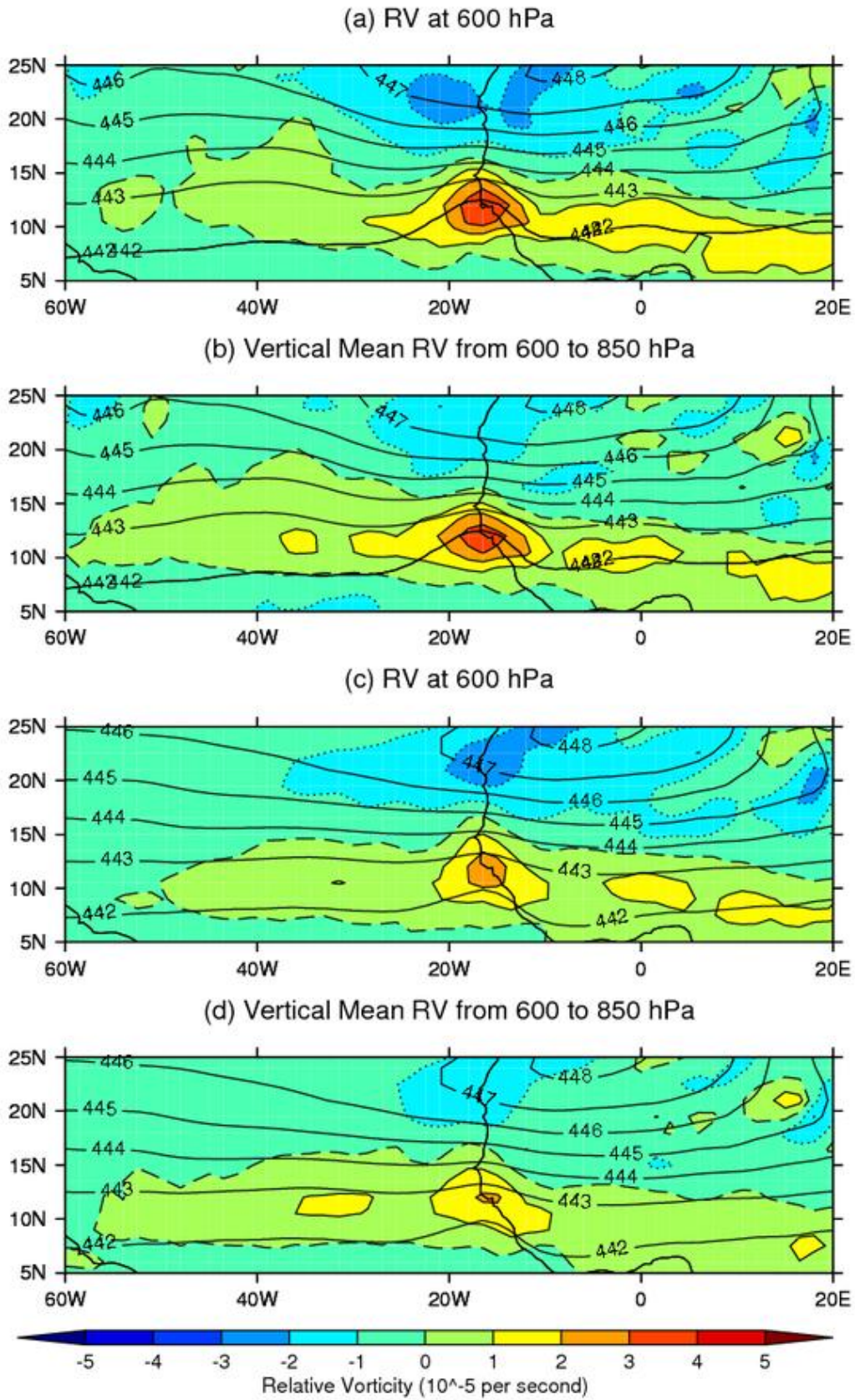


Fig 7.6.1: relative vorticity ($\times 10^{-5} \text{s}^{-1}$) overlaid with 600 hPa geopotential height contours (dm).
 (a) 600 hPa RV for developing AEWs; (b) vertical mean RV for developing AEWs
 (c) 600 hPa RV for non-developing AEWs; (d) vertical mean RV for non-developing AEWs

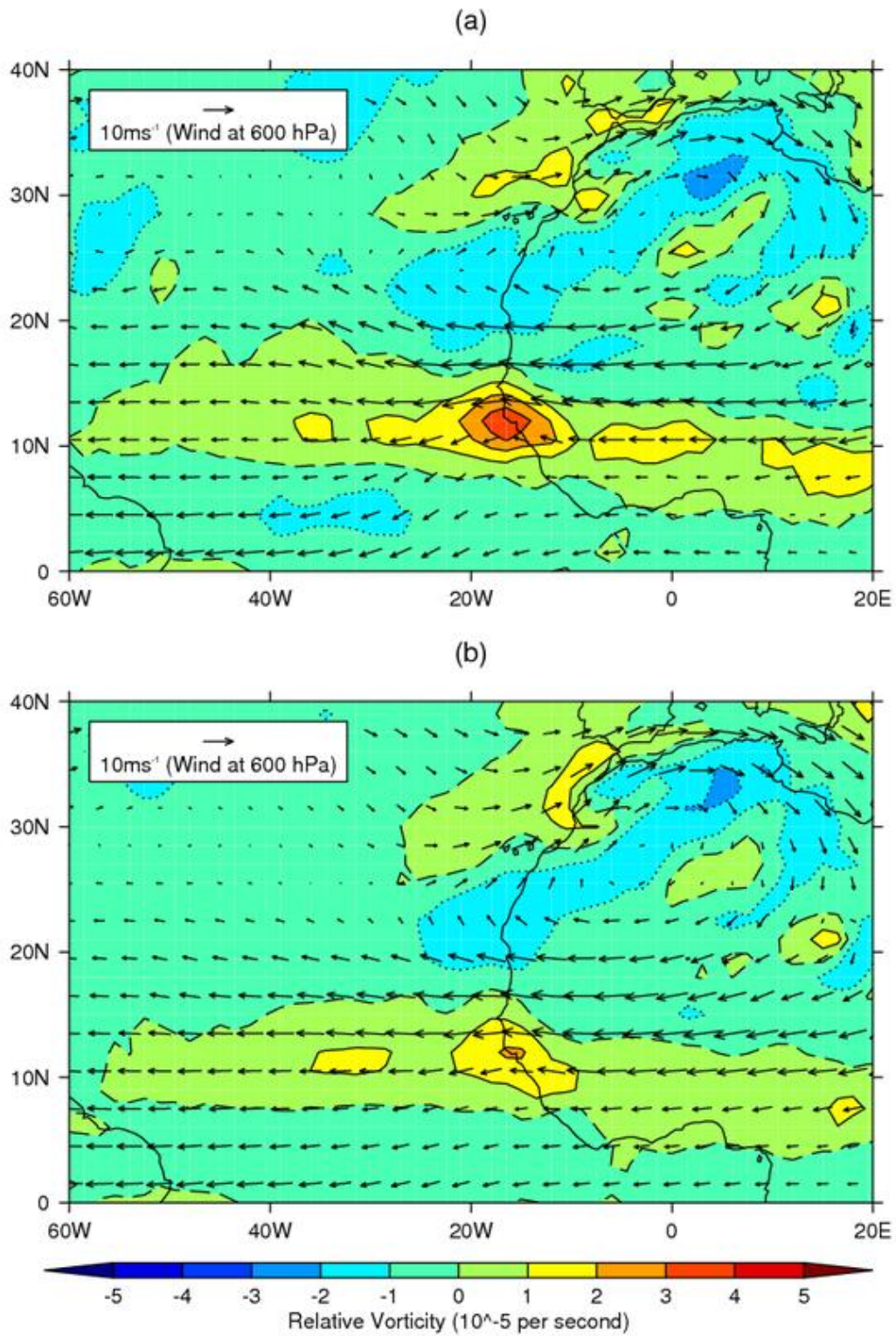


Fig 7.6.2: relative vorticity ($\times 10^{-5} \text{s}^{-1}$) overlaid with 600 hPa wind vectors (ms^{-1}) for (a) developing AEWs and (b) non- developing AEWs

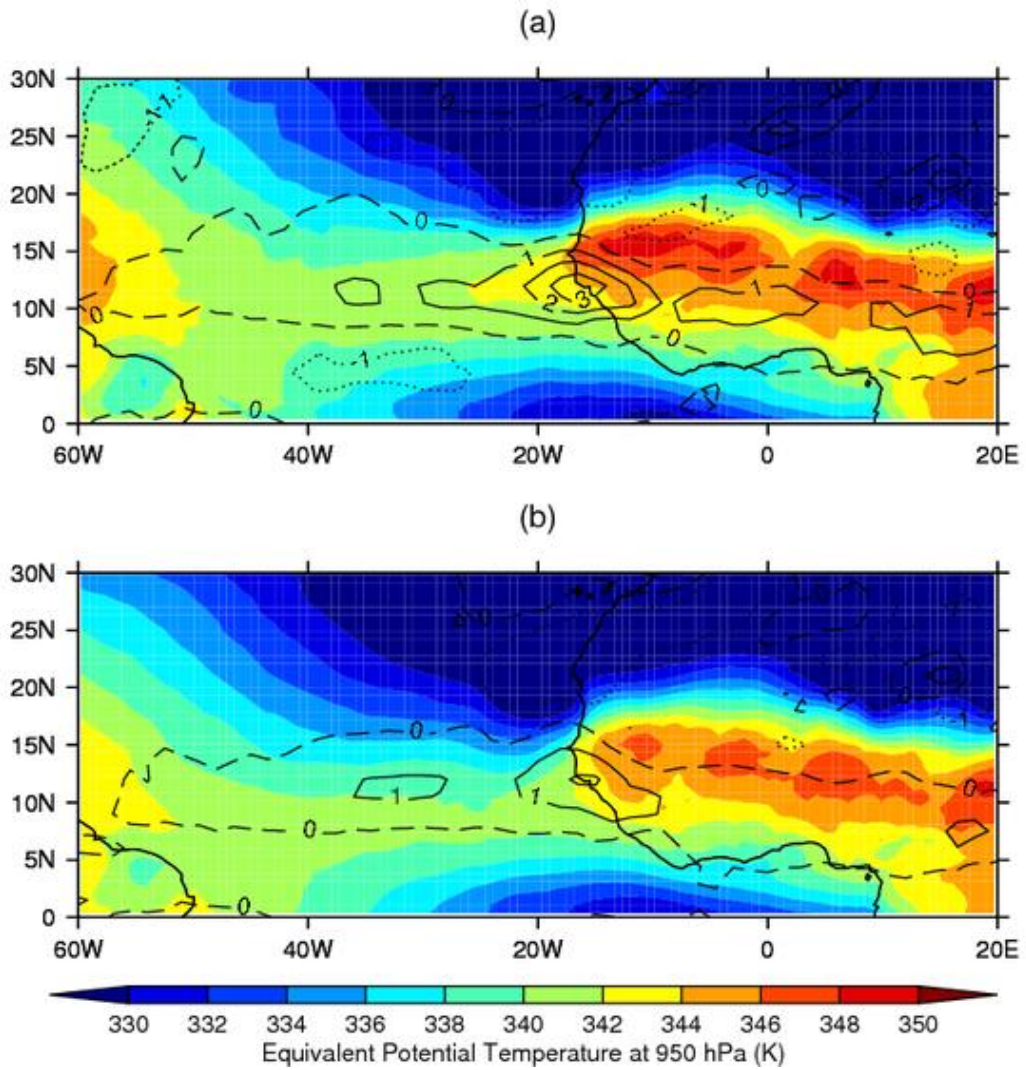


Fig 7.6.3: relative vorticity ($\times 10^{-5} \text{s}^{-1}$) overlaid with 950 hPa θ_e (K) for (a) developing AEWs and (b) non-developing AEWs

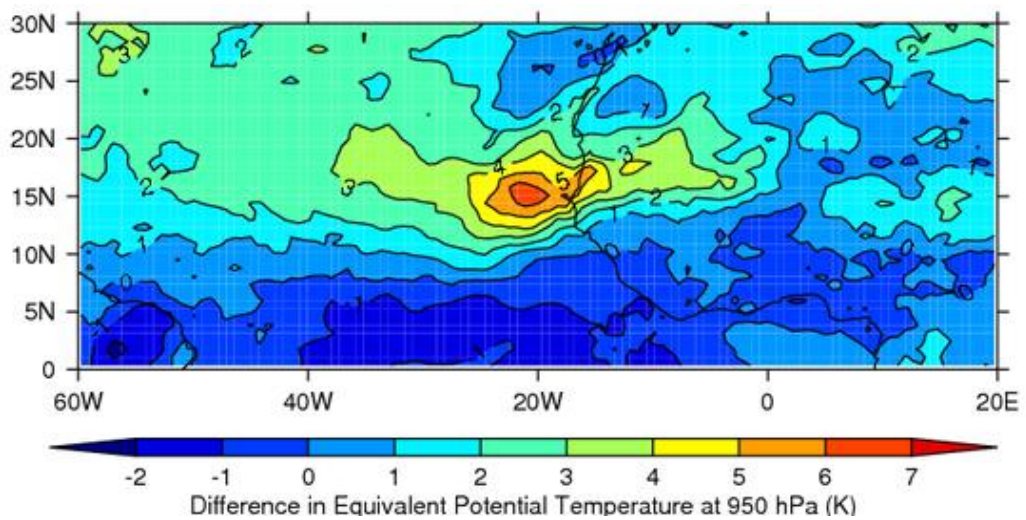


Fig 7.6.4: difference in 950 hPa θ_e (K) between developing and non-developing AEWs

8. Downstream Tracking and Identification of African Easterly Waves

Cyclogenesis depends very much on the downstream development of AEWs. The case studies showed that AEWs which are extremely strong at the West African coast can decay rapidly or carry on without developing further across the entire Atlantic, whereas some AEWs that are relatively weak at this point develop into full blown hurricanes over the Caribbean. The case studies also indicated that the strength of the AEJ going across the Atlantic with a particular AEW was strongly linked to any tropical depression development.

To bring a significant degree of statistical veracity to any conclusions it is vital to use the conditions from as many different AEWs as possible. To this end all of the developing and non-developing AEWs for the JJAS period of 2005 to 2009 which were tracked using the automatic relative vorticity tracking algorithm (*section 3.*) (*table 8.1*) were used.

Year	Non-developing AEWs	Developing AEWs
2005	31	8
2006	24	7
2007	30	5
2008	31	8
2009	30	6
Total	146	34

Table 8.1: numbers of AEWs for JJAS 2005 to 2009

One point immediately to note is that the numbers of developing AEWs do not seem to correlate with the known hurricane activity in each year – 2005, for example had so many that the naming system had to go over to the Greek alphabet. The reason for this is the timing of the data period, as in busy hurricane years a significant number occurred after the start of October (*table 8.2*).

Year	Post-JJAS Storms
2005	13
2006	0
2007	3
2008	6
2009	3

Table 8.2: post-JJAS storms for 2005-2009

A further complication is that while AEWs are mostly co-located when they cross the West African coast, once they pass over the central and western Atlantic they become widely spread due to the influence of the particular synoptic conditions at the time. This means that a particular temporal or spatial window cannot be used to capture data from different AEWs. The method used was to pick a particular point in each AEWs development and gather data in a 10 degree radius around that

particular point for the tropospheric conditions required, and then to average these individual data sets into two separate composites for the developing and non-developing cases.

The point chosen for each AEW was the point at which the automatic relative vorticity maximum tracking algorithm (Serra, et al., 2010) for the mean relative vorticity averaged between 850 to 600 hPa detected the AEW track in the Atlantic (or earlier if a developing AEW was tracked over Africa all the way until cyclogenesis). This development stage was chosen as it gives each AEW a common development stage, and does not depend on any criteria that will only be known later, e.g. “24 hours before declaration as a tropical depression”. There is no consistent difference in relative vorticity at the track start point between developing and non-developing AEWs (*table 8.3*), with developing AEWs on average having 28% more relative vorticity on detection. This varies greatly from year to year however and cannot be used as a reliable indicator of cyclogenesis potential.

Year	Developing AEW Relative Vorticity ($\times 10^{-5} \text{ s}^{-1}$) at Track Start	Non-Developing AEW Relative Vorticity ($\times 10^{-5} \text{ s}^{-1}$) at Track Start	% Difference in RV from non-developing to developing AEWs
2005	2.83	2.40	18%
2006	4.31	2.30	87%
2007	3.40	2.35	45%
2008	2.40	2.33	3%
2009	2.58	2.55	1%
Total	3.07	2.39	28%

Table 8.3: relative vorticity reading at the start of each AEW track

This choice of starting point gives a wide geographical spread of data locations for both developing (*Figure 8.1*) and non-developing (*Figure 8.2*) AEWs. The criteria for selection of these tracks was that they were present between 0°N and 20°N, and that for the non-developing ones they started either over the sea or just at the coast, so as to try and avoid significant land effects (e.g. surface heating). The AEJ is generally stronger over the African land mass due to the higher temperature gradient, and so the developing AEWs that have their initial track point over land have been removed from the wind analyses to avoid any bias. The scale indicates relative vorticity (10^{-5} s^{-1}) and shows a random spread of initial relative vorticity readings for the track start points. This reinforces the point that the choice of a particular stage of an AEW’s development is much more consistent than a particular time or regional filter.

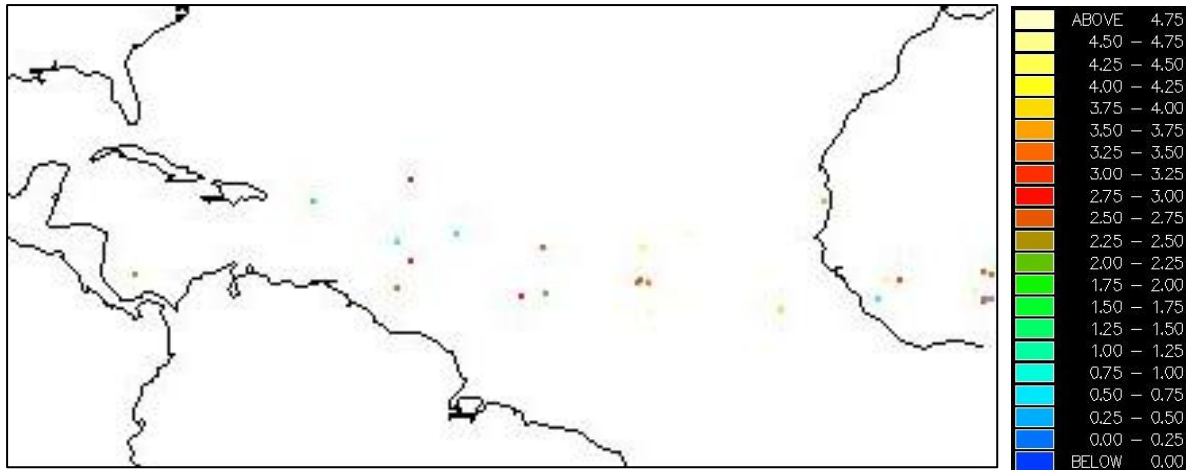


Fig 8.1: start points for developing AEW tracks, JJAS 2005 to 2009

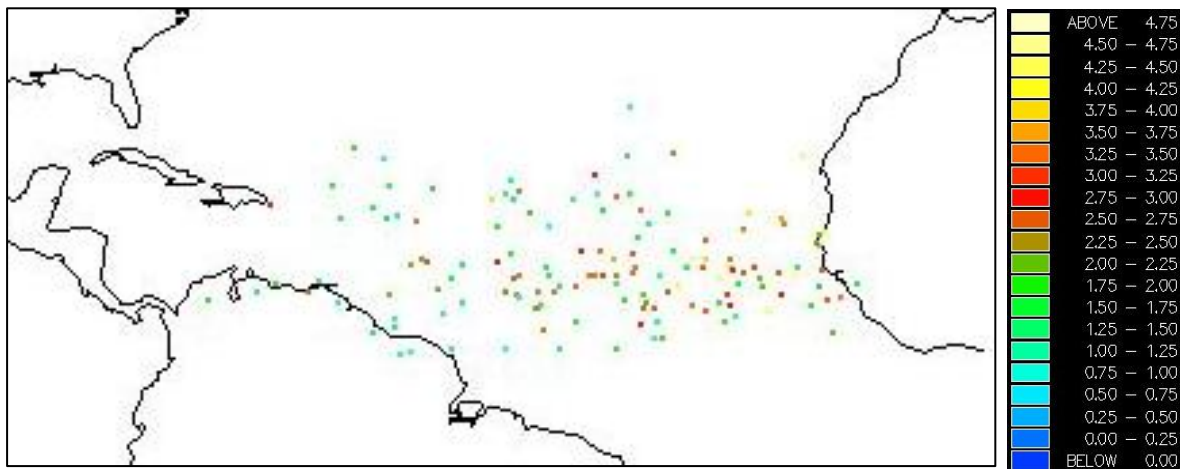


Fig 8.2: start points for non-developing AEW tracks, JJAS 2005 to 2009

9. The Compositing of Downstream Data for Developing and Non-Developing AEWs

After looking at several case studies it was hypothesised that the developing AEWs were usually accompanied by a stronger poleward jet at the 600 hPa level than non-developing ones. To test this, the conditions around the start points of the developing and non-developing tracks for JJAS 2005 to 2009 were individually collected into the two categories and analysed looking at wind speed, relative humidity, equivalent potential temperature (θ_e) and potential vorticity at the 315 K isentropic surface (PV315). The composites were oriented along the direction of each individual track, and are presented with the downtrack direction taken as due west. Therefore on any plan views due north represents 90° to the right of the mean track direction, due south 90° to the left of the mean track direction and due east directly behind the track start point (*Figure 9.1*). This technique has previously been extensively used and proved for extra-tropical systems by Catto (2009).

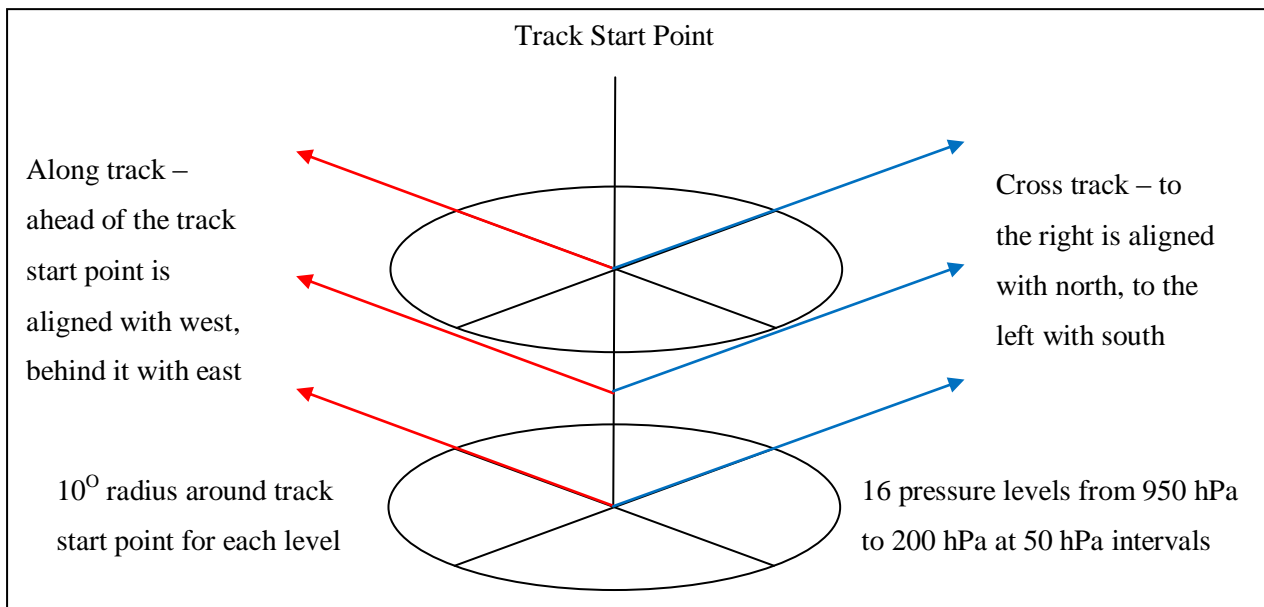


Fig 9.1: the downstream compositing volume and its orientation

9.1 Wind Speed Composites

The wind speed data here is the magnitude of the vector product of the zonal (u) and meridional (v) wind components. The cross track vertical section shows a marked difference between the developing AEW composite (*Figure 9.1.1 (a) and (b)*) and the non-developing one (*Figure 9.1.1 (c) and (d)*). There is a poleward jet at 650 hPa centred 4 degrees to the right of track in both cases, but the developing composite has both a faster central core (13 ms^{-1} compared to 11 ms^{-1}) and a wider one, with the 10 ms^{-1} or above region in the developing case being 6.5 degrees wide compared to 4.7 degrees wide for the non-developing case. Also, the difference between the wind speed left and right of track is different – the developing composite has a minimum wind speed of less than 5 ms^{-1} left of track giving a left/right difference of 8 ms^{-1} , compared to a 6 ms^{-1} difference in the non-developing one. The vertical sections along the track through the start point (*Figure 9.1.2 (a) and (b) for developing AEWs, (c) and (d) for non-developing ones*) also shows differences in magnitude and gradient, with a peak of 11 ms^{-1} ahead of the developing AEW start point, and a difference of 4 ms^{-1} with the region behind it, compared to 9 ms^{-1} and 2 ms^{-1} for the maximum and difference respectively for the non-developing composite.

The developing AEWs have had the ones that develop over land removed to avoid any wind speed bias from the stronger AEJ. This is actually a small effect, and is illustrated by the 200, 400, 600 and 850 hPa level plan views (*Figure 9.1.3* : left hand column for all the developing AEWs, central one for the developing AEWs that are first detected at sea, and the right hand column for the non-developing AEWs). This representation clearly show the proximity of the stronger 600 hPa poleward jet and the larger difference in wind speeds left and right of track in the developing composite compared to the non-developing one.

A noticeable point for further investigation is the difference in the 200 hPa level winds, which shows significantly more wind equatorward for the developing cases than the non-developing one, which is possibly the upper troposphere tropical easterly jet (Hastenrath, 1991). This is a possible cause of upper level divergence, which would in turn help low level convergence and convection (Hastenrath, 1991).

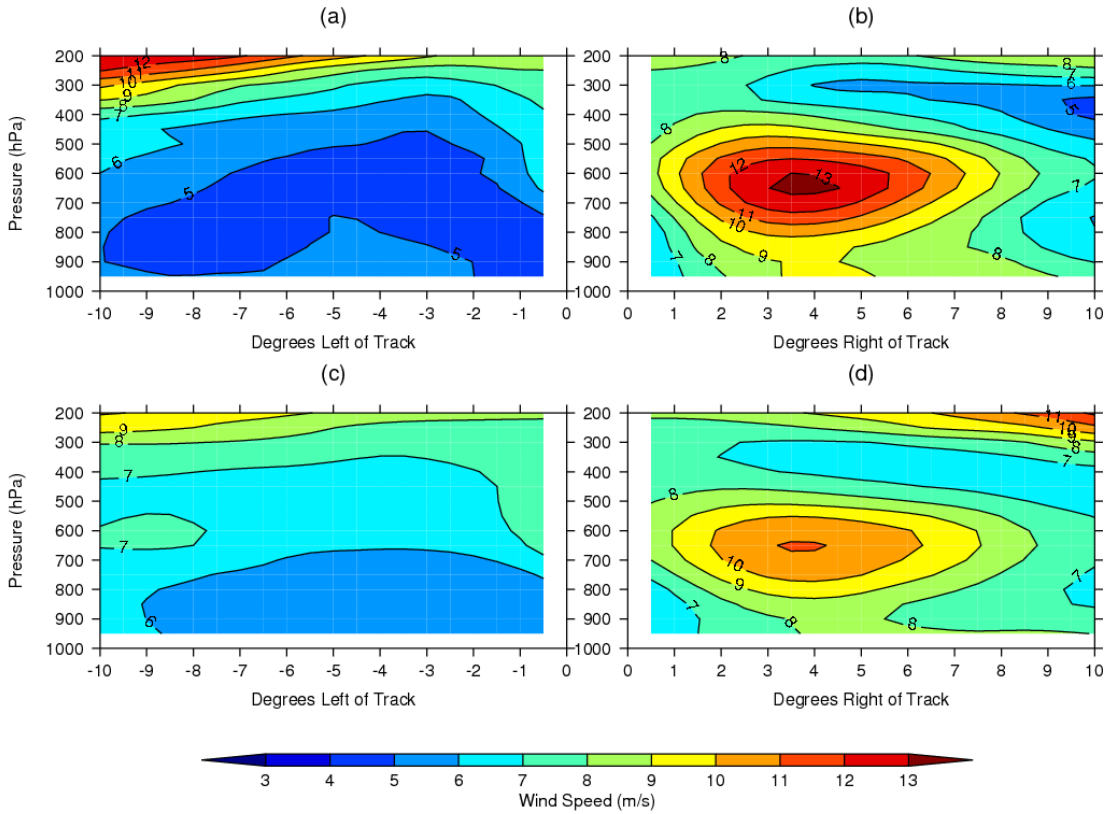


Fig 9.1.1: cross track vertical sections showing wind speed (ms^{-1}) left and right of the track start points of developing ((a) and (b)) and non-developing ((c) and (d)) AEWs

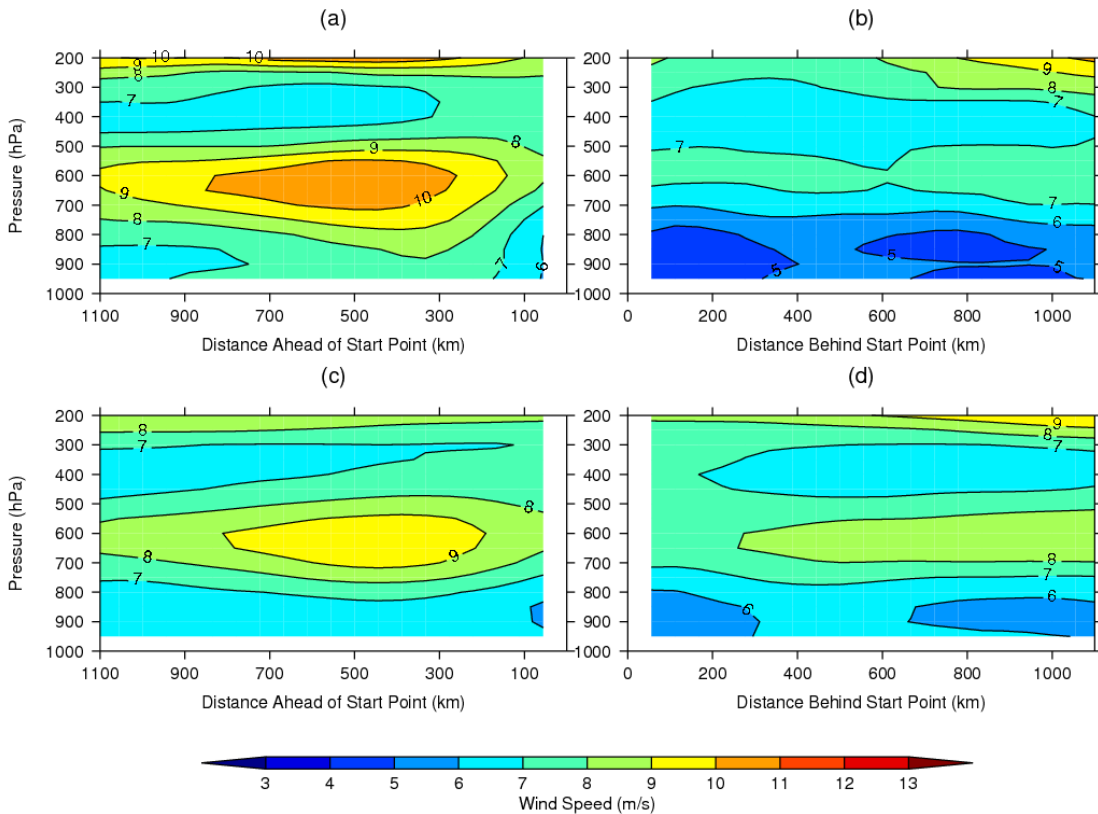


Fig 9.1.2: cross track vertical sections showing wind speed (ms^{-1}) ahead of and behind the track start points of developing ((a) and (b)) and non-developing ((c) and (d)) AEWs

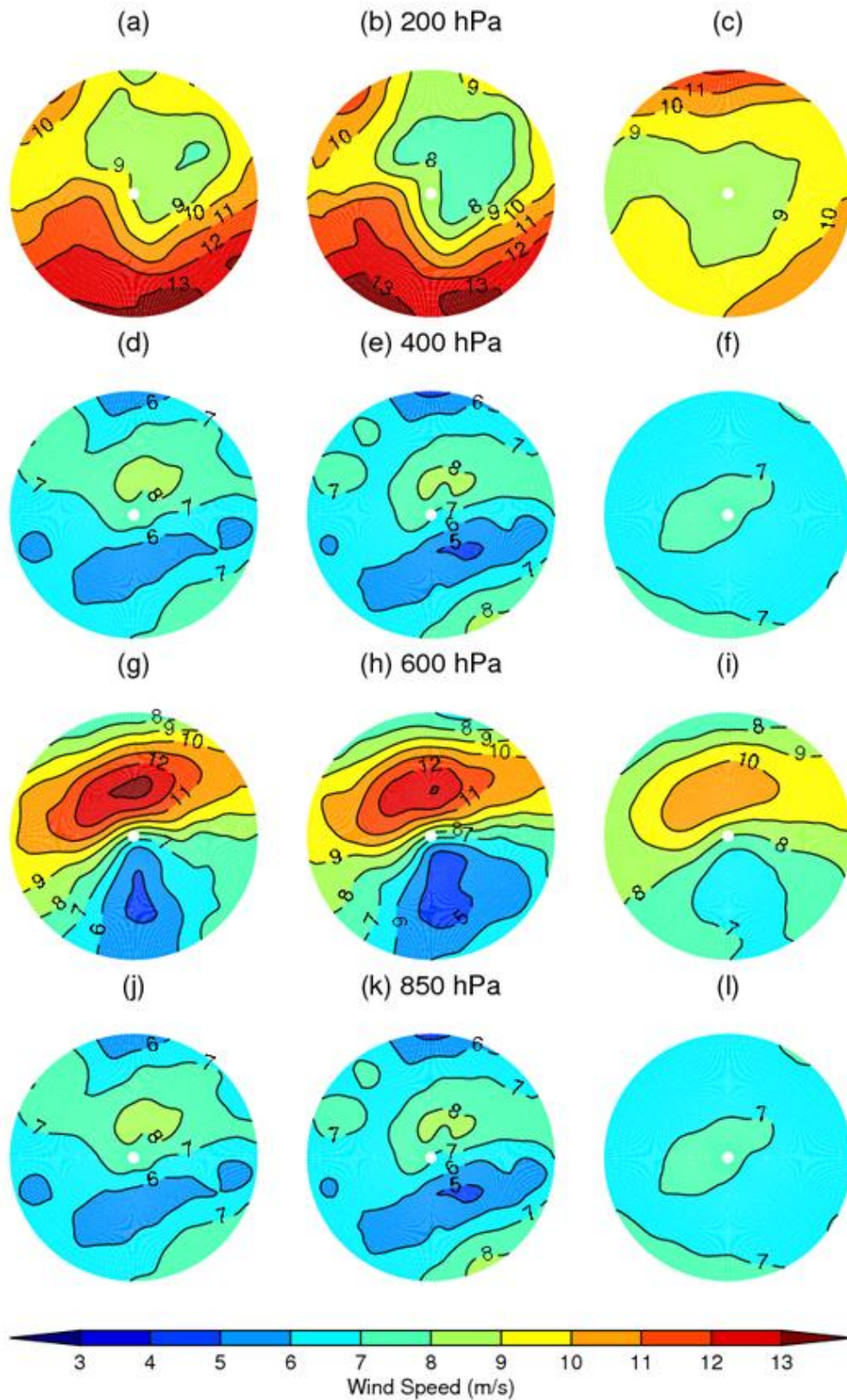


Fig 9.1.3: plan views with a 10° radius showing wind speed (ms^{-1}) at the 200 ((a), (b) & (c)), 400 ((d), (e) & (f)), 600 ((g), (h) & (i)) and 850 hPa ((j), (k) & (l)) levels around the track start points of all the developing (left hand column), the marine developing AEWs (central column) and non-developing (right hand column) AEWs

9.2 Relative Humidity Composites

The first thing that stands out when looking at the cross-track vertical section is that there is a column of more humid air with relative humidity values above 65% centred 2° left of track in the developing composite (*Figure 9.2.1 (a) and (b)*) compared to relative humidity values of above 45% for the same column in the non-developing composite (*Figure 9.2.1 (c) and (d)*). This impression is continued when looking at the vertical section along the track centred on the track start point, with the developing composite showing a region of relative humidity above 75% below 600 hPa up to 500 km behind the track start point (*Figure 9.2.2 (a) and (b)*), compared to an RH value of above 55% for the same region in the non-developing composite (*Figure 9.2.2 (c) and (d)*). The next significant feature is the upper level air ahead of the track start point – centred on 400 hPa the non-developing composite shows a tongue of drier air (less than 40 % RH) from immediately ahead compared to a gradual tapering off of relative humidity in the developing composite, which starts at 60% and only reaches 40% 650 km ahead of the track start point. The plan views are very useful for bringing the picture together. The developing composite at 400, 600 and 850 hPa (*Figure 9.2.3 (a) and (b) and (c)*) shows a region of more humid air over a larger volume located to the south east of the track start location when compared with the non-developing composite (*Figure 9.2.3 (d) and (e) and (f)*), with the difference becoming more marked with altitude with 85% compared to 80% at 850 hPa, 75% to 60% at 600 hPa and 70% to 45% at 400 hPa.

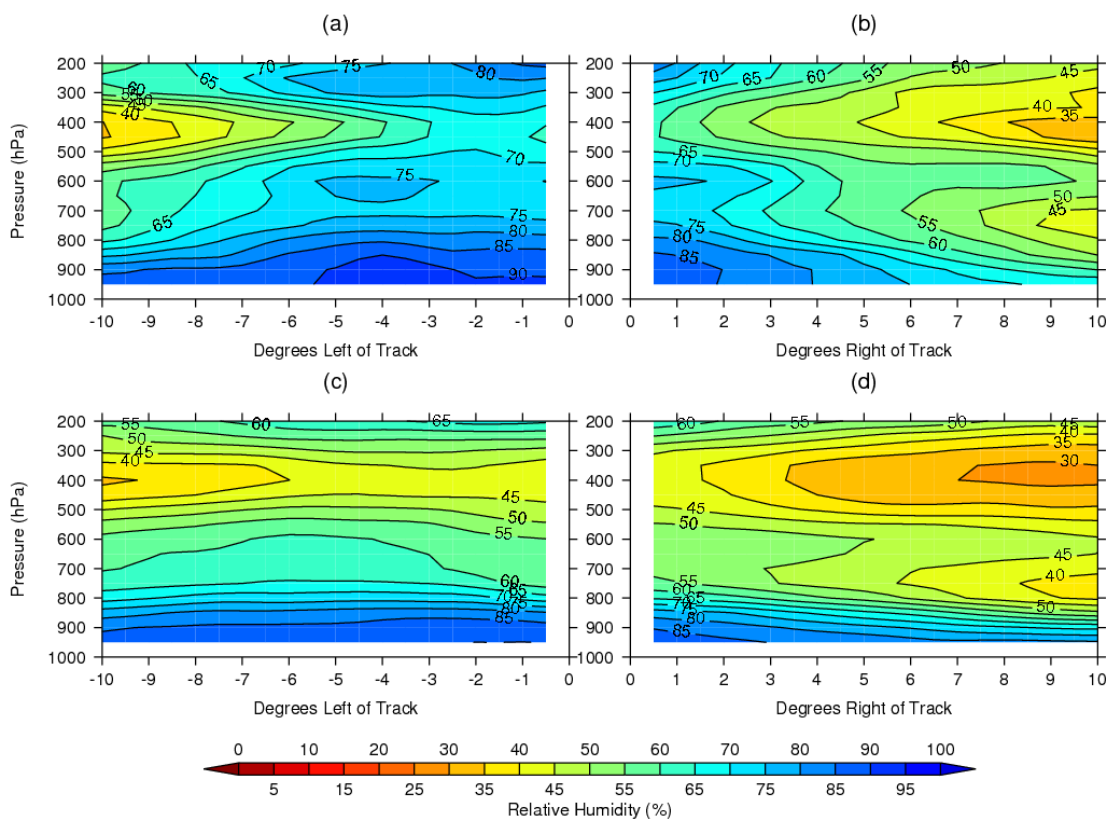


Fig 9.2.1: cross track vertical sections showing relative humidity (%) left and right of the track start points of developing ((a) and (b)) and non-developing ((c) and (d)) AEWs

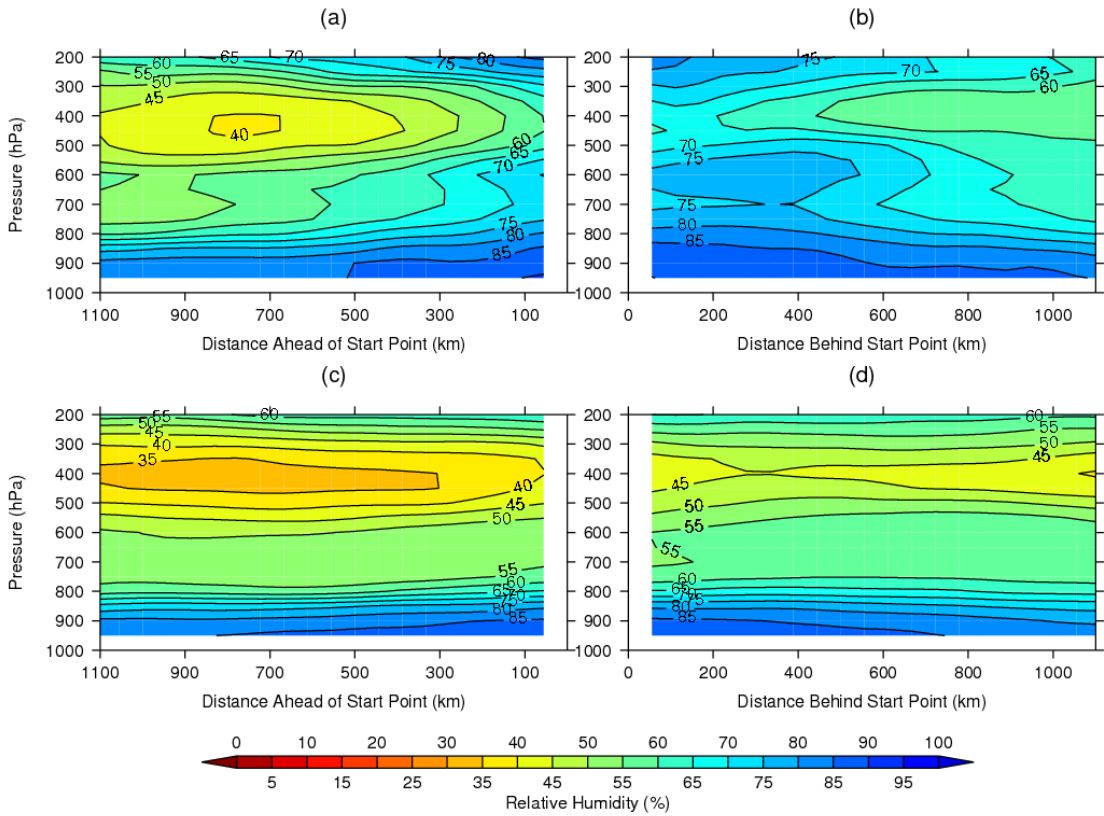


Fig 9.2.2: cross track vertical sections showing relative humidity (%) ahead of and behind the track start points of developing ((a) and (b)) and non-developing ((c) and (d)) AEWs

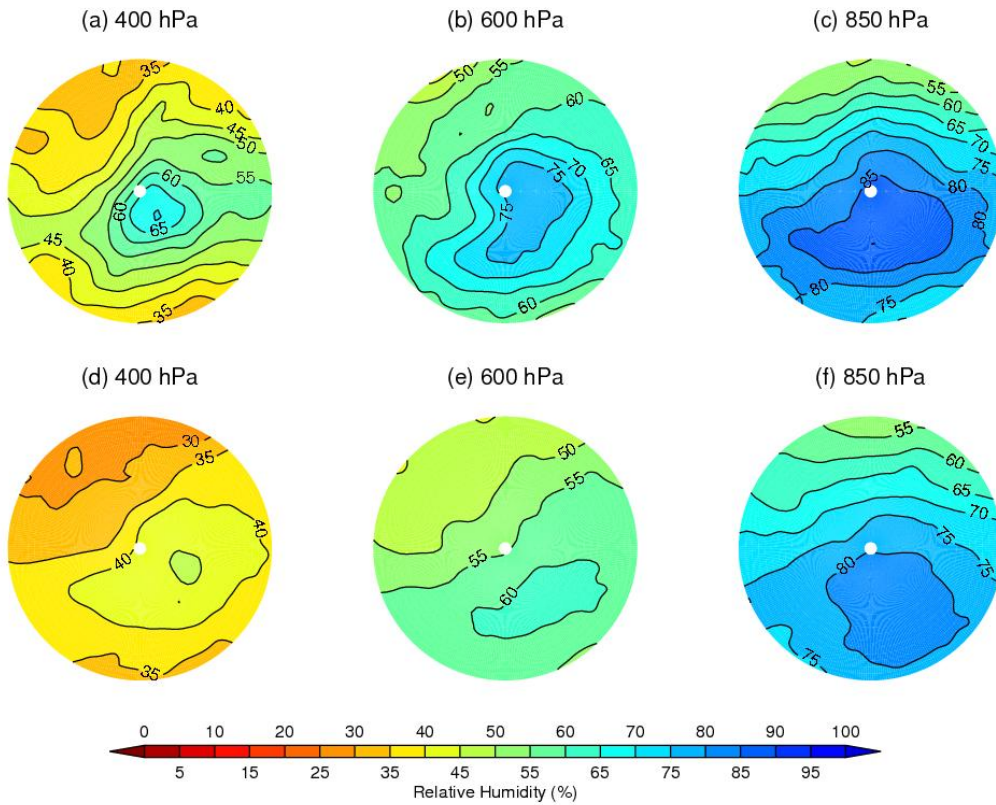


Fig 9.2.3: plan views with a 10° radius showing relative humidity (%) at the 400, 600 and 850 hPa levels around the track start points of developing ((a),(b) and (c)) and non-developing ((d), (e) and (f)) AEWs

9.3 Equivalent Potential Temperature Composites

θ_e is used as it is conserved no matter whether the air parcel is saturated or unsaturated. Just as with the relative humidity data the cross track vertical section through the track start point shows a column of air that has a minimum θ_e of 333 K approximately 2 degrees left of track (*Figure 9.3.1 (a) and (b)*) compared to 330 K in the same region of the non-developing composite (*Figure 9.3.1 (c) and (d)*).

The along track vertical section shows a value of 333 K at 600 hPa for the developing composite (*Figure 9.3.2 (a) and (b)*) compared to 329 K for the non-developing one (*Figure 9.3.2 (c) and (d)*).

The plan views complete the overall picture, with the developing composite at 400, 600 and 850 hPa (*Figure 9.3.3 (a), (b) and (c)*) showing a volume of air to the south east of the track start point which has a higher θ_e at all levels than the non-developing composite (*Figure 9.3.3 (d), (e) and (f)*), with 339 K compared to 335K at 850 hPa, 333 K to 331 K at 600 hPa and 339 K to 337 K at 400 hPa.

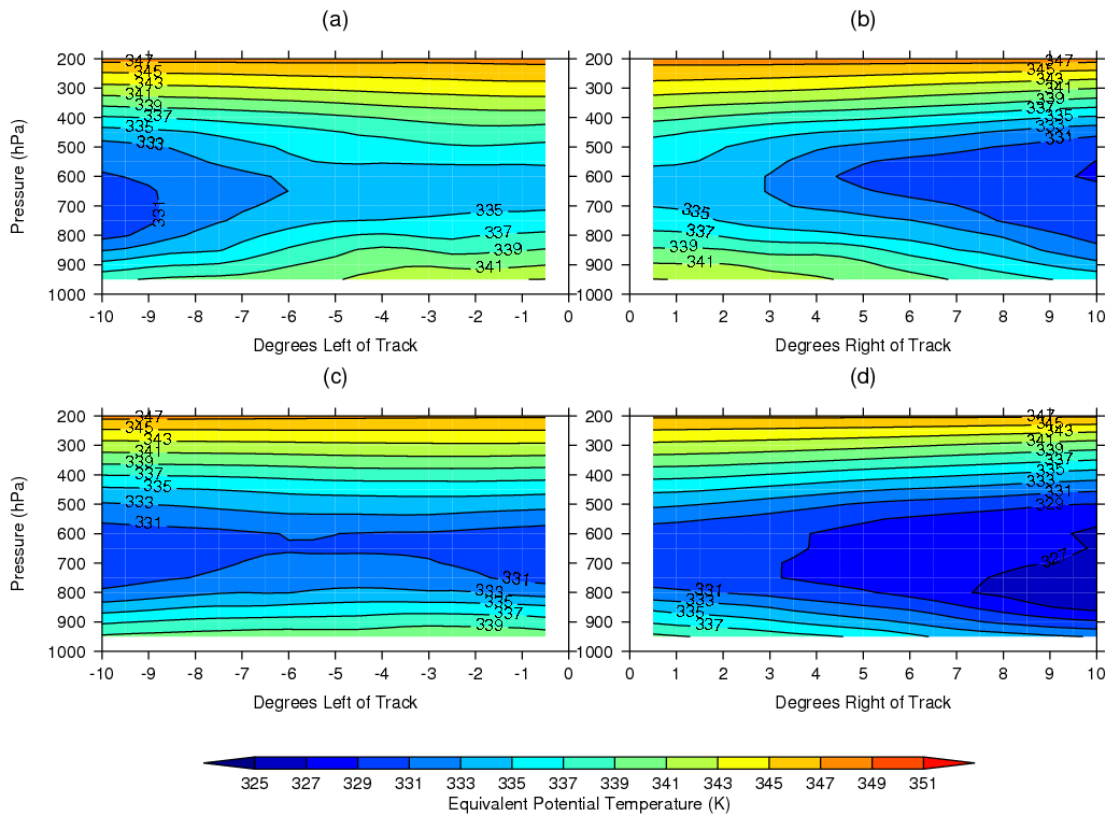


Fig 9.3.1: cross track vertical sections showing θ_e (K) left and right of the track start points of developing ((a) and (b)) and non-developing ((c) and (d)) AEWs

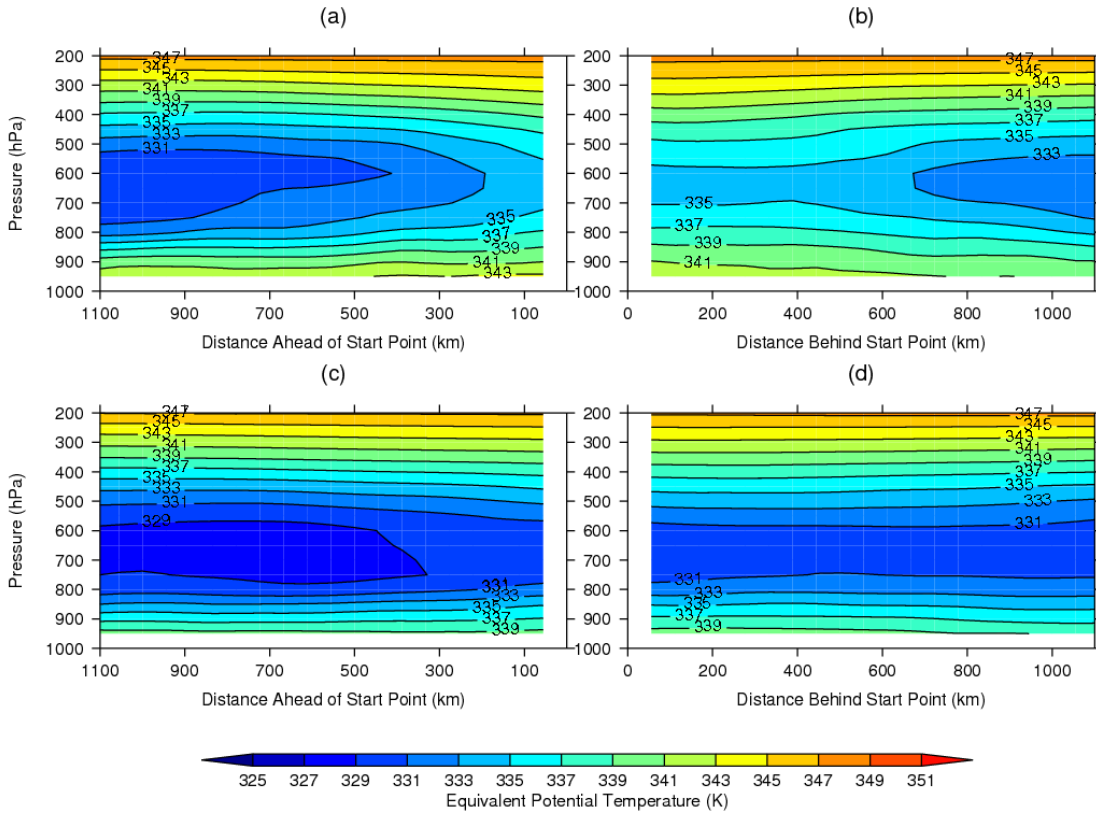


Fig 9.3.2: cross track vertical sections showing θ_e (K) ahead of and behind the track start points of developing ((a) and (b)) and non-developing ((c) and (d)) AEWs

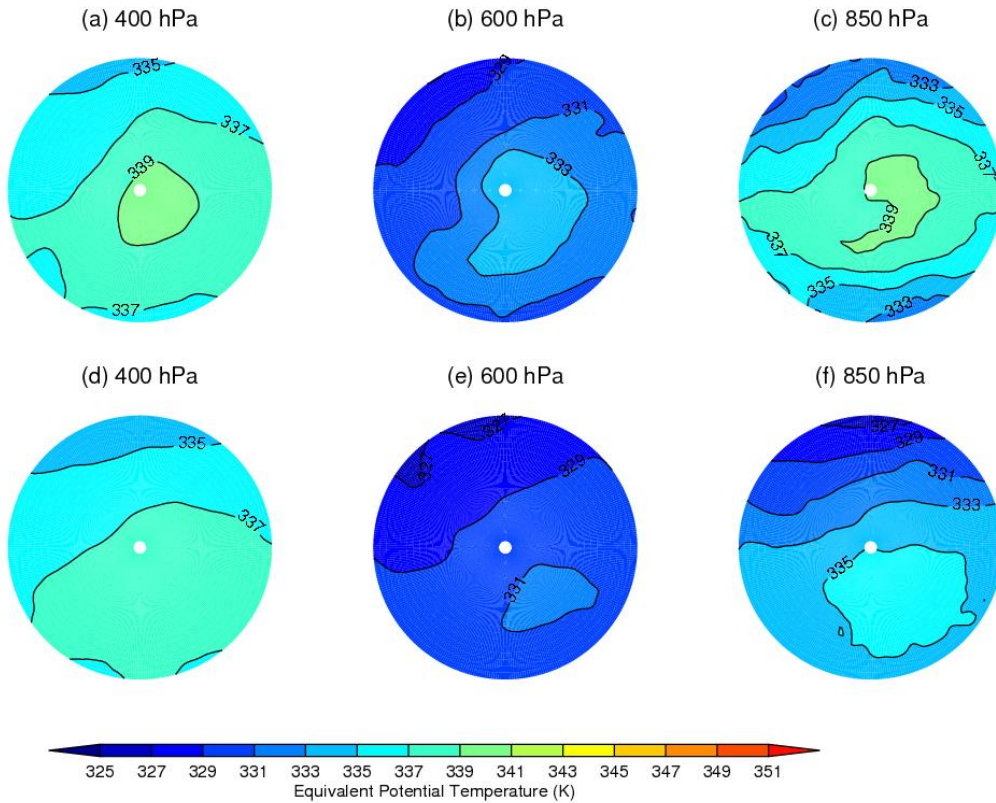


Fig 9.3.3: plan views with a 10^0 radius showing θ_e (K) at the 400, 600 and 850 hPa levels around the track start points of developing ((a),(b) and (c)) and non-developing ((d), (e) and (f)) AEWs

9.4 Potential Vorticity on the 315 K Isentropic Surface Composites

The plan view for PV315 (*Figure 9.4.1*) shows that the potential vorticity for the developing composite is both higher and has a greater gradient across the track direction than for the non-developing composite, with a maximum of 0.45 PVU and a gradient to the right of track of -0.063 PVU/degree, as compared to a maximum of 0.30 PVU and a gradient of -0.025 PVU for the non-developing composite. This demonstrates the greater baroclinic instability available for vortex generation (Fink, et al., 2004).

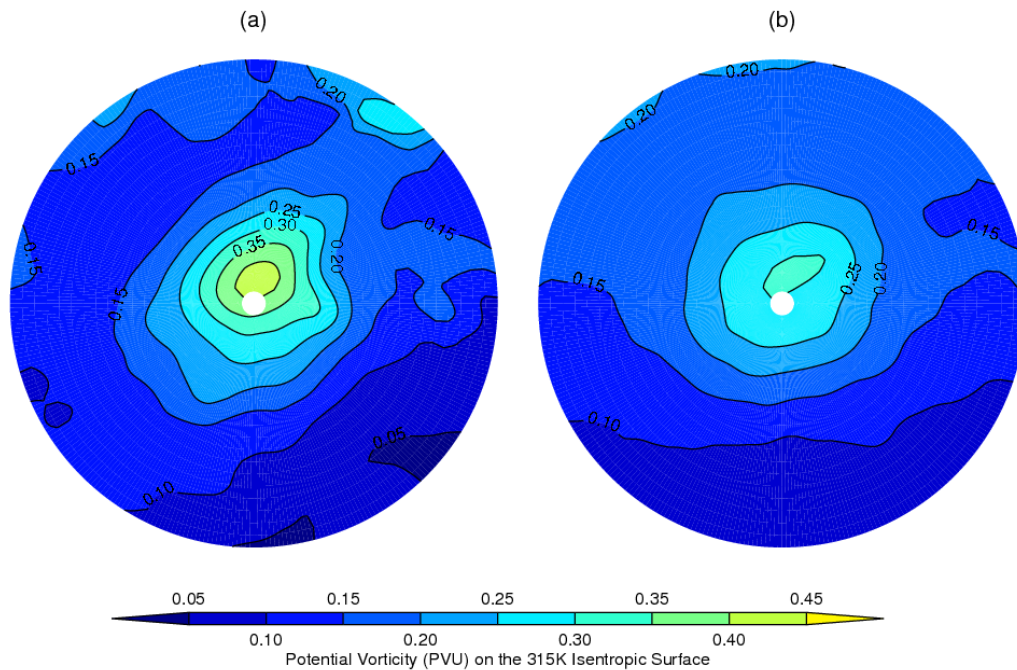


Figure 9.4.1: PV315 for (a) the developing and (b) the non-developing AEW composites

10. Discussion, Conclusions and Further Questions

10.1. Tracking and Identifying AEWs

The aim of this work was to construct composites and cross sections to test hypotheses on why some AEWs and not others develop near the West African coast and then transform into tropical cyclones. The first step in this was to track and identify AEWs as they propagate over West Africa and the tropical Atlantic, and the tracking of vertical mean relative vorticity maxima (Thorncroft & Hodges, 2001; Serra, Kiladis and Hodges, 2010) from 850 to 600 hPa was found to be the most consistent method in both detecting AEWs earlier and following the best track data of developing tropical cyclones over the Atlantic. To identify which AEW corresponded to which tropical cyclone for developing AEWs, and the time at which all AEWs crossed the West African coast it was found that manually analysing the 600 hPa relative vorticity maxima in conjunction with best track data (Tropical Prediction Center, 2010) was the simplest way. These two tracking and identification methods gave two sets of AEW references – firstly manually identified at the West African coast, and secondly automatically tracked downstream across the Atlantic.

10.2. Case Studies of Developing and Non-Developing AEWs

During the research process all the AEWs from JJAS 2005 to 2009 were observed crossing the West African coast, all the developing ones were followed across the Atlantic until they either made landfall or became extratropical storms and most of the non-developing ones were followed until they lost definition. Of these, two developing and two non-developing AEWs from the 2006 season were exhibited as case studies. Hurricane Ernesto and TS Chris were the developing AEWs chosen and they both exhibit similar characteristics as they evolved across the Atlantic. At the West African coast both have a strong AEJ ($>18 \text{ ms}^{-1}$) just to the north of the 600 hPa relative vorticity maximum, and both show significant convection. The northern 925 hPa relative vorticity maximum is strong in both cases due to the high Saharan surface temperatures. As these AEWs progress into the Atlantic the 925 hPa relative vorticity maximum decreases in strength, probably due to the drop in surface temperature over the relatively cool east Atlantic, but the 600 hPa vortex is still driven by the AEJ which remained coherent poleward of it. Looking at the vertical mean relative vorticity maximum in relation to the geopotential height it can be seen that the AEW wave structure remains thus, and the vertical mean relative vorticity remains generally co-located with the AEW trough. In the 48 hours before these AEWs are declared as tropical depressions, the 925 hPa relative vorticity maximum tends to increase as sea surface temperatures increase above 26°C to the west, and the 600 hPa relative vorticity maximum is still sustained by an organised local maximum of the AEJ immediately to the north, in both cases greater than 10 ms^{-1} . Also common to both cases is the presence of convection,

which when at the West African coast is in the form of fairly loose MSCs but becomes more organised with westward progress, developing bands of different levels of cloud by 52°W. AEWs 171 and 516 were chosen as the two non-developing AEWs to present as case studies, because both of them propagated most of the way across the Atlantic. At the West African coast they display many similarities to the developing AEWs, in that there is a discernable wave structure, weak in the case of AEW 171, easily visible relative vorticity maxima at 600 hPa, 925 hPa and for the vertically averaged case, and the presence of the AEJ poleward of the 600 hPa relative vorticity maximum. In AEW 171's case, the AEJ was relatively weak compared to the developing examples (12 ms⁻¹ compared to 18 ms⁻¹ or more), but for AEW 516 it was just as strong (20 ms⁻¹). Once the AEWs leave the coast, however, they evolve in very different ways to the developing AEWs, and it appears to be strongly related to the presence and behaviour of the AEJ. AEW 171 is associated with a weak offshoot of the AEJ which takes it down to the south and stalls there before dissipating entirely 6 days after leaving the West African coast. The AEJ associated with AEW 516 lasts longer, but again 5 days after leaving the coast the 600 hPa relative vorticity maximum is left disconnected from any poleward AEJ, and it dissipates. The behaviour of the convection associated with these non-developing systems is also markedly different. At the West African coast both have significant convection in the form of disorganised MSC systems associated with them. After 48 hours when the AEWs are both at approximately 31°W the convection has decreased significantly, with little organised presence, and a further 48 hours downstream has lost all organisation and is composed of isolated patches of medium height cloud.

The four case studies presented show the same general characteristics for all the individual AEWs observed during this research, in that the ones that developed all seemed to have a coherent AEJ component to the north of the vertical mean and 600 hPa relative vorticity maximum, even though they may not have had the strongest AEJ at the coast, while the non-developing AEWs all lost spatial connection with the AEJ, after which point they dissipated rapidly unless they were reinvigorated by another factor (e.g. passing over the South American continent). There were significant differences in the convection development, as described above between developing and non-developing AEJs, which would imply significant differences in their moisture content and vertical wind velocities.

10.3. Hypotheses for Experiments

It was hypothesised therefore that the developing AEWs had different AEJ, relative humidity and convective regimes (cf. Hopsch, et al., 2010) and these were investigated both at the West African coast and downstream. The West African coast is an obvious analysis point, as there is little geographic spread in the AEW tracks and also, equally importantly, the AEWs are at the same stage

developmentally before passing over the Atlantic. A volume from the Equator to 25°N, from 20° to 14°W and from 950 to 200 hPa was chosen as the coastal region for AEW analysis.

The choice of a downstream reference point is not so obvious, as developing AEWs take very different paths, as do non-developing ones to a lesser extent. The point at which the automatic relative vorticity maximum tracking algorithm (Serra, et al., 2010) for the mean relative vorticity averaged over 850 to 600 hPa detected the AEW track in the Atlantic was chosen as the analysis point, primarily because this means that each AEW has reached a similar development stage in at least one property, the relative vorticity field, and also because it does not depend on the relation to any future stage, for example 24 hours before declaration as a tropical depression. This initial tracking point was used as the reference point for a volume of radius 10° and height from 950 to 200 hPa.

The data for each AEW for JJAS 2005 to 2009 was individually taken at each of the two regions and times given above, and then these individual AEW data sets were composited into two overall subsets- developers and non-developers – for analysis.

10.4. AEW Development at the West African Coast

Analysis of the AEW composites as they crossed the West African coast showed that the AEWs that develop into tropical storms are on average accompanied by a stronger AEJ, and this is true not only of the maximum jet velocity, but also by its zonal extent and the change in zonal wind speed from south of the jet to north of it. Meridional wind has the smallest difference of any of the fields tested, with the only significant difference being a stronger equatorward flow at the top of the troposphere, perhaps indicative of more convection in the developing AEWs. This was definitely observed with the vertical wind component, which showed considerably more vertical motion for the developing composite compared to the non-developing one. This vertical motion is indicative of convection occurring, and this is also indicated by the relative humidity data, which shows a column of moister air throughout the troposphere associated with the relative vorticity maximum for developing AEWs as compared to non-developing ones. Also of note are the downstream relative humidity conditions – at low levels in the troposphere, illustrated by the 850 hPa level, there is up to 10% more relative humidity co-located with and to the north of the AEJ for the developing AEWs. The characteristics shown by the relative humidity data are mirrored by those of the equivalent potential temperature, which shows, unsurprisingly given the definition of θ_e (Emanuel, 1994), that the areas which have higher relative humidity generally also have higher θ_e and therefore more available potential energy.

The regional and downstream conditions at the time of the AEW coast crossing indicated that the position of the relative vorticity maximum with respect to synoptic and regional conditions showed

differences between developing and non-developing AEWs. AEWs are characterised by a trough axis, and the relative vorticity maximum for the developing AEW composite was on this axis, which would give neither positive nor negative vorticity advection, while for the non-developing AEW composite it was slightly upstream of the trough axis, which would lead to some negative vorticity advection. Just downstream of the AEW trough axis the lower atmosphere θ_e showed up to 6K more for the developing AEW composite than for the non-developing one. There was no significant difference seen in the average 600 hPa geopotential height conditions for the African continent between developing and non-developing AEWs.

10.5. AEW Downstream Development

The original hypothesis was that developing AEWs were characterised by a stronger easterly poleward jet at 650 hPa. This is the case, with the developing AEW composite having such a jet of stronger wind speed and greater horizontal extent. Also, and equally significant, there is the discovery that the change in wind speed from the south to the north of track is greater for developing AEWs, which gives immediate impetus to the development of relative vorticity maxima into actual closed circulations, and this is confirmed by both the maximum values and gradient of the PV315 field which show that conditions are better for the development of barotropic instability for the developing AEW composite than for the non-developing one (Pytharoulis, et al., 1999).

The fields of relative humidity and θ_e are closely linked, and show the existence of a warmer, moister volume of air to the south east of the developing AEWs, and drier air ahead of the non-developing AEWs. Bearing in mind that this snapshot of developing and non-developing AEWs is at the start of their detected tracks, just as or just before the developing AEWs start to show closed circulations, this can be thought of as a “reservoir” of warm, moist air, which, as it is drawn into the developing system, feeds energy and moisture into the convection. This would allow for the further development of organised convective systems, as demonstrated by the developing AEW case studies.

Also noted here but not investigated further is the discovery that developing AEWs have on average a significant jet at 200 hPa south of the vertical mean relative vorticity, whereas for non-developing AEWs it is the other way round. This jet is possibly the Tropical Easterly Jet (Hastenrath, 1991) and if so may have an effect on upper level convergence or divergence.

10.6. Overall Conclusions and Areas for Further Investigation

There is no one obvious characteristic of an AEW as it passes the West African coast that will allow it to be designated as a developer or a non-developer. Developing AEWs as a group have more convection (characterised by vertical wind velocity) and are driven by a stronger AEJ than non-developers at this point (cf. Hopsch, et al., 2010), but it is further downstream that the evolution to a tropical cyclone occurs and this is where significant differences are found. This evolution is supported by a noticeably stronger poleward adjacent AEJ and by a more humid volume of air with higher equivalent potential energy to the south and east of the vertical mean relative vorticity maximum. The stronger AEJ provides more energy from the barotropic instability deriving from the change in sign of the meridional potential vorticity gradient (Pytharoulis, et al., 1999) through the AEJ, and the volume of air of more relative humidity and equivalent potential energy provides a source of both moisture and energy to aid the growth of deep convection.

Areas for further research are:

- (a) an investigation into the effect of the 200 hPa level wind differences found between downstream developing and non-developing AEWs;
- (b) further investigation into the convective processes both at the West African coast and downstream, possibly including the effects of Saharan Air Layer dust particles as cloud condensation nuclei in combination with the moist air volume to the south and east of the relative vorticity vortices;
- (c) moving the downstream analysis through time from when the AEWs are first picked up until they develop closed circulation and are declared a tropical depression (or not, as the case may be).

References

- Avila, L. A., & Brown, D. P. (2006). *Tropical Cyclone Report - Tropical Storm Alberto*. National Hurricane Center. Miami: National Hurricane Center.
- Beven, J. (2006). *Tropical Cyclone Report - Hurricane Florence*. National Hurricane Center. Miami: National Hurricane Center.
- Blake, E. S. (2006). *Tropical Cyclone Report - Hurricane Gordon*. National Hurricane Center. Miami: National Hurricane Center.
- Blake, E. S., Rappaport, E. N., & Landsea, C. W. (2007). *The Deadliest, Costliest and Most Intense United States Tropical Cyclones from 1851 to 2006 (and Other Frequently Requested Hurricane Facts)*. National Hurricane Center. Miami: National Hurricane Center.
- Brown, D. P. (2006). *Tropical Cyclone Report - Hurricane Helene*. National Hurricane Center. Miami: National Hurricane Center.
- Burpee, R. W. (1972). The Origin and Structure of easterly Waves in the Lower troposphere of North Africa. *Journal of Atmospheric Science* , 29, 77-90.
- Carlson, T. N. (1969). Some Remarks on African Disturbances and their Progress over the Tropical Atlantic. *Monthly Weather Review* , 97 (10), 716-726.
- Catto, Jennifer (2009). Extratropical cyclones in HiGEM: climatology, structure and future predictions. PhD thesis, University of Reading.
- Chen, T.-C. (2006). Characteristics of African Easterly Waves Depicted by ECMWF Reanalyses for 1991-2000. *Monthly Weather Review* , 134, 3539-3566.
- Cornforth, R., Hoskins, B., & Thorncroft, C. (2009). The impact of moist processes on the African Easterly Jet - African Easterly Wave System. *Quarterly Journal of the Royal Meteorological Society* , 135, 894-913.
- ECMWF. (2010). *ERA-Interim Data*. Retrieved August 2010, from European Centre for Medium Range Weather Forecasts: http://data-portal.ecmwf.int/data/d/interim_daily/levtype=pt/
- Emanuel, K. A. (1994). *Atmospheric Convection*. New York, NY, USA: Oxford University Press.
- Fink, A., Vincent, D., Reiner, P., & Speth, P. (2004). Mean State and Wave Disturbances during Phases I, II and III of GATE Based on ERA-40. *Monthly Weather Review* , 132, 1661-1683.
- Franklin, J. L. (2006). *Tropical Cyclone Report - Tropical Storm Debby*. National Hurricane Center. Miami: National Hurricane Center.
- Gray, W. (1978). Hurricanes, their formation, structure and likely role in tropical circulation. In O. Shaw (Ed.), *Meteorology over the tropical oceans* (pp. 155-218). Bracknell: Royal Meteorological Society.
- Hastenrath, S. (1991). *Climate Dynamics of the Tropics*. Dordrecht, The Netherlands: Kluwer Academic Publishers.

- Hopsch, S. B., Thorncroft, C. D., & Tyle, K. R. (2010, April). Analysis of African Easterly Wave Structures and Their Role in Influencing Tropical Cyclogenesis. *Monthly Weather Review* , 1399 - 1419.
- Hopsch, S. B., Thorncroft, C. D., Hodges, K., & Aiyyer, A. (2007). West African Storm Tracks and Their Relationship to Atlantic Tropical Cyclones. *Journal of Climate* , 20, 2468-2483.
- Knabb, R. D., & Mainelli, M. (2006). *Tropical Cyclone Report - Hurricane Ernesto*. National Hurricane Center. Miami: National Hurricane Center.
- Knabb, R. D., Rhome, J. R., & Brown, D. P. (2006). *Tropical Cyclone Report, Hurricane Katrina, 23-30 August 2005*. Miami: National Hurricane Center.
- Lebel, T., & Ali, A. (2009). Recent Trends in the Central and Western Sahel rainfall regime (1990-2007). *Journal of Hydrology* , 375, 52-64.
- Mainelli, M. (2006). *Tropical Cyclone Report - Hurricane Isaac*. National Hurricane Center. Miami: National Hurricane Center.
- NERC Satellite Receiving Station, Dundee University, Scotland. (2010). *Geostationary Archive*. Retrieved from NEODASS, Dundee Satellite Receiving Station: <http://www.sat.dundee.ac.uk/geobrowse/geobrowse.php>
- Pasch, R. J. (2006). *Tropical Cyclone Report - Tropical Storm Beryl*. National Hurricane Center. Miami: National Hurricane Center.
- Philip's. (2002). *Philip's Atlas of the World*. London, UK: Philip's.
- Pytharoulis, I., & Thorncroft, C. (1999). The Low-Level Structure of African Easterly Waves in 1995. *Monthly Weather Review* , 127, 2266-2280.
- Serra, Y., Kiladis, G. N., & Hodges, K. I. (2010). Tracking and Mean Structure of Easterly Waves over the Intra-Americas Sea. *Draft* .
- Stewart, S. R. (2006). *Tropical Cyclone Report - Tropical Storm Chris*. National Hurricane Center. Miami: National Hurricane Center.
- Thorncroft, C., & Hodges, K. (2001). African Easterly Wave Variability and Its Relationship to Atlantic Tropical Cyclone Variability. *Journal of Climate* , 14, 1166-1179.
- Thorncroft, C., & Hoskins, B. (1994). An idealised study of African easterly waves. II: a non-linear view. *Quarterly Journal of the Royal Meteorological Society* , 120, 983-1015.
- Tropical Prediction Center. (2010). *Atlantic Tropical Storm Tracking By Year*. Retrieved 2010, from Unisys Weather: <http://weather.unisys.com/hurricane/index.html>
- UK Hydrographic Office. (2010). *Admiralty List of Radio Signals* (Vol. 3). Taunton, Somerset, UK: UK Hydrographic Office.
- UK Hydrographic Office. (1987). *Admiralty Ocean Passages for the World* (4 ed., Vol. NP 136). Taunton, Somerset, UK: UK Hydrographic Office.
- UK Hydrographic Office. (1998, March). A Planning Chart for the North Atlantic Ocean and Mediterranean Sea. *ARCS Chart 4004* . Taunton, Somerset, UK: UK Hydrographic Office.

Zipser, E. J., Twohy, C.H., Tsay, S., Thornhill, L., Tanelli, S., Ross, R., Krishnamurti, Q.J., Jenkins, G., Syed, I., Hsu, C., Hood, R., Heymsfield G.M., Heymsfield, A., Halverson, J., Goodman, H.M., Ferrare, R., Dunion, J.P., Douglas, M., Cifelli, R. Chen, G., Browell, E.V., Anderson, B. (2009, August). The Saharan Air Layer and the Fate of African Easterly Waves. *Bulletin of the American Meteorological Society* , 1137-1156.